

SELECTIVE SILENCING OF VERBETRATE  
NEURONS: STRATIGIES USING  
INVERTEBRATE LINGAND-GATED ION  
CHANNELS

Thesis by

Eric Slimko

In Partial Fulfillment of the Requirements for the

degree of

Doctor of Philosophy

CALIFORNIA INSTITUTE OF TECHNOLOGY

Pasadena, California

2006

(Defended June, 2006)

© 2006

Eric Slimko

All Rights Reserved

## ACKNOWLEDGEMENTS

First and foremost, I need to thank my advisor, Henry Lester, who throughout my years as a graduate student has shown what can only be called infinite patience. In addition, his guidance during my tenure has been unwavering, direct, enthusiastic, and largely right. I can think of several experiments in which had I pursued Henry's suggestions first instead of my own, I would have saved myself a remarkable amount of frustration and time. I consider it a high achievement that there are at least a few exceptions to this rule, where my approach turned out to be the fruitful one instead of Henry's. This is probably one of the central lessons of graduate school: *trust your mentors, but not too much.*

A variety of my Lab-mates have enhanced my experience dramatically, and not listing them here would be a disservice: Bal Khakh, now a professor at Cambridge, who's enthusiasm for all things neuroscience rivals that of my advisor; John Liete, for numerous lunch discussions of science and beyond; Sheri McKinney, without whose skill in neuronal culture techniques I would be hopelessly lost; and Johannes Schwartz, Raad Nashmi, and Carlos Fonck. A large part of graduate school is the time you spend with other scientists in various stages of their careers, and I am fortunate to have worked with these people.

After Henry, I owe a lot of motivation and ideas to David Anderson and several members of his Laboratory: Walter Lerchner, Wulf Haubensak, and Raymond Montegu. David, besides being a bottomless pit of ideas, has an intensity which leaves one wanting to perform far more experiments than one could reasonably perform. Also at CalTech, Christof Koch has added considerable color to my graduate years. Besides giving me the courage to tackle very hard problems, from Christof I will take one of his trademark quotes, to be used when in any argument, scientific or not: "*Trust me, I'm a scientist!*"

Finally, I must thank Herwig Baier of UCSF and his post-doc Ethan Scott. At my darkest of days a graduate student, the two of them managed to get the technique I had worked so hard on to function in zebrafish. This success provided a high-note at the end of my graduate career.

This work in part was supported by the National Institutes of Health Grants NS 11756 and MH 49176, by the Sidney Stern and Plum Foundations, and by the William T. Gimbal Discovery fund in Neuroscience.

## ABSTRACT

Selectively reducing the excitability of specific neurons will (1) allow for the creation of animal models of certain human neurological disorders and (2) provide insight into the roles of specific sets of neurons, both in the local circuit and in the behavior of the intact organism. This work focuses on a combined genetic and pharmacological approach to silence neurons electrically. We express invertebrate ivermectin (IVM)-sensitive chloride channels (*Caenorhabditis elegans* GluCl  $\alpha$  and  $\beta$ ) in vertebrate neurons first *in vitro* using viral and transfection techniques, and then finally *in vivo* using genetic techniques, to produce inhibition via a Cl<sup>-</sup> conductance when activated with IVM. We have considerably engineered these two genes by (1) re-coding the genes such that vertebrate-preferred codons are used throughout the sequences, (2) incorporating fluorescent tags within the proteins, and (3) finding a mutation to remove the undesirable glutamate sensitivity of the channel while retaining IVM efficacy. Expression of this new channel does not affect the normal spike activity of the target cell, yet the experimenter can effectively “shut-off” the cell with concentrations of as low as 5 nM IVM. Chapter 1 provides a broad overview of the many “selective silencing” approaches that experimenters have tried. In Chapter 2, the author describes the basic “GluCl/IVM” technique and initial experiments in cultured hippocampal neurons. Chapter 3 refines the technique by describing the strategy and mutation that allowed great reduction in the native glutamate response while maintaining the IVM response. Chapter 4 develops the final engineering of the channel: recoding the sequence for optimal expression and the introduction of fluorescent tags for identification. Finally, Chapters 5 and 6 discuss the successes and failures of *in vivo* work with what we now call the “GluCl/IVM method.”

## TABLE OF CONTENTS

Acknowledgements .....	iii
Abstract .....	v
Table of Contents.....	vi
List of Figures .....	vii
Chapter I: Introduction to Selective Silencing .....	1
Chapter II: Selective Electrical Silencing of Mammalian Neurons In Vitro by the Use of Invertebrate Ligand-Gated Chloride Channels .....	23
Chapter III: Selective elimination of glutamate activation and introduction Of fluorescent proteins into a <i>Caenorhabditis elegans</i> chloride channel ..	51
Chapter IV: Codon optimization of <i>Caenorhabditis elegans</i> GluCl ion Channel genes for mammalian cells dramatically improves expression levels .....	71
Chapter V: Usage of the “GluCl/IVM” method in zebrafish to understand the role of retinal ganglion cells .....	92
Chapter VI: Attempts to use the “GluCl/IVM” method in mice.....	110

## LIST OF FIGURES

<i>Number</i>	<i>Page</i>
1-1. <b>Inhibition of synaptic transmission of cerebellar granule cells by doxycycline (DOX)-dependant reversible expression of tetanus toxin (TeNT) .....</b>	6
1-2. <b>Silencing of cortical neurons with the AlstR/AL receptor/ligand system.....</b>	9
1-3. <b>Pharmacological stimulation of genetically designated target neurons .....</b>	12
2-1. <b>Modified pSinRep5 construct, pSinRep5tsgGluCl<math>\alpha\beta</math>EGFP .....</b>	28
2-2. <b>GluCl <math>\alpha</math> and <math>\beta</math> are both required for functional channels in HEK293 cells.....</b>	31
2-3. <b>Activation of GluCl conductance by IVM over a 100-fold concentration range .....</b>	33
2-4. <b>IVM silences GluCl-expressing neurons .....</b>	35
2-5. <b>There is a large variation in expression levels that seems to be culture dependent.....</b>	37
2-6. <b>Neurons cotransfected with separate plasmids encoding EYFP-tagged GluCl <math>\alpha</math> and ECFP-tagged GluCl <math>\beta</math> show fluorescence.....</b>	39
2-7. <b>IVM-induced chloride conductance deactivates several hours after IVM washout.....</b>	41
2-8. <b>Expression of GluCl does not alter glutamate or GABA-evoked currents .....</b>	42
3-1. <b>GluCl sequences in the extracellular ligand-binding domain and M1, compared with other nAChR superfamily members... </b>	58

3-2. Electrophysiological characterization of WT and three mutated GluCl constructs.....	60
3-3. GluCl $\alpha\beta$ (Y182F) eliminates glutamate sensitivity and retains ivermectin sensitivity .....	62
3-4. Functional expression of fluorescent protein-tagged constructs .....	66
4-1. Codon usage of native GluCl $\alpha$ and $\beta$ subunits compared with the optimized GluCl $\alpha$ and $\beta$ subunits synthesized in this study .....	78
4-2. Increase in channel expression as revealed by fluorescence microscopy .....	80
4-3. Increase in expression measured by fluorescence microscopy and electrophysiology .....	82
4-4. Correlation of signals in the two fluorescent channels.....	83
4-5. Dose-response relation for activation of optGluCl channel by IVM.....	85
4-6. Effects of optGluCl $\beta$ Y182F mutation.....	87
5-1. Schematic of the two visuomotor behaviors investigated in this study .....	95
5-2. Immunohistochemistry localization of GluCl.....	100
5-3. Results of Visual Background Adaptation (VBA) .....	102
5-4. Results from the Optomotor Response (OMR).....	104
5-5. Results for the Optokinetic Response (OKR).....	105
5-6. Spontaneous swimming activity .....	107
6-1. Constructs used for transgenic mice generation .....	115
6-2. RVLM sections .....	120
6-3. Infection of the hippocampus with AAV.....	122-123
6-4. mRNA <i>in-situ</i> s for wild-type and two lines .....	127-128
6-5. Immunohistochemistry of cerebellar slices.....	129

6-6. <b>Direct detection of ECFP and EYFP in L7 line 70</b> .....	131
6-7. <b>Acute dissociated Purkinje cell input conductance</b> .....	132
6-8. <b>Static rotarod performance</b> .....	134
6-9. <b>Learning rotarod paradigm</b> .....	135
6-10. <b>Ivermectin can kill mice</b> .....	137

*Chapter 1***Introduction to Selective Silencing**

*For example, it would be useful to be able to inactivate, preferably reversibly, a single type of neuron in a single area of the brain...Molecular biology is advancing so rapidly that it will soon have a massive impact on all aspects of neurobiology.*

Francis Crick wrote the above sentences while musing on new approaches required to “unscramble” the complicated systems we call brains (Crick, 1988; Wulff and Wisden, 2005). Simple invertebrate nervous systems have small networks of neurons that sometimes have only one or two cells of each type, lending them to exploration by current hyperpolarization. Such silencing can reveal how specific components of neural circuits influence network properties or even contribute to animal behavior (Greenspan, 2004). These are not the systems that Crick was discussing. Unfortunately, applying this approach for the study of complex brains found in vertebrate nervous systems is challenging, for two reasons: (1) there are often many cells of a given type, and (2) neuronal targets can be spatially dispersed populations (e.g. interneurons, Purkinje cells, or dopaminergic neurons in striatum. There are countless examples that will only expand as more unique molecular signatures are identified.)

For vertebrates, a cell-type-specific, reversible method for delicate analysis of circuitry that is able to work on the signaling timescale of the brain (milliseconds to seconds) does not yet exist (Steele et al., 1998; Miesenbock, 2004; Callaway, 2005; Wulff and Wisden, 2005). For the most part, experimenters have focused on either strictly genetic or strictly pharmacological techniques. Unfortunately, genetics alone cannot induce new protein expression on the timescale of brain activity, and pharmacology alone often lacks specificity. Rarely do naturally expressed receptors or ion channels provide unique drug targets of the experimenter’s choice. The logical extension is to combine genetics and pharmacology, and a variety of approaches have been proposed and explored at different levels. This thesis reports on the exploration of one of these approaches, called the

“GluCl/IVM method.” However, before a careful explanation of this technique we will first review the “Selective Silencing” field.

### ***Drosophila* selective silencing**

Many genes are used for reducing the excitability of neurons in a variety of preparations, both *in vitro* and *in vivo* (Table 1-1). Clearly, the largest successes are in the fruit fly *Drosophila*. In the *Drosophila* nervous system, the light chain of tetanus toxin (TeNT) was used to interrupt synaptic transmission and observe behavioral defects (Sweeney et al., 1995; Keller et al., 2002; Martin et al., 2002). TeNT cleaves the vesicle-associated membrane protein 2 (VAMP2 or synaptobrevin), which is required for Ca<sup>2+</sup>-regulated synaptic vesicle exocytosis. Thus, expression of TeNT will block synaptic transmission without directly killing the cell. The neuronal substrate of the olfactory escape response was studied in this fashion (Sweeney et al., 1995). Overexpression of K<sup>+</sup> channels, which clamps the neuron at its resting membrane potential, also works quite well in *Drosophila* (Baines et al., 2001; White et al., 2001a; White et al., 2001b). For example, this technique was used to show a disruption in circadian behavior of the animal due to electrical silencing of circadian pacemaker neurons, while leaving the light-dark driven molecular clock intact (Nitabach et al., 2002). Also in *Drosophila*, local expression of temperature-sensitive dynamin can transiently block synaptic transmission in minutes (Kitamoto, 2001, 2002). The *shibire* gene encodes a dynamin GTPase that is essential for synaptic vesicle recycling and maintaining the release pool of synaptic vesicles. *Shibire<sup>ts1</sup>* has a mutation making the protein inactive at temperatures >29 C. Rapidly shifting temperatures causes synaptic transmission to terminate at 32 C and reactivate at 25 C. The importance of mushroom bodies and dorsal paired medial neurons in *Drosophila* memory formation was demonstrated with this technique (Dubnau et al., 2001a; McGuire et al., 2001).

Unfortunately, the move to vertebrate systems has not been so straightforward as one might have predicted. Some of these *Drosophila* techniques have been applied in vertebrates and have met with limited success. The following text focuses on excitability modulation approaches in vertebrate systems.

<i>In vitro</i> applications		
<i>Gene</i>	<i>Target cells</i>	<i>Reference</i>
aK <sub>v</sub> 1.2	<i>Aplysia</i> neurons	(Kaang et al., 1992)
aK <sub>v</sub> 5.1	<i>Aplysia</i> neurons	(Zhao et al., 1994)
GFP-K <sub>v</sub> 1.4	Skeletal myoballs	(Falk et al., 2001)
dK <sub>v</sub> 1.1	Cardiac myocytes	(Johns et al., 1995)
rK <sub>ir</sub> 3.x (GIRKs)	Hippocampal neurons	(Ehrengruber et al., 1997)
GFP-K <sub>ir</sub> 2.1	SCG Neurons, hair cells	(Johns et al., 1999)
HERG	Cardiac myocytes	(Hoppe et al., 2001)
EKO	<i>Aplysia</i> neurons	(White et al., 2001b)
rK <sub>ir</sub> 1.1	Hippocampal neurons	(Nadeau et al., 2000)
hGABA <sub>C</sub> R	Hippocampal neurons	(Cheng et al., 2001)
ceGluCl	Mammalian neurons	(Slimko et al., 2002)
TeTxLC	<i>Aplysia</i> neurons	(Mochida et al., 1990)
DroAlstR	Ferret cortical neurons	(Lechner et al., 2002)
RASSL	COS-7 cells	(Coward et al., 1998)
<i>In vivo</i> applications		
<i>Gene</i>	<i>Target tissues</i>	<i>Reference</i>
xK <sub>v</sub> 1.1,xK <sub>v</sub> 1.2	<i>Xenopus</i> embryonic neurons	(Jones and Ribera, 1994)
EKO	<i>Drosophila</i> embryonic neurons	(White et al., 2001b)
	<i>Drosophila</i> larval muscles	(White et al., 2001b)
	<i>Drosophila</i> photoreceptors	(White et al., 2001b)
ceK <sub>v</sub> 3	<i>C. elegans</i> motor neurons	(Zhao and Nonet, 2000)
rK <sub>v</sub> 1.1,rK <sub>v</sub> 1.2	<i>C. elegans</i> sensory neurons	(Peckol et al., 1999)
TeTxLC	<i>Drosophila</i> photoreceptors	(Hiesinger et al., 1999)
	<i>Drosophila</i> embryonic neurons	(Sweeney et al., 1995)
	<i>Drosophila</i> sensory neurons	(Martin et al., 1998)
	<i>Drosophila</i> ventral lateral neurons	(Kaneko et al., 2000)
	<i>Drosophila</i> Ddc <sup>+</sup> neurons	(Blanchardon et al., 2001)
	<i>Drosophila</i> giant fiber neurons	(Allen et al., 1999)
	<i>Drosophila</i> pacemaker neurons	(Nitabach et al., 2002)
	Mouse cerebellar granule cells	(Yamamoto et al., 2003)
	Mouse olfactory neurons	(Yu et al., 2004)
GFP-K <sub>ir</sub> 2.1	<i>Drosophila</i> motor neurons	(Baines et al., 2001)
	<i>Drosophila</i> larval muscles	(Paradis et al., 2001)
	<i>Drosophila</i> photoreceptors	(Hardie et al., 2001)
Shi <sup>ts1</sup>	<i>Drosophila</i> photoreceptors	(Kitamoto, 2001)
	<i>Drosophila</i> peptidergic neurons	(Waddell et al., 2000)
	<i>Drosophila</i> MB neurons	(Dubnau et al., 2001b)
	<i>Drosophila</i> cholinergic neurons	(Kitamoto, 2001)
dK <sub>v</sub> 1.1	<i>Drosophila</i> muscles	(Zagotta et al., 1989)
	<i>Drosophila</i> neurons	(Zhao et al., 1995)
aK <sub>v</sub> 1.1	Mouse CNS	(Sutherland et al., 1999)
rSK3	Mouse myotubes	(Bond et al., 2000)
Dunc-18	<i>Drosophila</i> Neurons	(Wu et al., 1998)
Syt I	<i>Drosophila</i> neuromuscular junction	(Marek and Davis, 2002)
ceGluCl	Zebrafish retina	This work
α-bungarotoxin	Zebrafish neurons	(Ibanez-Tallon et al., 2004)
RASSL	Mouse heart	(Redfern et al., 1999)

Table 1-1: Various genes that have been employed to suppress the excitability of neurons. While such strategies have been successful in *Drosophila*, experiments in mammalian systems have been more challenging. Adapted and expanded from White et al, 2001. © (2001) Elsevier Science Ltd.

## Genetic ablation and inactivation

Careful analysis of deficits experienced by humans with damaged or missing brain parts has led to giant leaps in the understand of the vertebrate nervous system (Morris, 1999; Damasio, 2000; Goodale and Milner, 2003). Much of systems neuroscience is based on ablating brain regions or nuclei of a variety of animals (Izquierdo and Medina, 1998). While ablation of a brain region does not necessarily provide insight into its function, it does show its relationship to other regions, suggesting systems but not local mechanisms. Cell-type-specific ablation studies have been undertaken to address local mechanisms. This can be done a number of ways. For example, by using transgenic techniques to express toxins that directly kill the cell (Sato and Tanigawa, 2005) or by expressing proteins that bind an injected agent that then kills the cell (Kobayashi et al., 1995). Unfortunately, ablation, whether regional, cellular, or genetic, often causes compensations or adaptation, confusing the interpretation of these experiments (Greenspan, 2001). These unexpected compensations are interesting and have been studied. For example, the selective ablation of Golgi cells in the cerebellum was originally intended to study the function of these cells, but instead resulted in documenting compensatory mechanisms (Watanabe et al., 1998; Hirano et al., 2002). While perhaps not so helpful for the original purpose of studying the function of the cells destroyed, this provided an excellent example of long-term plasticity and genetic resilience of the nervous system. However, to achieve the ideal of a technique well-suited to circuit modulation and behavioral studies, the interference must be reversible, ideally on timescales from milliseconds to several minutes. Clearly, ablation does not fit this requirement.

Several genetic-only approaches to inactivation have been based on expression of  $K^+$  channels. Cultured sympathetic neurons have been silenced using viral infection of the Kir2.1 inwardly-rectifying potassium channel gene (Johns et al., 1999). DOX-regulation of this gene selectively expressed in olfactory sensory neurons *in vivo* was used to effectively silence them and thus demonstrate the role of activity in constructing a sensory map (Yu et al., 2004). Some success derived from transgenically overexpressing the Kir6.2 channel in forebrain neurons, resulting in a strong loss of spontaneous activity from neocortical and hippocampal neurons, although these mice were not inducible (Heron-Milhavet et al.,

2004). Not all potassium channels result in predictable changes in cell excitability, however. For example, ROMK1 caused apoptosis and is probably not suitable for *in vivo* work (Nadeau et al., 2000), and Shaker-type K<sup>+</sup> channels dysregulated native potassium gene expression (Sutherland et al., 1999).

The light chain of tetanus toxin (TeNT) approach from *Drosophila* was used to temporarily inactivate cerebellar granule cells in mice (Yamamoto et al., 2003). Cell-type-specificity and reversibility is achieved by using the tetracycline-controlled reverse (rtTA) activator system. The rtTA gene is expressed only in cerebellar granule cells driven by the GABA<sub>A</sub> receptor  $\alpha 6$  subunit promoter (Bahn et al., 1997). The rtTA protein is an inactive transcription factor unless it binds doxycycline (DOX); rtTA-DOX then translocates to a tetracycline-responsive element (TRE) in the promoter of a TeNT minigene and drives expression of the toxin (Figure 1-1a). The TRE-TeNT gene is inactive unless DOX is given in the animal's drinking water. High levels of TeNT were detected in cerebellar granule cells after five days of DOX treatment and these levels were maintained as long as DOX was given to the animals. Unfortunately, it took nearly two weeks for the levels of TeNT to decay once DOX was withdrawn from the animal's water supply. During DOX treatment, a behavioral phenotype consistent with cerebellar disruption was observed, namely a marked decrease in performance on the rotarod, a standard test for motor coordination. Two weeks after DOX removal, animals recovered their motor skills (Figure 1-1b,c,d) (Yamamoto et al., 2003). The slow kinetics of gene activation and deactivation are partly due to the pharmacokinetics of DOX; however an intrinsic limit on the speed of the deactivation and reactivation is the need for first RNA transcription and then protein synthesis followed by protein degradation. Hence, the technique is limited to exploring how chronic inactivation of activity over days to week effects behavior and network properties. A similar approach has been used to study the formation and maintenance of sensory maps in the mouse olfactory bulb (Yu et al., 2004); however, in this work no behavioral modulation was reported.

## FIGURE 1-1

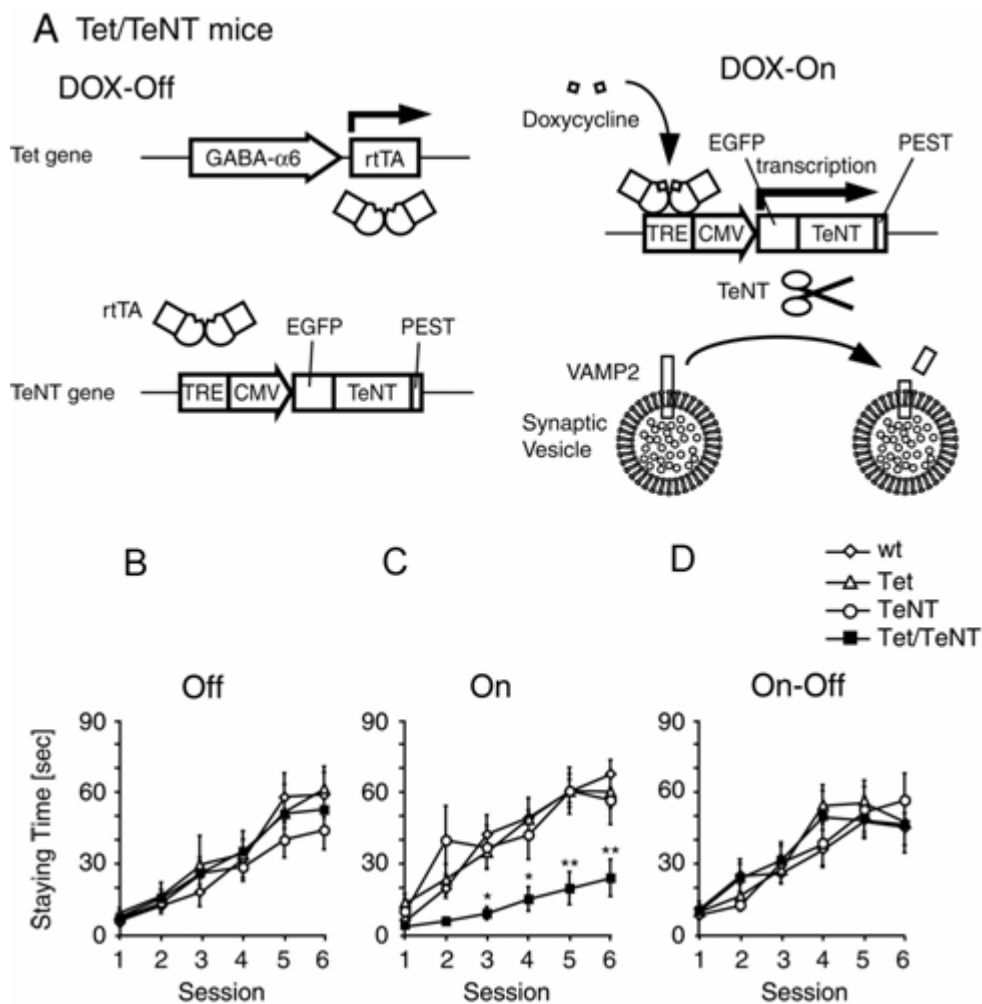


Figure 1-1: **Inhibition of synaptic transmission of cerebellar granule cells by doxycycline (DOX)-dependent reversible expression of tetanus toxin (TeNT).** A, in the absence of DOX, the tetracycline-controlled reverse activator (rtTA) transcription factor does not bind and no protein is produced. In the presence of DOX, rtTA binds the tetracycline response element (TRE) and activates transcription of the toxin, which subsequently cleaves VAMP2 and stops with synaptic transmission. B, In the absence of DOX, all mice genotypes have similar ability on the rotarod. C, in the presence of DOX for 13 days, only mice carrying both the rtTA gene and the TRE cassette lose the ability to perform on the rotarod. D, three weeks after the removal of DOX, these mice recover their ability to perform. All panels adapted from Yamamoto et al, 2003. © (2003) the Society for Neuroscience.

## **Pharmacological manipulations of brain activity**

Pharmacological disruptions of brain circuits are attractive because of their acute reversibility. GABA agonists, glutamate receptor antagonists, and short-acting anesthetics have been used to locally silence brain regions (Hupe et al., 1999; Riedel et al., 1999). The nervous system is unable to engage compensatory mechanisms because of the acute nature of these approaches. Unfortunately, these approaches are generally constrained to operate only on locally defined groups of neurons, as their target receptors are generally widely expressed. While these techniques have provided invaluable information to systems neuroscience, the field is still wanting of a higher precision technique.

## **The “Selective, Reversible, and Rapid” ideal of Selective Silencing**

The genetic techniques in vertebrates explored to date have been selective, and in some cases reversible; however they are far from rapid. On the other hand, pharmacological techniques have been rapid and reversible, but far from specific. The field appears to have been constrained to “pick two” elements of the ideal, and this has led a number of workers to attempt to develop more refined techniques. The natural extension of the genetic-only and pharmacological-only techniques is to try to combine the two and there have been a number of ambitious attempts to do exactly that.

## **Ligand-activated $K^+$ conductances**

As discussed previously, the static clamping of neuronal activity using inward-rectifying  $K^+$  channels has been demonstrated. However, for dissecting the roles of cell types in fast circuit signaling, a ligand-controlled  $K^+$  channel is needed to induce inhibition transiently. While there are no known directly ligand-gated  $K^+$  channels, many neurotransmitters modulate cellular  $K^+$  conductance through G-protein coupled receptors (GPCRs).

Conklin and colleagues engineered GPCRs to eliminate sensitivity to endogenous ligands but retain sensitivity to synthetic ligands in a technique they call RASSL (receptor activated solely by a synthetic ligand) (Redfern et al., 1999; Scarce-Levie et al., 2001). Many natural GPCRs could be platforms for RASSL design, and there are a variety of

synthetic agonists and antagonists available. The original RASSL strategy used a mutated  $\kappa$  opioid receptor to activate  $G_i$  (Coward et al., 1998), thus activating G protein-activated inward rectifier (GIRK) channels. This RASSL, termed Ro1, is insensitive to 21 natural opioid peptides but is activated by the drugs spiradoline and bremazocine. When transgenic mice expressing Ro1 in the heart were given the agonist spiradoline, their heart rates decreased by as much as 80% (Redfern et al., 1999). In a further example, Claeysen and colleagues made a RASSL of the 5-HT<sub>4</sub> receptor (Claeysen et al., 2003). The 5-HT<sub>4</sub>-RASSL stimulates, via G<sub>s</sub>, cAMP formation in response to the synthetic ligand GR 113808 but not to 5-HT. The difficulty with the technique is that the native receptors also respond to the synthetic ligands, so any mouse in which this is attempted would have to be done on a native receptor knockout to achieve interpretable results. A completely artificial RASSL-ligand system is desired.

Using a similar strategy, Lechner and colleagues exploited the *Drosophila* allatostatin GPCR (Lechner et al., 2002) (Figure 1-2). The receptor is unresponsive to mammalian peptide ligands such as somatostatin, galanin, or enkephalins, and the *Drosophila* allatostatin peptide does not activate any known mammalian receptors. The receptor opens GIRK channels via coupling to  $G_{i/o}$ . Neonatal ferret neocortex slices were cotransfected with plasmids encoding the *Drosophila* allatostatin receptor and mammalian GIRK channel subunits 1 and 2. Adding allatostatin peptide produced hyperpolarization within minutes that reversed upon removal of the peptide. The hyperpolarization combined with the additional resting conductance markedly increased the current required to elicit action potentials. When used in a cell-specific expression system, this method offers significant promise. However, any target neuron must have sufficient GIRK channels either naturally or transgenically expressed, and because allatostatin is a peptide it will not cross the blood brain barrier and must be directly infused into the target brain region. The requirement to express GIRK channels may have non-specific effects.

### **Channel-specific toxins**

A variety of ion channel types are blocked by channel-specific toxins. Ibanez-Tallon and colleagues expressed peptide toxins selective for specific ion channels on the neuronal

## FIGURE 1-2

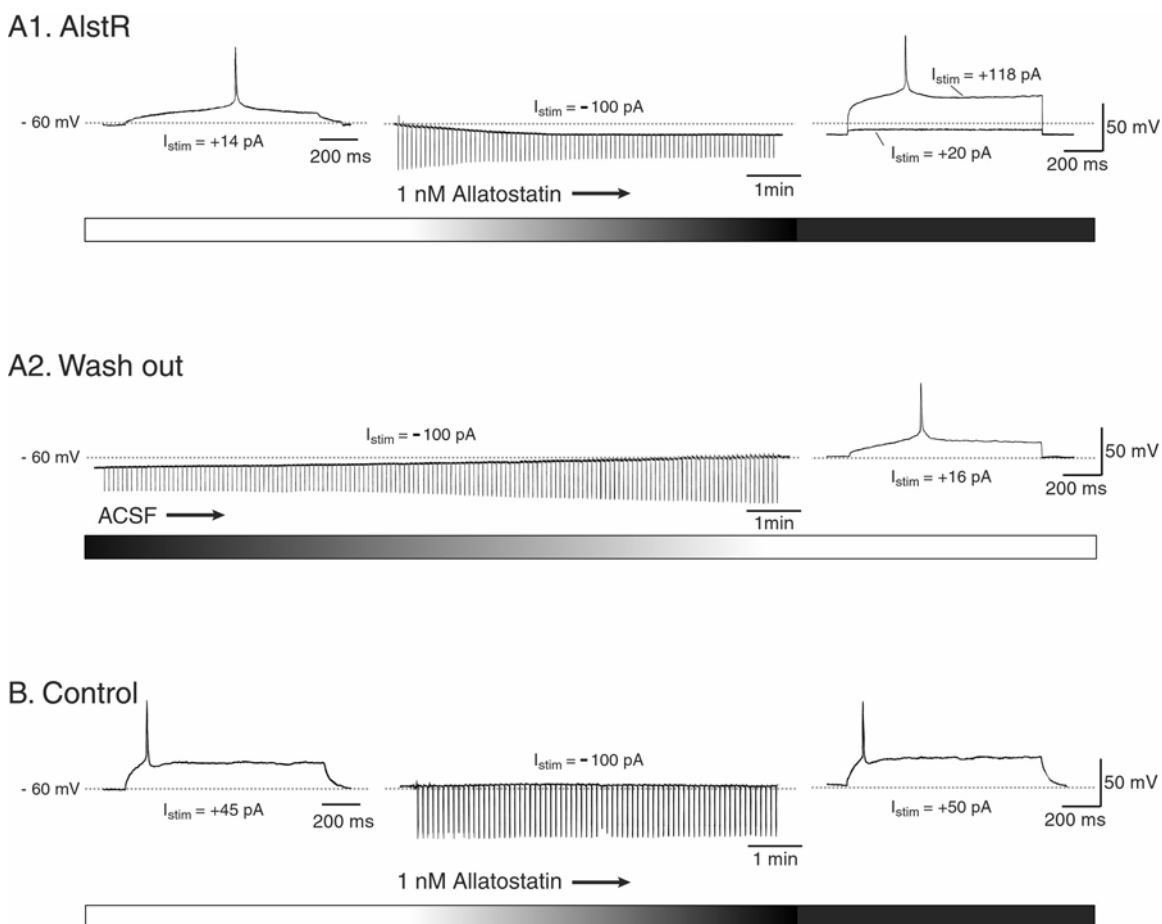


Figure 1-2: **Silencing of cortical neurons with the AlstR/AL receptor/ligand system.** *A1*, The spike threshold of a representative AlstR-transfected neuron was determined by a series of depolarizing current pulses ( $I_{stim}$ , 1 sec duration; *left panel*) before addition of allatostatin to the bath (*gradually shaded bar*). In this example, the spike threshold was found to be at +14 pA. Before and after the onset of perfusion with 1 nM AL, input resistance was monitored by hyperpolarizing current pulses at 5 sec intervals (*middle panel*). Input resistance and resting membrane potential decreased within minutes of AL application. The amount of current necessary to elicit an action potential in the presence of AL (+118 pA) was greatly increased with respect to the initial values (*right panel*). *A2*, The effects of AL were reversible over the course of several minutes by washing out AL with normal ACSF. Input resistance, membrane potential (*left panel*), and spike threshold (*right panel*) returned to approximately initial values after a perfusion time approximately equivalent to the time required for the exchange of one bath volume (see Results). *B*, Input resistance, membrane potential, and spike threshold of control neurons were unaffected by application of AL. All panels reproduced from Lechner et al, 2002 © (2002) The Society for Neuroscience.

surface by fusing them to a glycosylphosphatidylinositol anchor and linker (Ibanez-Tallon et al., 2004). Several toxin-receptor pairs are considered, including  $\alpha$ -bungrotoxin and nicotinic receptors,  $\mu$ O-conotoxin and Na<sup>+</sup> channels, and  $\omega$ -conotoxin and Ca<sup>+</sup> channels. In cells expressing the receptor associated with the toxin, the toxin binds and blocks the receptor. This technique is unique in that it targets input from specific receptors in a neuron, rather than targeting the excitability of the neuron itself. The blockage is not inducible other than with transcriptional control; however, it may be possible to cage the membrane-tethered toxin so that it could be stimulus-activated.

### **Selective, reversible, and rapid *excitation* of neurons**

While the above techniques have been developed to suppress neuronal activity, Zemelman and colleagues have developed a cell specific excitation approach. In the *Drosophila* retina, light causes depolarization rather than the hyperpolarization found in vertebrates. When the *Drosophila* phototransduction cascade (arrestin, rhodopsin and G<sub>q $\alpha$</sub> , together termed chARGe) is expressed in cultured hippocampal neurons, light triggers an excitatory response (Zemelman et al., 2002). The rhodopsin receptor couples to endogenous non-selective cation channels of the transient receptor family (TRP) through G<sub>q $\alpha$</sub> . Arrestin is necessary to inactivate and recycle the rhodopsin. Upon opening, the TRP channels depolarize the cell. Hippocampal neurons transfected with the chARGe phototransduction components showed no change in electrical properties while in the dark. Illumination of the cultures elicited action potential trains, provided that the chromophore retinal was supplemented (to generate rhodopsin from opsin). However, there was poor temporal coupling between stimulus and response; neurons continued firing for minutes after light removal. Expressing the three charge components in a targeted neuron *in vivo* could be demanding.

Another approach uses the vanilloid receptor TRPV1, which is gated by capsaicin or the receptor TRPM8 which is gated by methanol (Zemelman et al., 2003). Both receptors are homotetrameric non-selective cation channels. In mammals, these receptors are expressed in peripheral neurons but not in the CNS. Cultured hippocampal neurons transfected with either TRP receptor were slightly depolarized even with no ligand, suggesting a small leak

conductance through the channel. Strong spiking in neurons expressing the cognate receptors was evoked upon the addition of ligand (Figure 1-3). Photorelease of caged capsaicin increased the temporal and spatial precision: a 1 s UV-light pulse evoked an action potential volley within seconds. Repeated photostimulation gave reproducible responses without attenuation. The choice of activation trigger, light or ligand, gives flexibility. Delivery of the required ligands *in vivo* at sufficient concentrations will be challenging.

### **Gene delivery with viruses**

Clearly, all the techniques discussed above rely on the ability to selectively express one or more genes in a target set of neurons. The experimental goals set constraints on the ideal vector for transgene delivery. The target cells must first be susceptible to the vector under consideration with appropriate efficacy. Once the genetic material is inside, the cell must have the ability to express the transgene. Unfortunately, virologists have not been able to identify a “universal vector” that is capable of infecting any cell type at high efficiency (Callaway, 2005). Many different vectors have been used throughout the literature, including adeno-associated virus (AAV) (Davidson et al., 2000; Kaspar et al., 2002; Rabinowitz et al., 2002; Rabinowitz et al., 2004), lentiviruses (Naldini et al., 1996; Blomer et al., 1997), Sindbis viruses (Gwag et al., 1998), and herpes simplex virus (HSV) (Sandler et al., 2002). All of these vectors can deliver DNA (or RNA) efficiently to non-dividing adult neurons within 0.5-1.0 mm of an injection site. The vectors are replication incompetent and hence there is no further spread or toxicity. However, each of these viruses also has tropism for different neuronal subtypes, and the experimenter must first empirically determine if the target cell of interest is susceptible to infection by a given vector. The inherent tropism of these vectors may at first seem like a severe limitation. However, clever experimenters used it to advantage: it becomes part of the targeting scheme (Watson et al., 2002). Viruses were also engineered to have tropism for a particular cell type or to expand the range cell types that can be infected (Bartlett et al., 1999; Grandi et al., 2004).

## FIGURE 1-3

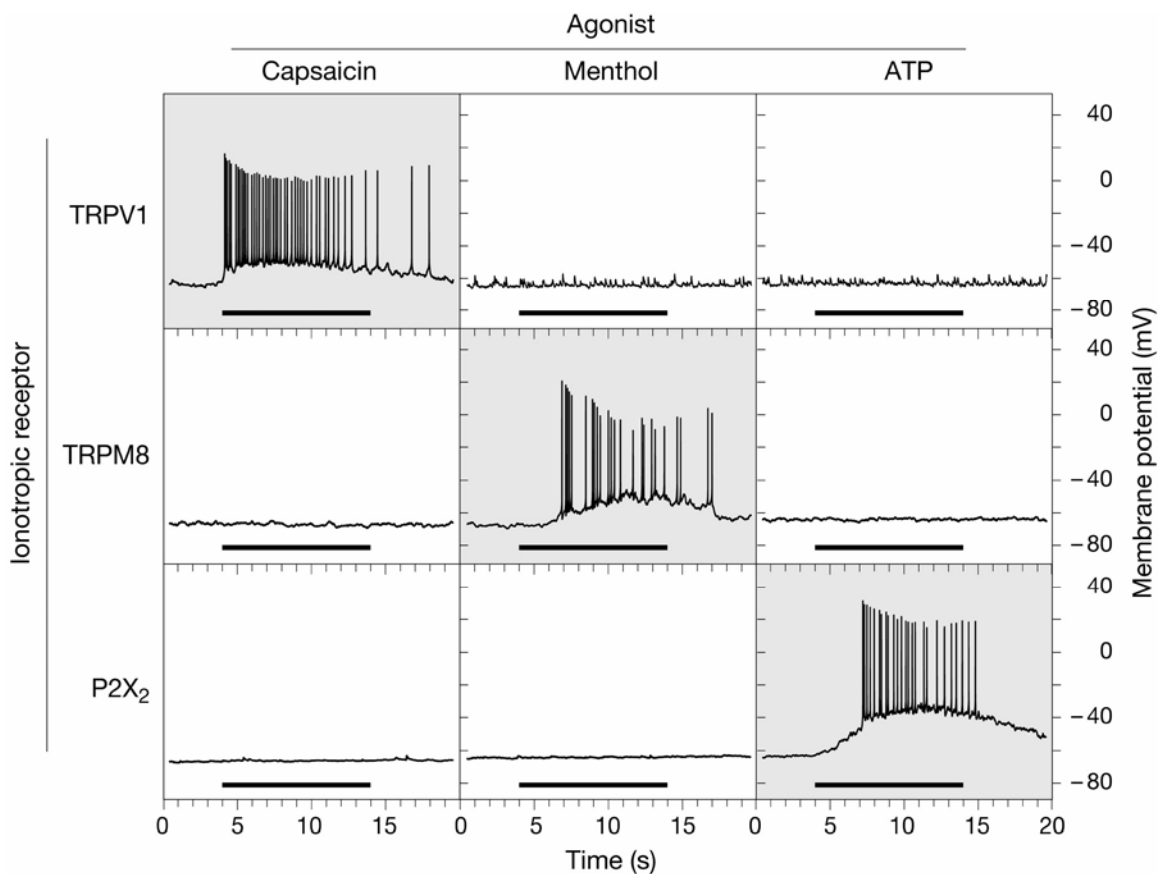


Figure 1-3: **Pharmacological stimulation of genetically designated target neurons.** The membrane potentials of hippocampal neurons expressing TRPV1 (*Top*), TRPM8 (*Middle*), and P2X<sub>2</sub> (*Bottom*) were recorded in whole-cell current-clamp mode. All neurons were challenged sequentially with 50 nM capsaicin (*Left*), 100  $\mu$ M menthol (*Center*), and 50  $\mu$ M ATP (*Right*); approximate periods of agonist application are indicated by horizontal bars. Only cognate matches between ionotropic receptor and agonist (shaded entries in the diagonal) elicit action potentials. Increased baseline noise of the TRPV1-expressing neuron after the application of capsaicin (*Top*, *Center* and *Right*) is caused by residual capsaicin in the perfusion system. Reproduced from Zemelman et al, 2003 © (2003) National Academy of Scientists.

Capacity is the major limitation of viral vectors. Often, cell-type-specific promoters are too large to fit within the viral genome. AAV and lentivirus can package genetic sequences up to ~5 kb and ~8kb, respectively (Samulski, 2000; Kafri, 2001), whereas the 152 Kb genome of HSV could potentially accept much larger genetic sequences. High-titer HSV amplicons incorporating bacterial artificial chromosomes (BACs) ~130 Kb in size have been reported (Wade-Martins et al., 2003; Xing et al., 2004). Cell-type-specificity is likely to be enhanced by further developments in these types of vectors.

### **Transgenic approaches to gene targeting**

By far the most common approach to achieve cell-type-specific targeting is to use a cell-type-specific promoter. For example, Purkinje cell protein 2 (Pcp2, also known as L7) is restricted to cerebellar Purkinje cells and retinal bipolar cells (Oberdick et al., 1990). The 2.9 Kb DNA sequence upstream from this gene was used to drive expression in these cell types (Zhang et al., 2001). Many other examples of cell-type-specific promoters are useful in generating mouse lines with targeting expression, but there are also many unsuccessful attempts. Generally, the probability of success and degree of specificity are greatly increased as longer stretches of DNA sequence are used, presumably because larger portions of the proper regulatory sequences are included. BAC transgenics, which can use more than 200 Kb of DNA, have been very successful (Heintz, 2001). The challenge arises because the mechanisms and sequences that regulate gene expression are poorly understood.

In addition to traditional transgenics and BAC transgenics, knock-in strategies allow for the expression of exogenous genetic sequences in specific cell-types, without the need to identify specific promoter elements. For example, given a silencing gene under consideration, one could knock that gene directly into the locus of another gene that is expressed exclusively in the target neurons, either by knocking out the target gene (and thereby using heterozygous animals) (Tamamaki et al., 2003) or by knocking in an internal ribosome entry site (IRES)-silencing gene cassette into the 3' untranslated region of the target gene (Lindeberg et al., 2004). In a more sophisticated approach, Yu and colleagues knocked in an IRES-tetracycline transcriptional activator cassette in the 3' untranslated

region of the OMP gene, and then crossed this mouse with a transgenic carrying a tetracycline response element (TRE)-silencing gene cassette (Yu et al., 2004). This work demonstrated the utility of combining traditional transgenics with knockins.

The use of cell-type-specific promoters with viral vectors is important, because it may not be desirable to modulate all neurons in a given geometric area (i.e., at the injection site). Instead, a given experiment is more likely to require affecting only a given cell type in that area. Hence, the vector must contain a cell-type-specific promoter to restrict the expression. From above, the major limitation on viral vectors is their cloning capacity. Hence, a considerable amount of trial-and-error work must be done to attempt to identify the minimum sequence required to achieve cell-type-specificity. Often, no such minimum sequence can be identified because there is no definitive method for localizing regulatory sequences, although this has been tried (Wasserman and Sandelin, 2004).

Neurons can differ not only in the genes they express, but also in the distant structures to which they project their efferent axons. It is possible to pseudotype a lentivirus with the envelope protein from rabies virus, enabling it to infect neurons efficiently through their axon terminals (Mazarakis et al., 2001; Wong et al., 2004). HSV infects neurons through their axon terminals (Sandler et al., 2002). Specific neurons can thus be targeted based upon their distant axonal projections.

### **Directions for the future**

Unique subsets of neurons are defined by their location, their morphology, their specific molecular components, or a combination of all three elements. Since the time of Cajal, brain anatomists have made great strides classifying cells via the first two elements. As the approximately 15,000 genes expressed in the mammalian brain are characterized and mapped, neurons are likely to be increasingly identified by the genes they express. Researchers in brain genomics have been surprised at the wide expression of several genes studied to date, but there are many genes left to explore. Tools that molecular biology can provide to help tease apart the function of these neuronal subsets and their roles in the local circuit and ultimately the organism's behavior will be valuable.

Researchers have developed predictive descriptions of circuits through modeling efforts, especially for highly stereotypic structures like the cerebellum and hippocampus (Medina and Mauk, 2000; Whittington and Traub, 2003). The actual consequences of manipulating the activity of a particular cell need to be tested in comparison to the model prediction. Giving a drug to an animal so that particular neuronal types in these circuits could be temporarily silenced or excited would be an incisive methodological advance (Wulff and Wisden, 2005). The field needs a spectrum of methods that can be tailored to particular applications, as each method is likely to have strengths and weaknesses. Using genes from invertebrate biology is promising, as often these animals employ transmitters not used in vertebrate brains, allowing direct transplantation of signaling systems (Miesenbock, 2004). Transgenic techniques as well as viral expression techniques will be vital for neuronal modulation in mice and other animals (Callaway, 2005). Bacterial artificial chromosomes (BACs) will allow the production of transgenic mice with a higher likelihood of resulting in a desired, consistent pattern of gene expression (Gong et al., 2003). Surprisingly, despite years of effort by several researchers, there has been only one “silencing” mouse that has linked changes in the excitability properties of target neurons to behavior of the animal (Yamamoto et al., 2003). The field is still open for unique approaches to selectively and reversibly inhibit or stimulate specific neuronal types in vertebrate systems.

## References

- Allen MJ, Shan X, Caruccio P, Froggett SJ, Moffat KG, Murphey RK (1999) Targeted expression of truncated *glued* disrupts giant fiber synapse formation in *Drosophila*. *J Neurosci* 19:9374-9384.
- Bahn S, Jones A, Wisden W (1997) Directing gene expression to cerebellar granule cells using gamma-aminobutyric acid type A receptor  $\alpha 6$  subunit transgenes. *Proc Natl Acad Sci U S A* 94:9417-9421.
- Baines RA, Uhler JP, Thompson A, Sweeney ST, Bate M (2001) Altered electrical properties in *Drosophila* neurons developing without synaptic transmission. *J Neurosci* 21:1523-1531.
- Bartlett JS, Kleinschmidt J, Boucher RC, Samulski RJ (1999) Targeted adeno-associated virus vector transduction of nonpermissive cells mediated by a bispecific F(ab' $\gamma$ )<sub>2</sub> antibody. *Nat Biotechnol* 17:181-186.

- Blanchardon E, Grima B, Klarsfeld A, Chelot E, Hardin PE, Preat T, Rouyer F (2001) Defining the role of *Drosophila* lateral neurons in the control of circadian rhythms in motor activity and eclosion by targeted genetic ablation and PERIOD protein overexpression. *Eur J Neurosci* 13:871-888.
- Blomer U, Naldini L, Kafri T, Trono D, Verma IM, Gage FH (1997) Highly efficient and sustained gene transfer in adult neurons with a lentivirus vector. *J Virol* 71:6641-6649.
- Bond CT, Sprengel R, Bissonnette JM, Kaufmann WA, Pribnow D, Neelands T, Storck T, Baetscher M, Jerecic J, Maylie J, Knaus HG, Seeburg PH, Adelman JP (2000) Respiration and parturition affected by conditional overexpression of the Ca<sup>2+</sup>-activated K<sup>+</sup> channel subunit, SK3. *Science* 289:1942-1946.
- Callaway EM (2005) A molecular and genetic arsenal for systems neuroscience. *Trends Neurosci* 28:196-201.
- Cheng Q, Kulli JC, Yang J (2001) Suppression of neuronal hyperexcitability and associated delayed neuronal death by adenoviral expression of GABA(C) receptors. *J Neurosci* 21:3419-3428.
- Claeyssen S, Joubert L, Sebben M, Bockaert J, Dumuis A (2003) A single mutation in the 5-HT<sub>4</sub> receptor (5-HT<sub>4</sub>-R D100(3.32)A) generates a Gs-coupled receptor activated exclusively by synthetic ligands (RASSL). *J Biol Chem* 278:699-702.
- Coward P, Wada HG, Falk MS, Chan SD, Meng F, Akil H, Conklin BR (1998) Controlling signaling with a specifically designed Gi-coupled receptor. *Proc Natl Acad Sci U S A* 95:352-357.
- Crick F (1988) *What Mad Pursuit: a Personal View of Scientific Discovery*. London: Penguin Books.
- Damasio A (2000) *The Feeling of What Happens*: Random House.
- Davidson BL, Stein CS, Heth JA, Martins I, Kotin RM, Derksen TA, Zabner J, Ghodsi A, Chiorini JA (2000) Recombinant adeno-associated virus type 2, 4, and 5 vectors: transduction of variant cell types and regions in the mammalian central nervous system. *Proc Natl Acad Sci U S A* 97:3428-3432.
- Dubnau J, Grady L, Kitamoto T, Tully T (2001a) Disruption of neurotransmission in *Drosophila* mushroom body blocks retrieval but not acquisition of memory. *Nature* 411:476-480.
- Dubnau J, Grady L, Kitamoto T, Tully T (2001b) Disruption of neurotransmission in *Drosophila* mushroom body blocks retrieval but not acquisition of memory. *Nature* 411:476-480.
- Ehrengruber ME, Doupnik CA, Xu Y, Garvey J, Jasek MC, Lester HA, Davidson N (1997) Activation of heteromeric G protein-gated inward rectifier K<sup>+</sup> channels over-expressed

- by adenovirus gene transfer inhibits the excitability of hippocampal neurons. *Proc Natl Acad Sci USA* 94:7070-7075.
- Falk T, Kilani RK, Yool AJ, Sherman SJ (2001) Viral vector-mediated expression of K<sup>+</sup> channels regulates electrical excitability in skeletal muscle. *Gene Ther* 8:1372-1379.
- Gong S, Zheng C, Doughty ML, Losos K, Didkovsky N, Schambra UB, Nowak NJ, Joyner A, Leblanc G, Hatten ME, Heintz N (2003) A gene expression atlas of the central nervous system based on bacterial artificial chromosomes. *Nature* 425:917-925.
- Goodale M, Milner D (2003) *Sight Unseen: an Exploration of Conscious and Unconscious Vision*: Oxford University Press.
- Grandi P, Wang S, Schuback D, Krasnykh V, Spear M, Curiel DT, Manservigi R, Breakefield XO (2004) HSV-1 virions engineered for specific binding to cell surface receptors. *Mol Ther* 9:419-427.
- Greenspan RJ (2001) The flexible genome. *Nat Rev Genet* 2:383-387.
- Greenspan RJ (2004) Systems neurobiology without backbones. *Curr Biol* 14:R177-179.
- Gwag BJ, Kim EY, Ryu BR, Won SJ, Ko HW, Oh YJ, Cho YG, Ha SJ, Sung YC (1998) A neuron-specific gene transfer by a recombinant defective Sindbis virus. *Brain Res Mol Brain Res* 63:53-61.
- Hardie RC, Raghu P, Moore S, Juusola M, Baines RA, Sweeney ST (2001) Calcium influx via TRP channels is required to maintain PIP<sub>2</sub> levels in *Drosophila* photoreceptors. *Neuron* 30:149-159.
- Heintz N (2001) BAC to the future: the use of bac transgenic mice for neuroscience research. *Nat Rev Neurosci* 2:861-870.
- Heron-Milhavet L, Xue-Jun Y, Vannucci SJ, Wood TL, Willing LB, Stannard B, Hernandez-Sanchez C, Mobbs C, Virsolvy A, LeRoith D (2004) Protection against hypoxic-ischemic injury in transgenic mice overexpressing Kir6.2 channel pore in forebrain. *Mol Cell Neurosci* 25:585-593.
- Hiesinger PR, Reiter C, Schau H, Fischbach KF (1999) Neuropil pattern formation and regulation of cell adhesion molecules in *Drosophila* optic lobe development depend on synaptobrevin. *J Neurosci* 19:7548-7556.
- Hirano T, Watanabe D, Kawaguchi SY, Pastan I, Nakanishi S (2002) Roles of inhibitory interneurons in the cerebellar cortex. *Ann N Y Acad Sci* 978:405-412.
- Hoppe UC, Marban E, Johns DC (2001) Distinct gene-specific mechanisms of arrhythmia revealed by cardiac gene transfer of two long QT disease genes, HERG and KCNE1. *Proc Natl Acad Sci U S A* 98:5335-5340.

- Hupe JM, Chouvet G, Bullier J (1999) Spatial and temporal parameters of cortical inactivation by GABA. *J Neurosci Methods* 86:129-143.
- Ibanez-Tallon I, Wen H, Miwa JM, Xing J, Tekinay AB, Ono F, Brehm P, Heintz N (2004) Tethering naturally occurring peptide toxins for cell-autonomous modulation of ion channels and receptors in vivo. *Neuron* 43:305-311.
- Izquierdo I, Medina JH (1998) On brain lesions, the milkman and Sigmunda. *Trends Neurosci* 21:423-426.
- Johns DC, Marx R, Mains RE, O'Rourke B, Marban E (1999) Inducible genetic suppression of neuronal excitability. *J Neurosci* 19:1691-1697.
- Johns DC, Nuss HB, Chiamvimonvat N, Ramza BM, Marban E, Lawrence JH (1995) Adenovirus-mediated expression of a voltage-gated potassium channel in vitro (rat cardiac myocytes) and in vivo (rat liver). A novel strategy for modifying excitability. *J Clin Invest* 96:1152-1158.
- Jones SM, Ribera AB (1994) Overexpression of a potassium channel gene perturbs neural differentiation. *J Neurosci* 14:2789-2799.
- Kaang BK, Pfaffinger PJ, Grant SG, Kandel ER, Furukawa Y (1992) Overexpression of an *Aplysia* shaker K<sup>+</sup> channel gene modifies the electrical properties and synaptic efficacy of identified *Aplysia* neurons. *Proc Natl Acad Sci U S A* 89:1133-1137.
- Kafri T (2001) Lentivirus vectors: difficulties and hopes before clinical trials. *Curr Opin Mol Ther* 3:316-326.
- Kaneko M, Park JH, Cheng Y, Hardin PE, Hall JC (2000) Disruption of synaptic transmission or clock-gene-product oscillations in circadian pacemaker cells of *Drosophila* cause abnormal behavioral rhythms. *J Neurobiol* 43:207-233.
- Kaspar BK, Vissel B, Bengoechea T, Crone S, Randolph-Moore L, Muller R, Brandon EP, Schaffer D, Verma IM, Lee KF, Heinemann SF, Gage FH (2002) Adeno-associated virus effectively mediates conditional gene modification in the brain. *Proc Natl Acad Sci U S A* 99:2320-2325.
- Keller A, Sweeney ST, Zars T, O'Kane CJ, Heisenberg M (2002) Targeted expression of tetanus neurotoxin interferes with behavioral responses to sensory input in *Drosophila*. *J Neurobiol* 50:221-233.
- Kitamoto T (2001) Conditional modification of behavior in *Drosophila* by targeted expression of a temperature-sensitive shibire allele in defined neurons. *J Neurobiol* 47:81-92.
- Kitamoto T (2002) Conditional disruption of synaptic transmission induces male-male courtship behavior in *Drosophila*. *Proc Natl Acad Sci U S A* 99:13232-13237.

- Kobayashi K, Morita S, Sawada H, Mizuguchi T, Yamada K, Nagatsu I, Fujita K, Kreitman RJ, Pastan I, Nagatsu T (1995) Immunotoxin-mediated conditional disruption of specific neurons in transgenic mice. *Proc Natl Acad Sci U S A* 92:1132-1136.
- Lechner HA, Lein ES, Callaway EM (2002) A genetic method for selective and quickly reversible silencing of mammalian neurons. *J Neurosci* 22:5287-5290.
- Lindeberg J, Usoskin D, Bengtsson H, Gustafsson A, Kylberg A, Soderstrom S, Ebendal T (2004) Transgenic expression of Cre recombinase from the tyrosine hydroxylase locus. *Genesis* 40:67-73.
- Marek KW, Davis GW (2002) Transgenically encoded protein photoinactivation (FlAsH-FALI): acute inactivation of synaptotagmin I. *Neuron* 36:805-813.
- Martin JR, Ernst R, Heisenberg M (1998) Mushroom bodies suppress locomotor activity in *Drosophila melanogaster*. *Learn Mem* 5:179-191.
- Martin JR, Keller A, Sweeney ST (2002) Targeted expression of tetanus toxin: a new tool to study the neurobiology of behavior. *Adv Genet* 47:1-47.
- Mazarakis ND, Azzouz M, Rohll JB, Ellard FM, Wilkes FJ, Olsen AL, Carter EE, Barber RD, Baban DF, Kingsman SM, Kingsman AJ, O'Malley K, Mitrophanous KA (2001) Rabies virus glycoprotein pseudotyping of lentiviral vectors enables retrograde axonal transport and access to the nervous system after peripheral delivery. *Hum Mol Genet* 10:2109-2121.
- McGuire SE, Le PT, Davis RL (2001) The role of *Drosophila* mushroom body signaling in olfactory memory. *Science* 293:1330-1333.
- Medina JF, Mauk MD (2000) Computer simulation of cerebellar information processing. *Nat Neurosci* 3 Suppl:1205-1211.
- Miesenbock G (2004) Genetic methods for illuminating the function of neural circuits. *Curr Opin Neurobiol* 14:395-402.
- Mochida S, Poulain B, Eisel U, Binz T, Kurazono H, Niemann H, Tauc L (1990) Exogenous mRNA encoding tetanus or botulinum neurotoxins expressed in *Aplysia* neurons. *Proc Natl Acad Sci U S A* 87:7844-7848.
- Morris GM (1999) Topographical knowledge survives hippocampal damage. *Curr Biol* 9:R890-892.
- Nadeau H, McKinney S, Anderson DJ, Lester HA (2000) ROMK1 (Kir1.1) causes apoptosis and chronic silencing of hippocampal neurons. *J Neurophysiol* 84:1062-1075.
- Naldini L, Blomer U, Gage FH, Trono D, Verma IM (1996) Efficient transfer, integration, and sustained long-term expression of the transgene in adult rat brains injected with a lentiviral vector. *Proc Natl Acad Sci U S A* 93:11382-11388.

- Nitabach MN, Blau J, Holmes TC (2002) Electrical silencing of *Drosophila* pacemaker neurons stops the free-running circadian clock. *Cell* 109:485-495.
- Oberdick J, Smeyne RJ, Mann JR, Zackson S, Morgan JI (1990) A promoter that drives transgene expression in cerebellar Purkinje and retinal bipolar neurons. *Science* 248:223-226.
- Paradis S, Sweeney ST, Davis GW (2001) Homeostatic control of presynaptic release is triggered by postsynaptic membrane depolarization. *Neuron* 30:737-749.
- Peckol EL, Zallen JA, Yarrow JC, Bargmann CI (1999) Sensory activity affects sensory axon development in *C. elegans*. *Development* 126:1891-1902.
- Rabinowitz JE, Bowles DE, Faust SM, Ledford JG, Cunningham SE, Samulski RJ (2004) Cross-dressing the virion: the transcapsidation of adeno-associated virus serotypes functionally defines subgroups. *J Virol* 78:4421-4432.
- Rabinowitz JE, Rolling F, Li C, Conrath H, Xiao W, Xiao X, Samulski RJ (2002) Cross-packaging of a single adeno-associated virus (AAV) type 2 vector genome into multiple AAV serotypes enables transduction with broad specificity. *J Virol* 76:791-801.
- Redfern CH, Coward P, Degtyarev MY, Lee EK, Kwa AT, Hennighausen L, Bujard H, Fishman GI, Conklin BR (1999) Conditional expression and signaling of a specifically designed Gi-coupled receptor in transgenic mice. *Nat Biotechnol* 17:165-169.
- Riedel G, Micheau J, Lam AG, Roloff EL, Martin SJ, Bridge H, de Hoz L, Poeschel B, McCulloch J, Morris RG (1999) Reversible neural inactivation reveals hippocampal participation in several memory processes. *Nat Neurosci* 2:898-905.
- Samulski RJ (2000) Expanding the AAV package. *Nat Biotechnol* 18:497-498.
- Sandler VM, Wang S, Angelo K, Lo HG, Breakefield XO, Clapham DE (2002) Modified herpes simplex virus delivery of enhanced GFP into the central nervous system. *J Neurosci Methods* 121:211-219.
- Sato M, Tanigawa M (2005) Production of CETD transgenic mouse line allowing ablation of any type of specific cell population. *Mol Reprod Dev* 72:54-67.
- Scearce-Levie K, Coward P, Redfern CH, Conklin BR (2001) Engineering receptors activated solely by synthetic ligands (RASSLs). *Trends Pharmacol Sci* 22:414-420.
- Slimko E, McKinney S, Anderson D, Davidson N, Lester HA (2002) Selective electrical silencing of mammalian neurons in vitro using invertebrate ligand-gated chloride channels. *J Neurosci* (in press).
- Steele PM, Medina JF, Nores WL, Mauk MD (1998) Using genetic mutations to study the neural basis of behavior. *Cell* 95:879-882.

- Sutherland ML, Williams SH, Abedi R, Overbeek PA, Pfaffinger PJ, Noebels JL (1999) Overexpression of a Shaker-type potassium channel in mammalian central nervous system dysregulates native potassium channel gene expression. *Proc Natl Acad Sci U S A* 96:2451-2455.
- Sweeney ST, Broadie K, Keane J, Niemann H, O'Kane CJ (1995) Targeted expression of tetanus toxin light chain in *Drosophila* specifically eliminates synaptic transmission and causes behavioral defects. *Neuron* 14:341-351.
- Tamamaki N, Yanagawa Y, Tomioka R, Miyazaki J, Obata K, Kaneko T (2003) Green fluorescent protein expression and colocalization with calretinin, parvalbumin, and somatostatin in the GAD67-GFP knock-in mouse. *J Comp Neurol* 467:60-79.
- Waddell S, Armstrong JD, Kitamoto T, Kaiser K, Quinn WG (2000) The amnesiac gene product is expressed in two neurons in the *Drosophila* brain that are critical for memory. *Cell* 103:805-813.
- Wade-Martins R, Saeki Y, Chiocca EA (2003) Infectious delivery of a 135-kb LDLR genomic locus leads to regulated complementation of low-density lipoprotein receptor deficiency in human cells. *Mol Ther* 7:604-612.
- Wasserman WW, Sandelin A (2004) Applied bioinformatics for the identification of regulatory elements. *Nat Rev Genet* 5:276-287.
- Watanabe D, Inokawa H, Hashimoto K, Suzuki N, Kano M, Shigemoto R, Hirano T, Toyama K, Kaneko S, Yokoi M, Moriyoshi K, Suzuki M, Kobayashi K, Nagatsu T, Kreitman RJ, Pastan I, Nakanishi S (1998) Ablation of cerebellar Golgi cells disrupts synaptic integration involving GABA inhibition and NMDA receptor activation in motor coordination. *Cell* 95:17-27.
- Watson DJ, Kobinger GP, Passini MA, Wilson JM, Wolfe JH (2002) Targeted transduction patterns in the mouse brain by lentivirus vectors pseudotyped with VSV, Ebola, Mokola, LCMV, or MuLV envelope proteins. *Mol Ther* 5:528-537.
- White B, Osterwalder T, Keshishian H (2001a) Molecular genetic approaches to the targeted suppression of neuronal activity. *Curr Biol* 11:R1041-1053.
- White BH, Osterwalder TP, Yoon KS, Joiner WJ, Whim MD, Kaczmarek LK, Keshishian H (2001b) Targeted attenuation of electrical activity in *Drosophila* using a genetically modified K(+) channel. *Neuron* 31:699-711.
- Whittington MA, Traub RD (2003) Interneuron diversity series: inhibitory interneurons and network oscillations in vitro. *Trends Neurosci* 26:676-682.
- Wong LF, Azzouz M, Walmsley LE, Askham Z, Wilkes FJ, Mitrophanous KA, Kingsman SM, Mazarakis ND (2004) Transduction patterns of pseudotyped lentiviral vectors in the nervous system. *Mol Ther* 9:101-111.

- Wu MN, Littleton JT, Bhat MA, Prokop A, Bellen HJ (1998) ROP, the *Drosophila* Sec1 homolog, interacts with syntaxin and regulates neurotransmitter release in a dosage-dependent manner. *Embo J* 17:127-139.
- Wulff P, Wisden W (2005) Dissecting neural circuitry by combining genetics and pharmacology. *Trends Neurosci* 28:44-50.
- Xing W, Baylink D, Kesavan C, Mohan S (2004) HSV-1 amplicon-mediated transfer of 128-kb BMP-2 genomic locus stimulates osteoblast differentiation in vitro. *Biochem Biophys Res Commun* 319:781-786.
- Yamamoto M, Wada N, Kitabatake Y, Watanabe D, Anzai M, Yokoyama M, Teranishi Y, Nakanishi S (2003) Reversible suppression of glutamatergic neurotransmission of cerebellar granule cells in vivo by genetically manipulated expression of tetanus neurotoxin light chain. *J Neurosci* 23:6759-6767.
- Yu CR, Power J, Barnea G, O'Donnell S, Brown HE, Osborne J, Axel R, Gogos JA (2004) Spontaneous neural activity is required for the establishment and maintenance of the olfactory sensory map. *Neuron* 42:553-566.
- Zagotta WN, Germeraad S, Garber SS, Hoshi T, Aldrich RW (1989) Properties of ShB A-type potassium channels expressed in Shaker mutant *Drosophila* by germline transformation. *Neuron* 3:773-782.
- Zemelman BV, Lee GA, Ng M, Miesenbock G (2002) Selective photostimulation of genetically chARGed neurons. *Neuron* 33:15-22.
- Zemelman BV, Nesnas N, Lee GA, Miesenbock G (2003) Photochemical gating of heterologous ion channels: remote control over genetically designated populations of neurons. *Proc Natl Acad Sci U S A* 100:1352-1357.
- Zhang X, Baader SL, Bian F, Muller W, Oberdick J (2001) High level Purkinje cell specific expression of green fluorescent protein in transgenic mice. *Histochem Cell Biol* 115:455-464.
- Zhao B, Rassendren F, Kaang BK, Furukawa Y, Kubo T, Kandel ER (1994) A new class of noninactivating K<sup>+</sup> channels from *Aplysia* capable of contributing to the resting potential and firing patterns of neurons. *Neuron* 13:1205-1213.
- Zhao H, Nonet ML (2000) A retrograde signal is involved in activity-dependent remodeling at a *C. elegans* neuromuscular junction. *Development* 127:1253-1266.
- Zhao ML, Sable EO, Iverson LE, Wu CF (1995) Functional expression of Shaker K<sup>+</sup> channels in cultured *Drosophila* "giant" neurons derived from Sh cDNA transformants: distinct properties, distribution, and turnover. *J Neurosci* 15:1406-1418.

*Chapter 2***Selective electrical silencing of mammalian neurons *in vitro* using invertebrate ligand-gated chloride channels**

Text of this chapter is reproduced, with minor editing, from:

Slimko EM, McKinney S, Anderson DJ, Davidson N, Lester HA. (2002) Selective electrical silencing of mammalian neurons *in vitro* using invertebrate ligand-gated chloride channels. *J. Neurosci* 22(17):7373-7379

## Abstract

Selectively reducing the excitability of specific neurons will (1) allow for the creation of animal models of human neurological disorders and (2) provide insight into the global function of specific sets of neurons. We focus on a combined genetic and pharmacological approach to silence neurons electrically. We express invertebrate ivermectin (IVM)-sensitive chloride channels (*C. elegans* GluCl  $\alpha$  and  $\beta$ ) with a Sindbis virus, then activate these channels with IVM to produce inhibition via a  $\text{Cl}^-$  conductance. We constructed a three-cistron Sindbis virus that expresses the  $\alpha$  and  $\beta$  subunits of GluCl along with the green fluorescent protein (EGFP) marker. Expression of the *C. elegans* channel does not affect the normal spike activity or GABA/glutamate postsynaptic currents of cultured E18 hippocampal neurons. At concentrations as low as 5 nM, IVM activates a  $\text{Cl}^-$  current large enough to effectively silence infected neurons. This conductance reverses in eight hours. These low concentrations of IVM do not potentiate GABA responses. Comparable results are observed with plasmid transfection of yellow fluorescent protein (EYFP) tagged GluCl  $\alpha$  and cyan fluorescent protein (ECFP) tagged GluCl  $\beta$ . The present study provides an *in vitro* model mimicking conditions that can be obtained in transgenic mice and in viral mediated gene therapy. These experiments demonstrate the feasibility of using invertebrate ligand-activated  $\text{Cl}^-$  channels as an approach to modulate excitability.

## Introduction

This paper focuses on an approach to understanding the role of individual neuronal cell types in development, information processing, and behavior. Several investigators have suggested that such information can be obtained by employing gene transfer *in vitro*, or transgenic animals, to produce spatially and temporally controlled inactivation of specific neurons (White et al., 2001a). Recent studies report using transcriptional induction of various K<sup>+</sup> channels (Johns et al., 1999; Falk et al., 2001), and this method silences *Drosophila* neurons or muscle *in vivo* (Paradis et al., 2001; White et al., 2001b; Nitabach et al., 2002), providing useful insights into the role of defined neuronal populations. We previously studied the possibilities for neuronal silencing using expressed GIRK channels (Ehrengruber et al., 1997), weakly inward rectifying K<sup>+</sup> channels (Nadeau et al., 2000), and neuron restrictive silencing factor (Nadeau and Lester, 2002). However, there are indications that K<sup>+</sup> channels may cause unwanted side effects, such as apoptosis due to sustained K<sup>+</sup> efflux, in the cultured mammalian CNS neurons used to test this strategy (Nadeau et al., 2000).

The emerging genetic techniques seem to present some advantages over previous exclusively pharmacological strategies. Target areas and nuclei have indeed been inactivated *in vivo* through focal application of a GABA agonist, muscimol (Jasnow and Huhman, 2001; Maren et al., 2001). This procedure has been valuable in determining the role of the amygdala and hippocampus in fear conditioning (Helmstetter and Bellgowan, 1994; Muller et al., 1997; Holt and Maren, 1999; Wilensky et al., 1999, 2000). However, the muscimol strategy suffers from limitations, such as the inability to know exactly

which neurons were silenced, the inability to silence specific cell types in a given brain region, the inability to silence distributed but functionally related neuronal populations, and the irreproducible localization of focal injections. Also, specific neuronal populations have been irreversibly ablated (Kobayashi et al., 1995; Sawada et al., 1998; Watanabe et al., 1998; Isles et al., 2001), but further insights could arise from a reversible technique.

We suggest a strategy that combines the genetic and acute pharmacological manipulations. Because GABA and glycine are the major inhibitory neurotransmitter in the brain, and because GABA<sub>A</sub> and glycine receptors inhibit activity by activating a Cl<sup>-</sup> conductance, we have explored the possibility of using ligand-activated Cl<sup>-</sup> channels as silencing genes. The GluCl family of ligand-gated Cl<sup>-</sup> channels, found in several invertebrate phyla, is the target for various pesticides, anthelmintic, and antiparasitic drugs, including ivermectin (IVM) (Cully et al., 1994). GluCl channels are part of the nicotinic receptor superfamily, characterized by four transmembrane segments and a large N-terminus, and are most similar to GABA<sub>A</sub> and glycine receptors. Glutamate is the putative *in vivo* ligand for these channels. No GluCl channels have yet been detected in mammals (Martin et al., 1998; Xue, 1998).

The GluCl channels may represent a promising set of silencing genes. We have used a recombinant Sindbis virus to express these channels in cultured neurons, then tested whether the expressed channels can be activated with high sensitivity and high selectivity by IVM. Indeed we do find that that IVM at low nM concentrations induces a large Cl<sup>-</sup> conductance in some infected neurons, effectively clamping the membrane at a potential near the original resting potential. As a result, neither current injection nor focal

application of excitatory transmitter elicits action potentials. We also studied possible unwanted additional effects of either GluCl channel expression or IVM application, and found these potential side effects to be minimal or non-existent. The inducible and reversible nature of this inactivation, which we term the GluCl / IVM method, represents a potential powerful new technique for use in probing the contributions of specific regions of the nervous system to the global function.

## Materials and Methods

*Viral Vectors and Preparation.* Wild-type *C. Elegans* GluCl  $\alpha$  and GluCl  $\beta$  genes (Cully et al., 1994) cloned into pBluescript II SK+ were a kind gift from Merck Research Laboratories (Whitehead, NJ), the Sindbis vector pSinRep5dsgEGFP was a kind gift from Drs. H. Nawa and M. Kawamura of Niigata University, Niigata, Japan. The oligos pSG1: 5'-6CG ACG TCA TCT CTA CGG TGG TCC TAA ATA GTT TAA ACG CAT G -3' and pSG2: 5'-6CG TTT AAA CTA TTT AGG ACC ACC GTA GAG ATG ACG TCG CAT G-3' were annealed and ligated into the SphI site of pSinRep5dsgEGFP, resulting in pSinRep5tsgEGFP. GluCl  $\alpha$  was then amplified by PCR with the primers 5'-ATA GAT ACG CGT TCA ATA CTG CAT AAA T-3' and 5' TAG ATT CAC GTG AAA GCA TTC TCG ATC A 3' and cloned into the MluI and AatII sites of pSinRep5tsgEGFP, resulting in pSinRep5tsgGluCl $\alpha$ EGFP. GluCl  $\beta$  was then amplified by PCR with the primers: 5' AAT GCA GCA TGC ACT ACA CCT AGT TCA T 3' and 5' ACC GGT GCA TGC TAT GAT GTT TGC AAA T 3' and cloned into the SphI site of pSinRep5tsgGluCl $\alpha$ EGFP resulting in pSinRep5tsgGluCl $\alpha$  $\beta$ EGFP (Figure 2-1). This plasmid was then used to generate recombinant Sindbis virus according to the

## FIGURE 2-1

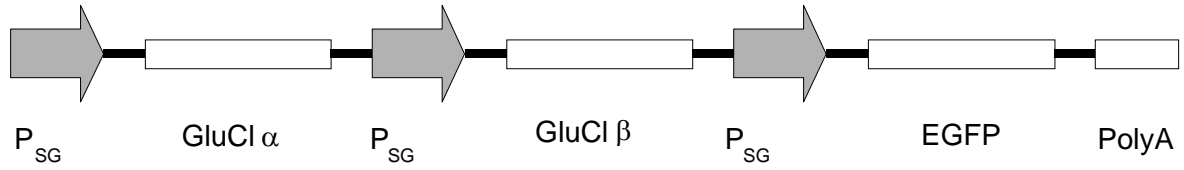


Figure 2-1: Modified pSinRep5 construct, pSinRep5tsgGluClαβEGFP, designed to express three genes with three subgenomic promoters: the GluCl α subunit, the GluCl β subunit, and the reporter EGFP. The resulting Sindbis virus is vSinGluClαβEGFP.

manufacturer's instructions. Briefly, RNA was transcribed from this plasmid and the DB-26S helper plasmid using the Invitrogen InvitroScript kit (Carlsbad, CA). These two RNA species were transfected by electroporation into baby hamster kidney cells and incubated for 48 h. The supernatant was collected and filtered at 0.2  $\mu\text{m}$ , and the viral particles (termed vSinGluCl $\alpha$  $\beta$ EGFP) were concentrated by centrifugation at 35,000 rpm for 1 h.

*Neuronal Culture.* Rat embryonic day 18 hippocampal neurons were prepared as described (Li et al., 1998). Hippocampal cultures were then infected with 1 to 5  $\mu\text{l}$  of the above virus stocks per 35 mm culture dish containing ~ 2 ml of media. Neurons were infected after 12–16 days in culture, and recordings were made 24–48 h later. For neuron transfection experiments, Lipofectamine 2000 from Invitrogen (Carlsbad, CA) was used in conjunction with Nupherin-neuron from Biomol Research Laboratories (Plymouth Meeting, PA) per manufacturer's instructions. Briefly, 5  $\mu\text{g}$  DNA of each tagged subunit was incubated with 120  $\mu\text{g}$  of Nupherin-neuron in 400  $\mu\text{l}$  of Neurobasal medium without phenol red, while 10  $\mu\text{l}$  of Lipofectamine 2000 was mixed in 400  $\mu\text{l}$  Neurobasal. After 15 min, the two solutions were combined and incubated 45 min. Neuronal cultures in 35 mm culture dishes were incubated in the resulting 800  $\mu\text{l}$  mixture for 5 min, spun in a swinging bucket centrifuge at 1000 rpm for 5 min, incubated for 4 h, and then the mixture was removed and replaced with the original 2 ml medium. Recordings were made 24–48 h later.

*Electrophysiology.* The bath solution was (in mM): 110 NaCl, 5.4 KCl, 1.8 CaCl<sub>2</sub>, 0.8 MgCl<sub>2</sub>, 10 HEPES, and 10 D-glucose, pH 7.4, osmolarity 230 mOsm. Patch pipettes were

filled with a solution containing (in mM): 100 K gluconate, 0.1 CaCl<sub>2</sub>, 1.1 EGTA, 5 MgCl<sub>2</sub>, 10 HEPES, 3 ATP, 3 phosphocreatine, and 0.3 GTP, pH 7.2, 215 mOsm. Whole-cell voltage clamp was maintained using an Axopatch-1D amplifier controlled by a personal computer running pCLAMP 8 software via a Digidata 1200 interface (Axon Instruments). Data were filtered at 2 kHz and digitized at 5 kHz. Drugs were applied focally to single voltage- and current-clamped neurons using a Picospritzer with a U-tube system providing the wash (Khakh et al., 1995).

*Statistics.* Pooled data are shown as means  $\pm$  SEM.

## Results

Initial experiments were performed on transfection of the GluCl  $\alpha$  and  $\beta$  subunits into HEK cells. Robust responses to IVM (500 nM) were detected only in cells that expressed both the  $\alpha$  and  $\beta$  subunits (Figure 2-2A and B). Unlike recordings from *Xenopus* oocytes (Cully et al., 1994), the current was transient; however, when we used successive voltage ramps to measure the conductance and reversal potential of the current, we found that the conductance remained relatively constant and the reversal potential changed after application of IVM (Figure 2-2C and D). In experiments not shown, we found that the IVM-induced conductance was stable for at least 30 min. These results encouraged us to design and construct the Sindbis virus, vSinGluCl $\alpha\beta$ EGFP, which expressed three genes: GluCl $\alpha$ , GluCl $\beta$ , and GFP as a reporter for infected cells.

FIGURE 2-2

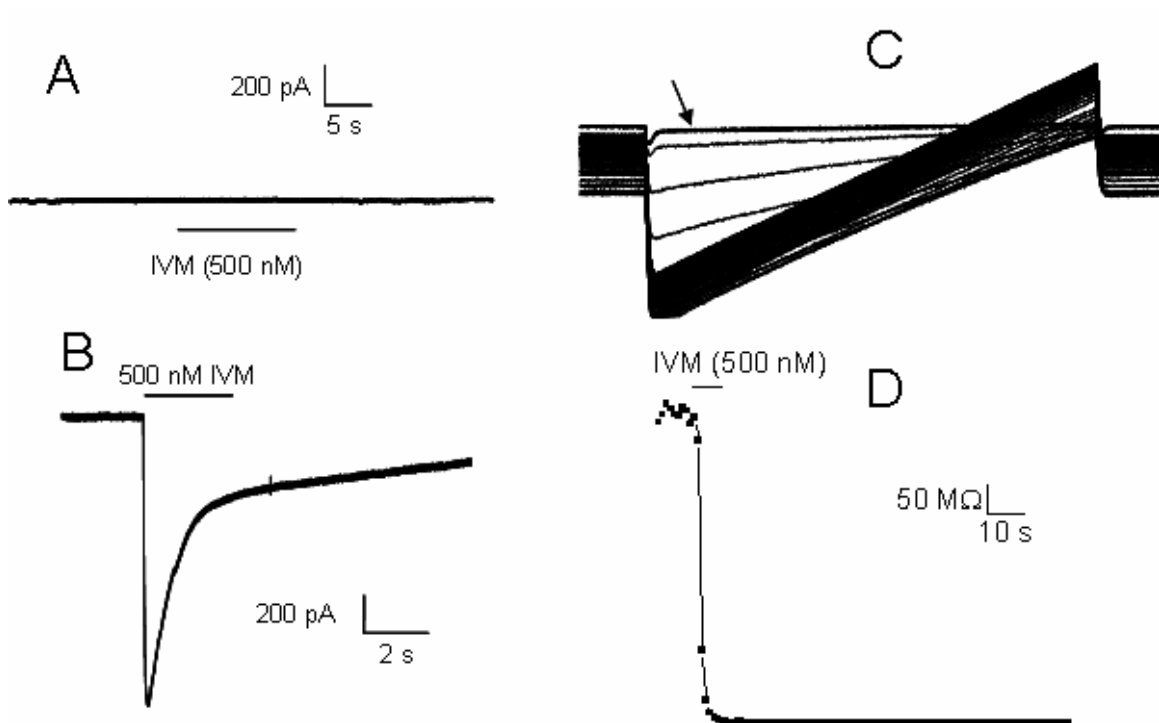


Figure 2-2 **GluCl  $\alpha$  and  $\beta$  are both required for functional channels in HEK293 cells.** A, Voltage-clamp record of a HEK293 cell transfected with GluCl  $\alpha$  and EGFP shows that this subunit alone does not respond to applications of 500 nM IVM. 5 out of 5 cells showed no response to this subunit alone. B, Voltage clamp record of a HEK293 cell transfected with GluCl  $\alpha$  and  $\beta$  subunits shows a transient IVM-induced current. 5 out of 5 cells transfected in this fashion showed a robust response to IVM. C, Voltage ramps from  $-90$  mV to  $-40$  mV before (arrow), during, and after the application of 500 nM IVM. The increasing slopes show the IVM-induced conductance. The waveforms also show a clear change in reversal potential during the development of the conductance. Ramps 100 ms in duration were delivered at 1 s intervals. D, Input resistance of the cell in panel C. A conductance develops and then remains relatively constant after application of IVM.

### **The GluCl / IVM method suppresses neuronal excitability**

We infected 10 to 14 days-in-culture rat E18 hippocampal cultures with vSinGluCl $\alpha\beta$ EGFP or the control virus vSinEGFP. As expected from previous studies (Khakh et al., 2001), the cultures were readily infected by either Sindbis virus, showing robust GFP expression in 20 to 50% of the neurons as early as 6 h post infection.

Previous studies also show that Sindbis-infected neurons die after ~ 48 h, presumably because the virus recruits all the ribosomes of the cell and thereby effectively shuts off host protein synthesis (Frolov and Schlesinger, 1994; Perri et al., 2000); therefore, we carried out our experiments at 24 hours post infection. Neurons infected with vSinGluCl $\alpha\beta$ EGFP and vSinEGFP had morphology indistinguishable from uninfected controls at this stage and appeared to be healthy (data not shown).

In approximately 20% of GFP-positive cells infected with vSinGluCl $\alpha\beta$ EGFP, we detected a robust conductance increase upon application of 5 nM to 500 nM IVM (bottom panels of Figure 2-3A,B, and C). The time to activate this current was dose-dependent; the time constant decreased from 500 s at 5 nM to 6 s at 500 nM. Surprisingly, the maximal conductance did not seem to vary in this concentration range. Also shown in the top panels of Figure 2-3 is the robust silencing effect of this conductance increase. Spontaneously firing cells subject to application of IVM stopped firing action potentials, and the membrane potential moved to values between -50 and -65 mV, which is near the value of  $E_{Cl}$  for solutions that we used. Importantly, vSinEGFP-infected neurons and uninfected neurons showed no responses to IVM at these concentrations (data not shown).

## FIGURE 2-3

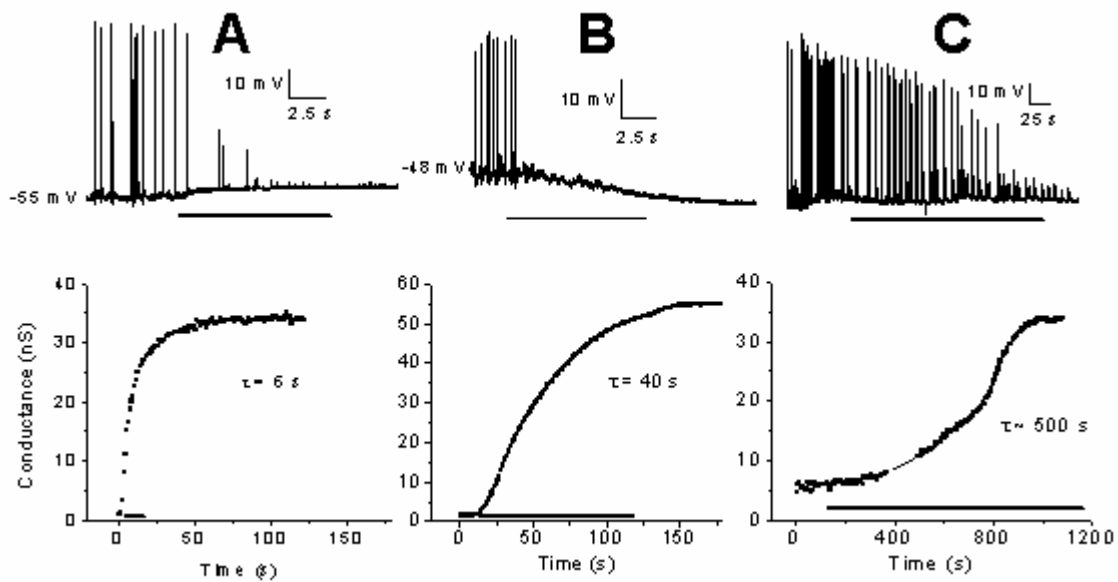


Figure 2-3: **Activation of GluCl conductance by IVM over a 100-fold concentration range.**

(A, 500 nM; B, 50 nM; C, 5 nM). Top panels show current-clamp data from cells that displayed spontaneous activity. Bottom panels show input conductance measured with voltage-clamp ramps from  $-80$  mV to  $-50$  mV 200 ms in duration at intervals of 1 s. Each panel represents data from a different cell. Uninfected and GFP-infected neurons had no response to IVM applied similarly.

Glutamate is the major excitatory transmitter in the brain, and brief applications of glutamate strongly elicit action potentials in hippocampal neurons (Storm-Mathisen, 1981; Crunelli et al., 1983). The major goal of the GluCl / IVM method is to insure that once a GluCl $\alpha\beta$  positive cell is activated by IVM, it no longer fires action potentials in response to excitatory input. Figure 2-4A demonstrates this effect. The left panel shows that an infected neuron fires volleys of action potentials in response to 10 ms pulses of 100  $\mu$ M glutamate; the right panel shows that, in the presence of 5 nM IVM, the same neuron no longer responds to identical glutamate pulses. Below (Figure 2-8), we show that neurons expressing this invertebrate glutamate receptor display no changes in glutamate responses.

Additionally, neurons infected with vSinGluCl $\alpha\beta$ EGFP and activated with IVM show extreme reductions in impulse firing elicited by direct current injection. The top panel of Figure 2-4B shows current-clamp records from a vSinGluCl $\alpha\beta$ EGFP-infected neuron. Increasing current pulses (up to 30 pA) elicit current-dependent firing. The bottom panel shows records from a similar neuron, incubated with 5 nM IVM. This neuron does not respond at all to the same current injection protocol. Moreover, injection of up to 200 pA (data not shown) failed to elicit a spike. Figure 2-4C shows the same experiments for an uninfected control cell; 5 nM IVM did not affect the excitability. This lack of IVM effect was observed in all of 103 uninfected or 55 vSinEGFP-infected neurons, respectively.

## FIGURE 2-4

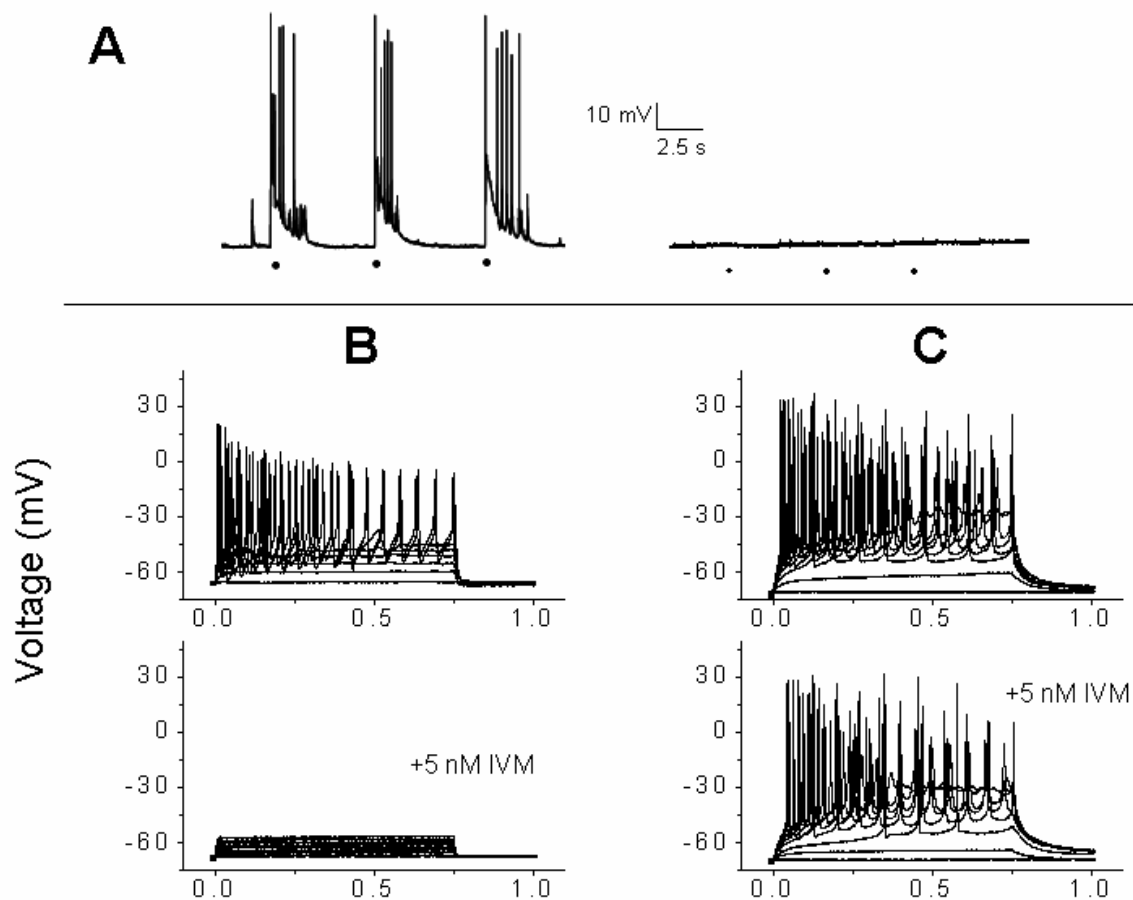


Figure 2-4. **IVM silences GluCl-expressing neurons.**

A, Silenced cells no longer respond to glutamate. Current clamp traces from a GluCl infected cell. Dots indicate 10 ms applications of 100  $\mu$ M glutamate. Left panel, prior to activation with IVM, the cell responds to glutamate with action potentials. Right panel, after activation with 5nM IVM, the cell no longer responds to the same glutamate application. One second applications of glutamate could produce a slight depolarization, but no action potentials (data not shown). B, GluCl infected cells in current clamp, showing responses to depolarizing current pulses (0 to 30 pA, 5 pA increments). In control solutions, cells responded with action potentials; but the IVM (5 nM)-induced Cl<sup>-</sup> conductance prevented action potentials (bottom panel). Cells remained silenced even in responses to current pulses as high as 200 pA (data not shown). C, an uninfected cell, showing no reduction in excitability by 5 nM IVM.

### **Sindbis expression produces highly variable results**

Previous reports show large cell-to-cell variability in expression levels, based on measurements using dual promoters to express an ion channel subunit with Sindbis virus (Okada et al., 2001). We expected similar cell-to-cell variability in our experiments. Unexpectedly, we found that the major variability in IVM responses occurred between culture dishes rather than within neurons in a given culture (Figure 2-5). Each point in Figure 2-5 represents the average of five infected neurons in a single infected culture. Some cultures respond well while others do not. We could observe no clear morphological differences or GFP fluorescence intensity differences between cultures that expressed well and those that expressed poorly. We attempted, with no success, to minimize this variability by varying the age of the cultures, the time after infection, temperature and position in the incubator, preparation of the virus, sonication of the virus, and glutamate concentration in the culture medium. In control dishes infected with vSinEGFP, there was no significant difference between the IVM+ and IVM- input conductance in any culture tested (data not shown). Because of this culture-to-culture variation, we selected only cultures that had neurons responding well to IVM for the measurement studies presented above. We found similar dish-to-dish variability in HEK293 cultures infected with vSinGluCl $\alpha\beta$ EGFP, but not in HEK cultures transfected with both plasmids encoding the GluCl subunits; therefore we believe that this variability is a characteristic of the Sindbis expression system rather than an inherent limitation of the GluCl / IVM method.

FIGURE 2-5

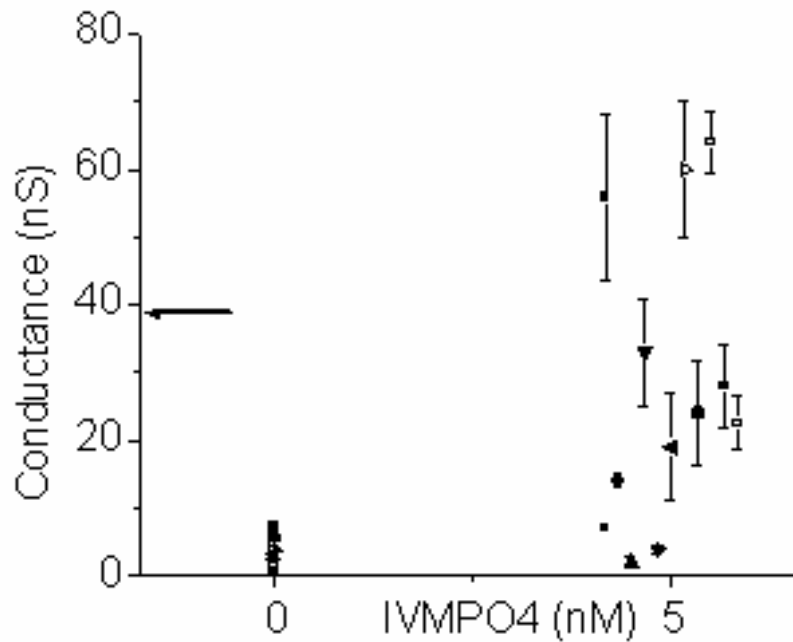


Figure 2-5: **There is a large variation in expression levels that seems to be culture dependent.** Each point represents the average of 5 cells in a culture dish. Roughly half of the cultures surveyed have no response to 500 nM IVM, and these cultures were excluded from the plot. The points plotted here represent the cultures that do respond to 500 nM IVM. Note that this graph represents data taken at 0 and 5 nM IVM; the points have been spread out to enhance visualization. The arrow represents average cell conductance in 0 nM IVM, 100  $\mu$ M muscimol for comparison.

**In Nupherin-mediated transfection, all fluorescent cells respond to IVM.**

We sought an expression method that could overcome the variability of the Sindbis system. We employed the newly developed Nupherin-neuron transfection system to transfect GluCl channels into hippocampal cultures. In these experiments, we modified the GluCl coding sequence to include fluorescent proteins (yellow fluorescent protein, YFP; and cyan fluorescent protein, CFP) in the M3-M4 loop of each construct (GluCl $\alpha$  and  $\beta$  subunits, respectively, as shown in Figure 2-6A). Figure 2-6C, D, and E show images from an exemplar hippocampal culture. Each of 30 fluorescent cells in three cultures responded to 5 nM IVM with a conductance greater than 30 nS, similar to the results with neurons in responsive Sindbis infected cultures (Figure 2-6B). This figure shows that neurons transfected with the GluCl  $\alpha$  subunit alone do not develop a conductance in the presence of IVM. The variability between cultures is substantially less with Nupherin-mediated expression than with Sindbis-mediated expression.

**IVM-induced Cl<sup>-</sup> conductance is reversible**

In previous reports, IVM has been described as acting irreversibly on GluCl channels expressed in *Xenopus* oocytes (Cully et al., 1994) on a time scale of several min. Ligand binding experiments show that IVM does dissociate from its receptor (presumably the GluCl channels), with a rate constant of 0.005 - 0.006 min<sup>-1</sup> (Cully and Paress, 1991). Therefore we sought to measure reversibility of IVM action on a time scale of several hundred min. We infected cultures of hippocampal neurons, incubated in 5 nM IVM, and

## FIGURE 2-6

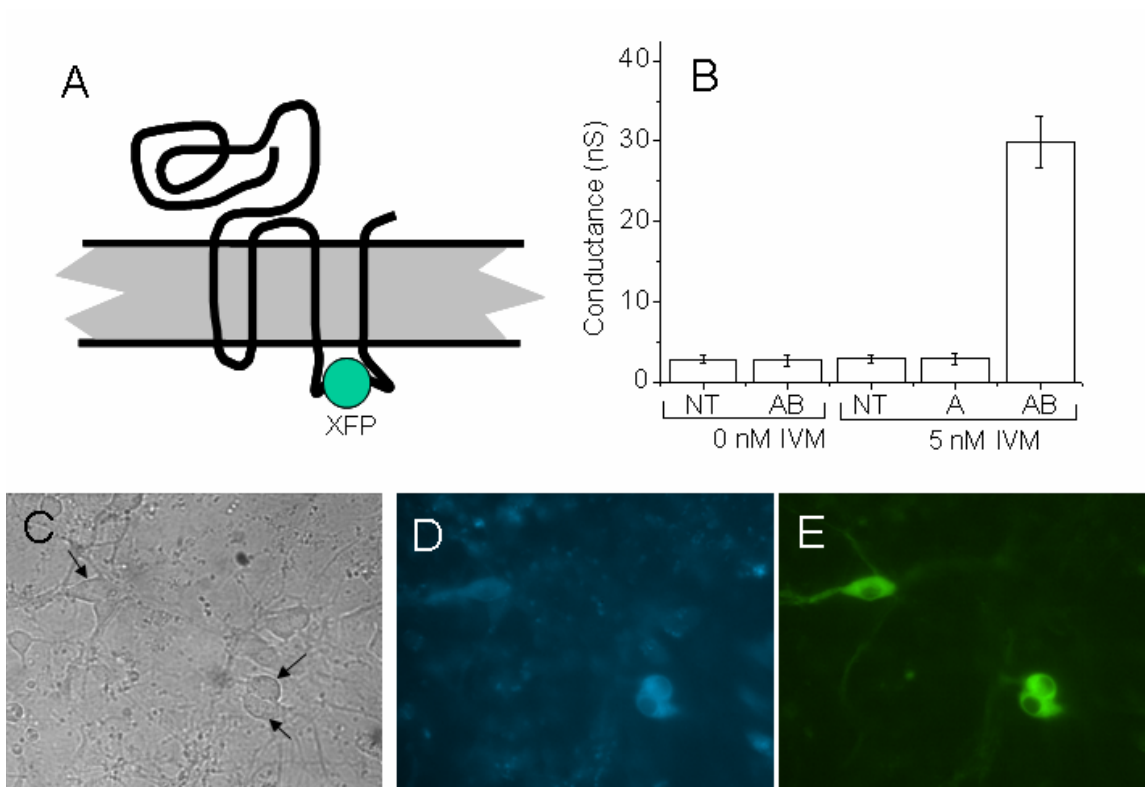


**Figure 2-6: Neurons cotransfected with separate plasmids encoding EYFP-tagged GluCl  $\alpha$  and ECFP-tagged GluCl  $\beta$  show fluorescence.**

A, Cartoon indicating that the fluorescent protein was inserted in the M3-M4 loop of each subunit.

B, Measured input conductance of neurons transfected with the GluCl  $\alpha$ -EYFP fusion and GluCl  $\beta$ -ECFP fusion. NT, neurons that have not been transfected; AB, neurons transfected with both subunits; A, neurons transfected with only the GluCl  $\alpha$ -EYFP subunit. All bars represent data from three independent cultures, 10 cells per culture.

C, A brightfield image at 40x showing several neurons, with arrows indicating three neurons that have been transfected.

D, The field of view in panel B imaged with an ECFP filter set.

E, The field of view in panel B imaged with an EYFP filter set.

measured the input conductance of the neurons to verify that the channels were activated. We then washed the cultures, and recorded the input conductance after one hour or eight hours. Figure 2-7 summarizes these results. At 1 h, the conductance has not significantly changed from the activated conductance, whereas by eight hours, the conductance has returned nearly to baseline. The final bar shows that IVM can subsequently reactivate the channels. Formally, it is not possible to distinguish between the possibility that the reversibility is caused by IVM washing off the GluCl receptors or the possibility that the reversibility is due to receptor turnover, but the important feature here is that the technique appears to be reversible in terms of electrical activity.

#### **Neither GluCl expression nor IVM application affects other synaptic properties**

In experiments to examine possible unwanted additional effects of IVM, we employed 5 nM IVM, since this concentration produces adequate silencing in most neurons. Because of the homology between GluCl channels and GABA<sub>A</sub> receptors, we were concerned that one or both of these subunits might heteromultimerize with native GABA<sub>A</sub> receptor subunits. We therefore compared the amplitude, rise time, and decay time of GABA-evoked responses. The left panel of Figure 2-8A shows that these three parameters do not significantly differ between infected and uninfected cells, providing confidence that heteromultimerization with GABA subunits did not take place or at least had no functional consequences. After measuring the evoked responses, we applied 5nM IVM to these cultures to ensure that these cultures were expressing the GluCl receptor at high levels.

FIGURE 2-7

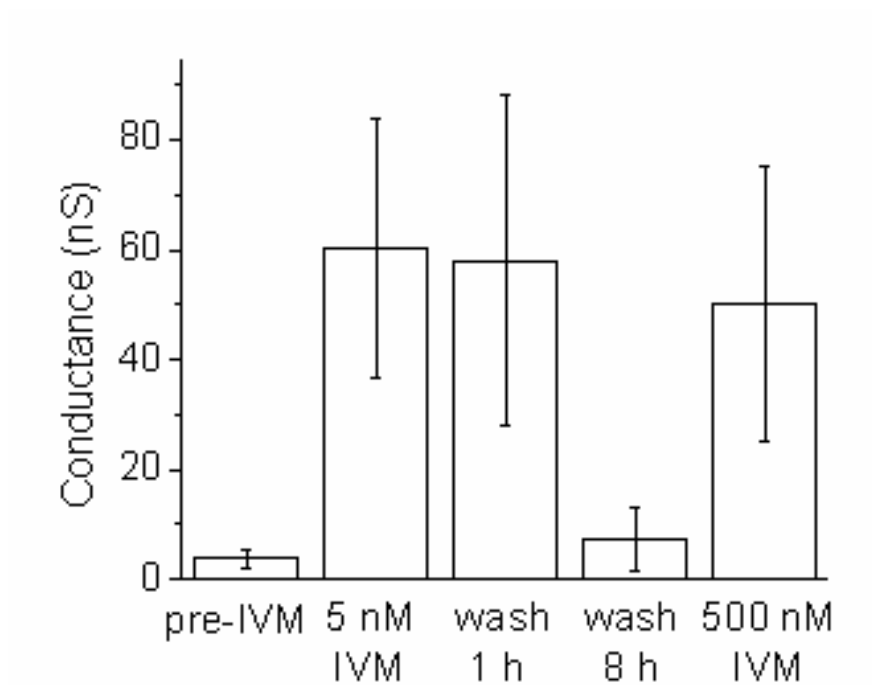
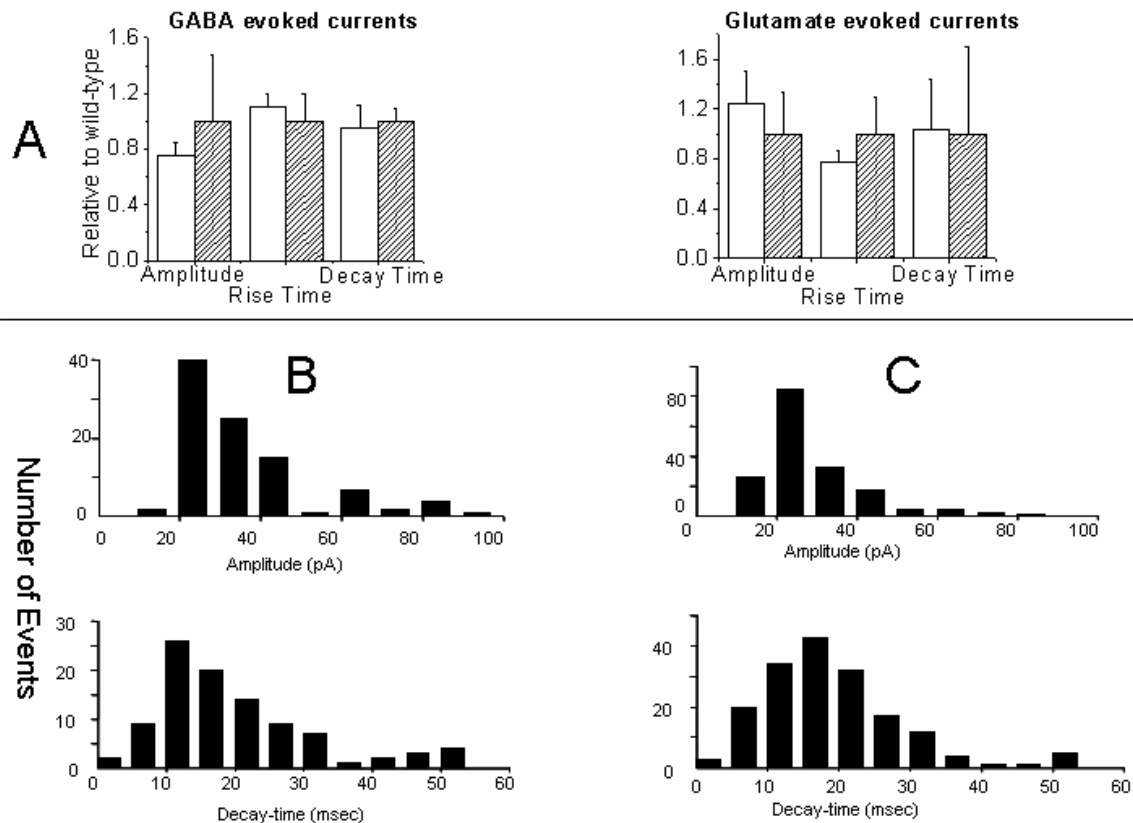


Figure 2-7: **IVM-induced chloride conductance deactivates several hours after IVM washout.** The input conductance of cells infected with vSin $\alpha$  $\beta$ EGFP was first measured without IVM, and then in the presence of 5 nM IVM. After 1 h of washing, there is little recovery in cell conductance, whereas after 8 h the conductance returns to uninfected levels. The last bar shows that IVM-induced conductance can be reactivated. Each bar represents 10 cells in two cultures and the error bars are standard errors.

## FIGURE 2-8



**Figure 2-8: Expression of GluCl does not alter glutamate or GABA-evoked currents.** A, Evoked currents were measured in GluCl-infected and uninfected neurons with 10 ms agonist puffs (100  $\mu$ M GABA, 1 mM glutamate). The amplitude, rise time, and decay time were measured. The plot shows these three parameters relative to the measurements in uninfected cells. GABA responses are shown in the left panel, glutamate responses on the right. For each of the two ligands, the bars represent data pooled from 10 cells from two different cultures. B, C, analysis of GABA mIPSCs in the absence (B) and presence (C) of 5 nM IVM. The peak amplitude histogram (top panel) and decay time histogram (bottom panel) are shown. The amplitude data are shown in 10 pA bins and the decay time data are shown in 10 ms bins. Note that there is no apparent difference in histogram shape between the 0 and 5 nM IVM case for either measurement. In (B) data are pooled from 20 events each from 5 neurons in one culture, and in (C) data are pooled from 30 events each from 5 neurons in one culture.

The GluCl  $\alpha$  and  $\beta$  heteromultimer is a glutamate receptor (Cully et al., 1994). We were concerned that this response might add to or distort the endogenous glutamate response of the neuron. The right panel of Figure 2-8A addresses these concerns in an experiment using Sindbis-mediated expression: the glutamate response did not change significantly between uninfected and GluCl $\alpha\beta$  expressing neurons. As above, we used only cultures that responded well to IVM for these experiments. These experiments were performed with CsCl in the internal recording solution and voltage-clamped at  $-60\text{mV}$ , so that any additional conductance caused by glutamate activation of GluCl would result in an increase in amplitude or perhaps an increase in decay time. In infected cultures treated with CNQX and APV to block endogenous glutamate receptors, we found that steady application of  $10\ \mu\text{M}$  glutamate (the estimated steady concentration of glutamate in CSF) produced no detectable conductance increases ( $< 0.1\ \text{nS}$ ). Steady application of  $2\ \text{mM}$  glutamate, however, produced slow, large ( $\sim 30\ \text{nS}$ ) conductances.

IVM has various effects on other ion channels, including GABA (Krusek and Zemkova, 1994), P2X<sub>2</sub> (Khakh et al., 1999), and nAChR (Krause et al., 1998). These effects occur with concentrations of IVM higher than  $5\ \text{nM}$ . However, we chose to study what we regard as the most likely side effect, GABA potentiation, with our target silencing IVM concentration of  $5\ \text{nM}$ . Figure 2-8B presents histograms of the amplitude and decay time of the GABAergic synaptic miniature IPSCs (mIPSCs) recorded from uninfected neurons in the presence of the glutamate receptor blockers CNQX and APV and the Na<sup>+</sup> channel blocker TTX. Figure 2-8C presents the same type of data, with the

addition of 5 nM IVM in the recording media. There is no apparent potentiation of GABA receptors at this concentration of IVM.

## Discussion

We describe a procedure that combines advantages of genetically based and pharmacologically based silencing by inhibitory ion channels. Our results demonstrate that the GluCl / IVM method modifies neuronal excitability in an inducible and reversible manner. Expression of GluCl alone seems to leave the excitability of the neuron unaltered, and IVM application to uninfected neurons within the effective range for silencing GluCl expressing neurons never produces a detectable conductance. However, many GluCl-expressing neurons display a reduction in excitability when exposed to low concentrations of IVM. The reduction in excitability silences many neurons, and this silencing can be reversed by ~ 8 h of washing. These are the desired results of the GluCl / IVM silencing method.

With the Sindbis virus construct, there was an inherently high level of variability of expression among infected cells. Despite numerous attempts to understand and control this variability, we found no parameters to explain it. Both HEK cells transfected with the GluCl  $\alpha$  and  $\beta$  subunits, and *Xenopus* oocytes injected with RNA for this channel, nearly always show expression, reinforcing our belief that this variability results from an aspect of Sindbis viral biology. Nupherin-mediated expression yields more consistent data, supporting this interpretation. Because our long-term goal involves transgenic methods to express the GluCl channels, the variability does not appear to be a source of significant concern for the GluCl / IVM silencing method.

Neurons expressing the channel at a high level are strongly silenced by 5 nM IVM. This low concentration is important, for previous reports show that IVM at considerably higher concentrations in the mammalian brain is toxic. Studies done with radiolabeled IVM in blood brain barrier-impaired mice indicate that the toxic concentration of IVM in the brain is ~ 500 nM (Schinkel et al., 1994), which is two orders of magnitude above the concentration we are using. This gives us some confidence that *in vivo* applications of the GluCl / IVM method may succeed. A related complexity is the delivery of IVM to the brain. The blood-brain barrier contains mechanisms, primarily involving *mdr1*, that appear to pump IVM out of the brain, and this might prevent systemically applied IVM from reaching GluCl channels in the brain. However, a clinically relevant intraperitoneal dose, 0.2 mg/kg, results in 1.5 ng/g of IVM in brain tissue (Schinkel et al., 1994), or approximately 2 nM. This is very close to the concentration we believe necessary for silencing neurons expressing GluCl. Perhaps *in vivo* applications of the GluCl / IVM method will require relatively simple methods of IVM delivery to the animal. Of course, more sophisticated options exist for easing drug delivery, such as using blood-brain disrupting drugs (Jette et al., 1995) or using mice with disrupted drug-pumping at the blood-brain barrier, as the foundation for transgenic mice expressing this channel.

Previous reports suggest that IVM “irreversibly” activates GluCl channels, an unusual situation for ligand-gated channels. The impression of irreversibility may arise from the limited time scale of previous experiments on *Xenopus* oocytes, or from drug retention by the large yolk volume of the cells. Data from our washout experiments (Figure 2-7), suggesting reversibility after 8 h, are roughly consistent with the

disassociation constant determined in biochemical binding experiments (Cully and Paress, 1991). Both the onset and recovery from silencing will depend on the pharmacokinetics of IVM in the animal; for instance, IVM can be stored in the fat.

In addition to the channel-based silencing strategies noted in the Introduction, other investigators have utilized genetic manipulations of synaptic transmission, for instance utilizing tetanus toxin (Baines et al., 2001). It is unclear whether tetanus toxin-based procedures are reversible. Additionally, exogenous expression of  $K^+$  channels has been used to modulate biochemical signaling pathways in HEK293 cells (Holmes et al., 1997).

There are several potential applications for the GluCl / IVM method, or for improved versions, in research and in therapeutics. One application would involve cell-specific expression of GluCl channels under the control of appropriate promoter(s). This strategy may enable genetic manipulation of excitability at selected times in development and in specific regions in the CNS. The requirement for both the GluCl  $\alpha$  subunit and the GluCl  $\beta$  subunit may at first seem like a complication; however, this gives the experimenter the flexibility to use different promoters to drive the two genes, so that only neurons in which both promoters are active will be silenced upon administration of IVM. Additionally, it may be possible to construct viruses with these two genes that can be used *in vivo*. Stereotaxic injection of such viruses may then circumvent the need for promoters that drive expression in specific brain nuclei. From a clinical standpoint, a targeted and controlled “excitability modulator” may form the basis for new treatments of epilepsy, chronic pain, or other diseases arising from excess neuronal activity. It may be possible to titrate silencing by varying the dose of IVM.

## References

- Baines RA, Uhler JP, Thompson A, Sweeney ST, Bate M (2001) Altered electrical properties in *Drosophila* neurons developing without synaptic transmission. *J Neurosci* 21:1523-1531.
- Crunelli V, Forda S, Kelly JS (1983) Blockade of amino acid-induced depolarizations and inhibition of excitatory post-synaptic potentials in rat dentate gyrus. *J Physiol* 341:627-640.
- Cully DF, Paress PS (1991) Solubilization and characterization of a high affinity ivermectin binding site from *Caenorhabditis elegans*. *Mol Pharmacol* 40:326-332.
- Cully DF, Vassilatis DK, Liu KK, Paress PS, Van der Ploeg LH, Schaeffer JM, Arena JP (1994) Cloning of an avermectin-sensitive glutamate-gated chloride channel from *Caenorhabditis elegans*. *Nature* 371:707-711.
- Ehrengruber MU, Doupnik CA, Xu Y, Garvey J, Jasek MC, Lester HA, Davidson N (1997) Activation of heteromeric G protein-gated inward rectifier K<sup>+</sup> channels overexpressed by adenovirus gene transfer inhibits the excitability of hippocampal neurons. *Proc Natl Acad Sci U S A* 94:7070-7075.
- Falk T, Kilani RK, Yool AJ, Sherman SJ (2001) Viral vector-mediated expression of K<sup>+</sup> channels regulates electrical excitability in skeletal muscle. *Gene Ther* 8:1372-1379.
- Frolov I, Schlesinger S (1994) Comparison of the effects of Sindbis virus and Sindbis virus replicons on host cell protein synthesis and cytopathogenicity in BHK cells. *J Virol* 68:1721-1727.
- Helmstetter FJ, Bellgowan PS (1994) Effects of muscimol applied to the basolateral amygdala on acquisition and expression of contextual fear conditioning in rats. *Behav Neurosci* 108:1005-1009.
- Holmes TC, Berman K, Swartz JE, Dagan D, Levitan IB (1997) Expression of voltage-gated potassium channels decreases cellular protein tyrosine phosphorylation. *J Neurosci* 17:8964-8974.
- Holt W, Maren S (1999) Muscimol inactivation of the dorsal hippocampus impairs contextual retrieval of fear memory. *J Neurosci* 19:9054-9062.
- Isles AR, Ma D, Milsom C, Skynner MJ, Cui W, Clark J, Keverne EB, Allen ND (2001) Conditional ablation of neurones in transgenic mice. *J Neurobiol* 47:183-193.

- Jasnow AM, Huhman KL (2001) Activation of GABA(A) receptors in the amygdala blocks the acquisition and expression of conditioned defeat in Syrian hamsters. *Brain Res* 920:142-150.
- Jette L, Murphy GF, Leclerc JM, Beliveau R (1995) Interaction of drugs with P-glycoprotein in brain capillaries. *Biochem Pharmacol* 50:1701-1709.
- Johns DC, Marx R, Mains RE, O'Rourke B, Marban E (1999) Inducible genetic suppression of neuronal excitability. *J Neurosci* 19:1691-1697.
- Khakh BS, Humphrey PP, Surprenant A (1995) Electrophysiological properties of P2X-purinoceptors in rat superior cervical, nodose and guinea-pig coeliac neurones. *J Physiol* 484:385-395.
- Khakh BS, Proctor WR, Dunwiddie TV, Labarca C, Lester HA (1999) Allosteric control of gating and kinetics at P2X<sub>4</sub> receptor channels. *J Neurosci* 19:7289-7299.
- Khakh BS, Smith WB, Chiu CS, Ju D, Davidson N, Lester HA (2001) Activation-dependent changes in receptor distribution and dendritic morphology in hippocampal neurons expressing P2X<sub>2</sub>-green fluorescent protein receptors. *Proc Natl Acad Sci U S A* 98:5288-5293.
- Kobayashi K, Morita S, Sawada H, Mizuguchi T, Yamada K, Nagatsu I, Fujita K, Kreitman RJ, Pastan I, Nagatsu T (1995) Immunotoxin-mediated conditional disruption of specific neurons in transgenic mice. *Proc Natl Acad Sci U S A* 92:1132-1136.
- Krause RM, Buisson B, Bertrand S, Corringer PJ, Galzi JL, Changeux JP, Bertrand D (1998) Ivermectin: a positive allosteric effector of the alpha7 neuronal nicotinic acetylcholine receptor. *Mol Pharmacol* 53:283-294.
- Krusek J, Zemkova H (1994) Effect of ivermectin on gamma-aminobutyric acid-induced chloride currents in mouse hippocampal embryonic neurones. *Eur J Pharmacol* 259:121-128.
- Li YX, Zhang Y, Lester HA, Schuman EM, Davidson N (1998) Enhancement of neurotransmitter release induced by brain-derived neurotrophic factor in cultured hippocampal neurons. *J Neurosci* 18:10231-10240.
- Maren S, Yap SA, Goosens KA (2001) The amygdala is essential for the development of neuronal plasticity in the medial geniculate nucleus during auditory fear conditioning in rats. *J Neurosci* 21:RC135.
- Martin RJ, Murray I, Robertson AP, Bjorn H, Sangster N (1998) Anthelmintics and ion-channels: after a puncture, use a patch. *Int J Parasitol* 28:849-862.
- Muller J, Corodimas KP, Fridel Z, LeDoux JE (1997) Functional inactivation of the lateral and basal nuclei of the amygdala by muscimol infusion prevents fear

- conditioning to an explicit conditioned stimulus and to contextual stimuli. *Behav Neurosci* 111:683-691.
- Nadeau H, Lester HA (2002) NRSF causes cAMP-sensitive suppression of sodium currents in cultured hippocampal neurons. *J Neurophysiol* in press.
- Nadeau H, McKinney S, Anderson DJ, Lester HA (2000) ROMK1 (Kir1.1) causes apoptosis and chronic silencing of hippocampal neurons. *J Neurophysiol* 84:1062-1075.
- Nitabach MN, Blau J, Holmes T (2002) Electrical Silencing of Drosophila Pacemaker Neurons Stops the Free-Running Circadian Clock. *Cell* 109:485-495.
- Okada T, Yamada N, Kakegawa W, Tsuzuki K, Kawamura M, Nawa H, Iino M, Ozawa S (2001) Sindbis viral-mediated expression of Ca<sup>2+</sup>-permeable AMPA receptors at hippocampal CA1 synapses and induction of NMDA receptor-independent long-term potentiation. *Eur J Neurosci* 13:1635-1643.
- Paradis S, Sweeney ST, Davis GW (2001) Homeostatic control of presynaptic release is triggered by postsynaptic membrane depolarization. *Neuron* 30:737-749.
- Perri S, Driver DA, Gardner JP, Sherrill S, Belli BA, Dubensky TW, Jr., Polo JM (2000) Replicon vectors derived from Sindbis virus and Semliki forest virus that establish persistent replication in host cells. *J Virol* 74:9802-9807.
- Sawada H, Nishii K, Suzuki T, Hasegawa K, Hata T, Nagatsu I, Kreitman RJ, Pastan I, Nagatsu T, Kobayashi K (1998) Autonomic neuropathy in transgenic mice caused by immunotoxin targeting of the peripheral nervous system. *J Neurosci Res* 51:162-173.
- Schinkel AH, Smit JJ, van Tellingen O, Beijnen JH, Wagenaar E, van Deemter L, Mol CA, van der Valk MA, Robanus-Maandag EC, te Riele HP, et al. (1994) Disruption of the mouse *mdr1a* P-glycoprotein gene leads to a deficiency in the blood-brain barrier and to increased sensitivity to drugs. *Cell* 77:491-502.
- Storm-Mathisen J (1981) Glutamate in hippocampal pathways. *Adv Biochem Psychopharmacol* 27:43-55.
- Watanabe D, Inokawa H, Hashimoto K, Suzuki N, Kano M, Shigemoto R, Hirano T, Toyama K, Kaneko S, Yokoi M, Moriyoshi K, Suzuki M, Kobayashi K, Nagatsu T, Kreitman RJ, Pastan I, Nakanishi S (1998) Ablation of cerebellar Golgi cells disrupts synaptic integration involving GABA inhibition and NMDA receptor activation in motor coordination. *Cell* 95:17-27.
- White B, Osterwalder T, Keshishian H (2001a) Molecular genetic approaches to the targeted suppression of neuronal activity. *Curr Biol* 11:R1041-1053.

- White BH, Osterwalder TP, Yoon KS, Joiner WJ, Whim MD, Kaczmarek LK, Keshishian H (2001b) Targeted attenuation of electrical activity in *Drosophila* using a genetically modified K<sup>+</sup> channel. *Neuron* 31:699-711.
- Wilensky AE, Schafe GE, LeDoux JE (1999) Functional inactivation of the amygdala before but not after auditory fear conditioning prevents memory formation. *J Neurosci* 19:RC48.
- Wilensky AE, Schafe GE, LeDoux JE (2000) The amygdala modulates memory consolidation of fear-motivated inhibitory avoidance learning but not classical fear conditioning. *J Neurosci* 20:7059-7066.
- Xue H (1998) Identification of major phylogenetic branches of inhibitory ligand-gated channel receptors. *J Mol Evol* 47:323-333.

*Chapter 3***Selective elimination of glutamate activation and introduction of fluorescent proteins into a *C. elegans* chloride channel**

Text of this chapter is reproduced, with minor editing, from:

Li P, Slimko EM, Lester HA (2002) Selective elimination of glutamate activation and introduction of fluorescent proteins into a *Caenorhabditis* chloride channel. *FEBS Letters* 528 (2002) 77-82.

## Abstract

Glutamate-gated (GluCl) chloride channels from invertebrates can be activated by ivermectin (IVM) to produce electrical silencing in mammalian neurons. To improve this GluCl/IVM strategy, we sought to mutate the *C. elegans* GluCl channels so that they become insensitive to glutamate but retain their sensitivity to IVM. Based on structure-function studies of nAChR superfamily members, we tested in oocytes 19 point mutants at 16 residues in the  $\beta$  subunit likely to be involved in the response to glutamate. Y182F reduces the glutamate response by greater than 6 fold, with little change to IVM responses, when coexpressed with WT GluCl  $\alpha$ . For GluCl  $\alpha\beta$ (Y182F), the  $EC_{50}$  and Hill coefficient for glutamate is similar to those of WT, indicating that the mutant decreases the efficacy of glutamate, but not the potency. Also, fluorescent proteins (EGFP, EYFP, ECFP; XFP) were inserted into the M3-M4 loop of the GluCl  $\alpha$ ,  $\beta$  and  $\beta$ (Y182F). We found no significant functional difference between these XFP-tagged receptors and WT receptors. The modified GluCl channel, without glutamate sensitivity but with a fluorescent tag, may be more useful in GluCl silencing strategies.

## Introduction

Several recent studies describe expression of exogenous ion channels in order to change the electrical properties of neurons (Johns et al., 1999; Sutherland et al., 1999; Nadeau et al., 2000; Falk et al., 2001; Okada et al., 2001; Scarce-Levie et al., 2001; White et al., 2001a; White et al., 2001b). Our laboratory has developed a procedure that employs the glutamate-gated chloride (GluCl) channels from *C. elegans* (Cully et al., 1994; Xue, 1998; Slimko et al., 2002). Because the anthelmintic ivermectin (IVM) activates these channels at concentrations too low to affect other mammalian ion channels, it is possible to envision a procedure that selectively silences the target neurons. The GluCl channels would be expressed in the target neurons either by local injection of viral vectors or in transgenic animals under cell-specific promoters.

The GluCl/IVM technique could be improved in two ways. First, the GluCl channels should be rendered insensitive to glutamate, which is present in CSF and released during synaptic transmission. Second, the expression of the GluCl channels should be physically verifiable by a technique that has higher throughput than electrophysiology. Fluorescent proteins are widely employed for such purposes; and the channels could be fused to fluorescent proteins.

We chose the GluCl channels in part because they are members of the nicotinic receptor superfamily, which has been widely studied by mutagenesis (Corringer et al., 2000). Therefore several precedents suggest ways to re-engineer the GluCl channels (Etter et al., 1999; Dougherty and Lester, 2001; Han et al., 2001). For the goal of eliminating glutamate responses while retaining IVM responses, one considers the residues in the N-terminal region known to bind agonists (Figure 3-1) (Pedersen et al.,

1986; Curtis et al., 2000). For the goal of introducing fluorescent proteins, previous results suggest that the intracellular loop between the M3 and M4 domains is the appropriate region (Gensler et al., 2001).

## Materials and Methods

### *Mutagenesis*

Wild type *C. elegans* GluCl  $\alpha$  and GluCl  $\beta$  genes (Cully et al., 1994) cloned into pBluescript II SK+ were a gift from Merck Research Laboratories. In our present study (Slimko et al., 2002), they were cloned into pcDNA 3.1 (ClonTech, Palo Alto, CA) with KpnI and Not I. Site-directed mutagenesis was performed on the GluCl  $\beta$  subunit using the QuikChange mutagenesis kit (Stratagene, La Jolla, CA), and the mutations were confirmed by sequencing.

### *2.2 Fluorescent protein-tagged constructs*

Green fluorescent protein (EGFP), yellow fluorescent protein (EYFP), and cyan fluorescent protein (ECFP) were obtained from ClonTech (Palo Alto, CA). The PCR primers 5'-TCCACCGGGCCGGCAAATGGTGAGCAAGGGC-3' and 5'-GTCGCGGCGCCGGCGCTTGTACAGCTCGTCCA-3' were used to PCR amplify EYFP or EGFP, and the resultant PCR product was ligated into the NgoMIV site of GluCl  $\alpha$ , which positions the tag immediately after the arginine at residue 408, the 49<sup>th</sup> out of 73 residues in the M3-M4 loop. The PCR primers 5'-CACCGGTCTTCGAAATGGTGAGCAAGGGC-3' and 5'-TCGCGGCCTTCGAACTTGTACAGCTCGTCC-3' were used to PCR amplify ECFP, and the resultant PCR product was ligated into the Csp45I site of GluCl  $\beta$ , which

positions the tag immediately after the phenylalanine at residue 373, the 43<sup>rd</sup> out of 69 residues in the M3-M4 loop.

#### *Expression of GluCl cRNAs*

The cDNAs were linearized by NotI. All cRNAs were transcribed *in vitro* using the T7 mMESSAGE mMACHINE kit (Ambion, Austin, TX) as appropriate. RNAs were then quantitated by RiboGreen<sup>TM</sup> RNA Quantitation Kit (Molecular Probes, Eugene, OR). Stage V to VI *Xenopus laevis* oocytes were harvested and injected with 50 nl/oocyte of a mixture containing 25 to 375 pg per subunit of cRNAs for wild-type, mutant and XFP constructs, in equimolar amounts of  $\alpha$  and  $\beta$ . The size of the XFP coding region is  $\sim$  0.7 kb and that of the GluCl subunits is  $\sim$  1.4 kb, thus 1.5 times greater mass of an XFP-tagged subunit cRNAs was injected compared with WT subunits. After injection, oocytes were incubated at 18 °C in ND-96 solution (96 mM NaCl, 2 mM KCl, 1 mM MgCl<sub>2</sub>, 1.8 mM CaCl<sub>2</sub> and 5 mM HEPES, pH 7.5, osmolarity 230 mOsm) supplemented with 50  $\mu$ g/ml gentamicin, 2.5 mM pyruvate and 0.6 mM theophylline.

#### *Electrophysiology*

Recordings were carried out 24 to 36 h after injection. Membrane potential was held at  $-60$  mV in Ca<sup>2+</sup>-free ND-96 with two electrodes (filled with 3 M KCl, resistance 0.5–3 M $\Omega$ ) using a GeneClamp 500 circuit and a Digidata 1200 digitizer from Axon Instruments, Inc. (Foster City, CA) interfaced with an IBM-compatible PC running pCLAMP 8.0 software from Axon. Drugs were applied with a dead time of 1 s. Typical drug application times for glutamate and IVM were 10 s and 30 s, respectively. Experiments were conducted at room temperature (22 °C). Ivermectin was stored frozen as a 10 mM stock solution in dimethyl sulfoxide for up to 2 weeks. When dissolved into

the perfusion solution, the final concentration of dimethyl sulfoxide was no more than 0.1%. Glutamate was also prepared from stock solution at concentration of 100 mM (in water).

#### *Data Analysis*

The glutamate dose-response relations were measured by applying a series of glutamate concentrations to each oocyte. Because IVM responses did not reverse on the time scale of the experiments, only a single concentration was applied to each oocyte. This response was normalized to the amplitude of the response to 5  $\mu$ M IVM in oocytes (a saturating concentration) of the same batch. Glutamate and IVM responses to various drug concentrations were fitted to the Hill equation by a nonlinear routine,  $I/I_{\max} = 1/(1 + (EC_{50}/[A])^n)$ , where  $I$  is agonist-induced current at concentration  $[A]$ ,  $I_{\max}$  is the maximum current,  $EC_{50}$  is the concentration inducing half-maximum response, and  $n$  is the Hill coefficient. Statistical analyses were performed using unpaired two-population Student's  $t$  test (as appropriate), with a significance level of  $p < 0.05$ . All Data were presented as mean  $\pm$  S.D.

#### *Drugs and restriction endonucleases*

Glutamate and IVM were purchased from Sigma (St. Louis, MO); Csp45I was purchased from Promega (Madison, WC); and all the other restriction endonucleases were purchased from New England Biolabs (Beverly, MA).

## Results and Discussion

### Mutations in the ligand-binding domain and M1 of GluCl $\beta$

To eliminate sensitivity to glutamate, we mutated the GluCl  $\beta$  subunit, because this subunit is required for glutamate sensitivity (Cully et al., 1994). Glutamate-gated chloride (GluCl) channels are members of the nicotinic acetylcholine receptor (nAChR) superfamily (Xue, 1998). Based on structure-function studies of the glycine receptor (Shan et al., 2001) and the crystal structure of the ACh binding protein (Brejc et al., 2001; Dougherty and Lester, 2001), we identified 16 residues likely to be involved in the response to glutamate but not to IVM.

Figure 3-1 shows the alignment between GluCl $\beta$ s and four other nAChR family members. Residues in red type are completely conserved; green and blue type denotes partial conservation. The first two Cys residues define the “signature loop” common to all nAChR superfamily subunits, and the second two Cys define Loop C (nAChR terminology). Y182 in the GluCl  $\beta$  subunit, aligns with W149 at nAChR, the site of a cation- $\pi$  interaction with the ligand (Zhong et al., 1998; Brejc et al., 2001). T229 and Y232 align with the crucial nAChR Y190 and Y198, respectively. The glycine receptor is the closest homolog of GluCl $\beta$ s in vertebrates. Relevant site-directed mutagenesis experiments on human glycine receptors indicate that I244A eliminates glycine sensitivity but retains IVM sensitivity (Shan et al., 2001). I269 at the GluCl  $\beta$  subunit aligns with this position. These 4 residues were mutated in the first round (highlighted in yellow, Figure legends, Figure 3-1). The mutations Y182A and Y232A abolished both glutamate and IVM responses; at these residues, we then performed 4 “milder” mutations (Y $\rightarrow$ F, W). We have not succeeded in generating a cDNA for Y232F.

## FIGURE 3-1

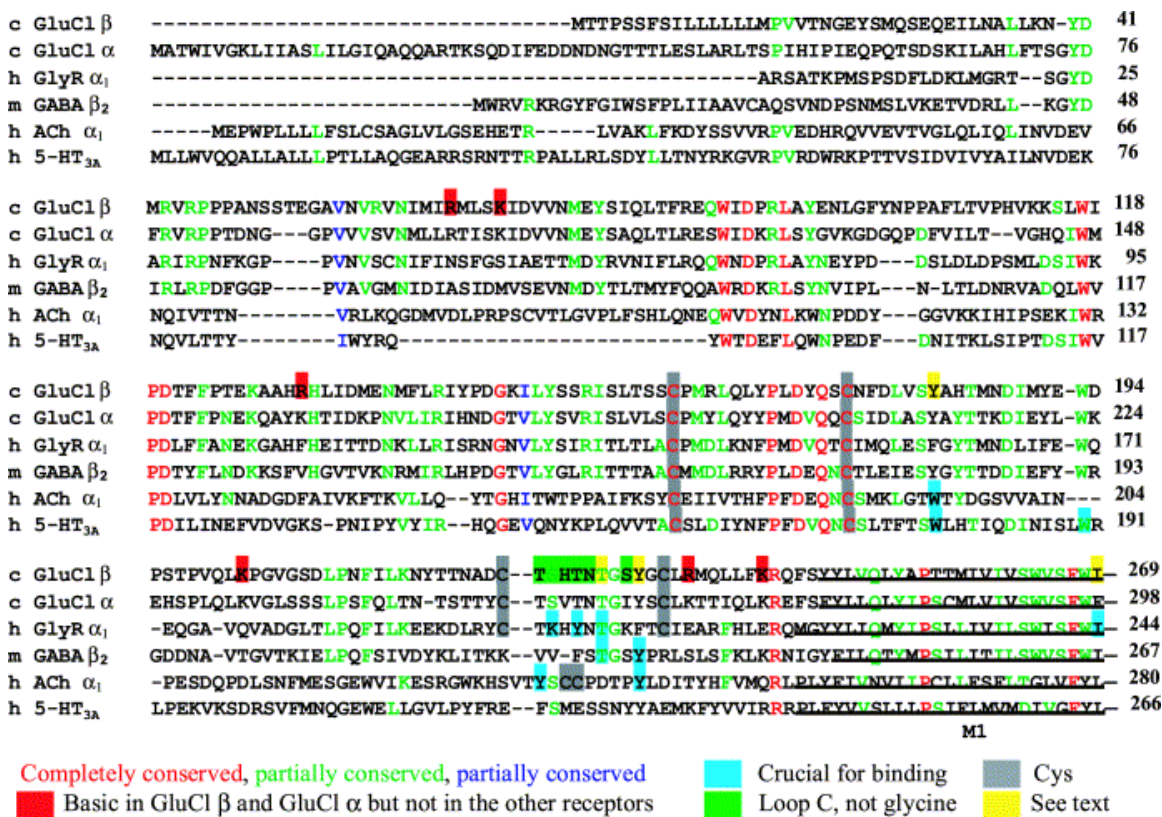


Figure 3-1: **GluCl sequences in the extracellular ligand-binding domain and M1, compared with other nAChR superfamily members.** The *C. elegans* GluCl β subunit and α subunit (c GluCl β; c GluCl α; GenBank accession numbers U14525 and U14524) were aligned with each other and the human glycine receptor α<sub>1</sub> subunit (h GlyR α<sub>1</sub>; Swiss-Prot P23415), mouse GABA receptor β<sub>2</sub> subunit (m GABA β<sub>2</sub>; Swiss-Prot P15432), human α<sub>1</sub> nicotinic acetylcholine receptor subunit (h Ach α<sub>1</sub>; Swiss-Prot P02708) and human 5-HT<sub>3A</sub> subunit (h 5-HT<sub>3A</sub>; Swiss-Prot P46098), using MULTALIN ([http://pbil.ibcp.fr/cgi-bin/align\\_multalin.pl](http://pbil.ibcp.fr/cgi-bin/align_multalin.pl)). The first two Cys residues define the signature loop common to all nAChR superfamily subunits, and the second two Cys define Loop C in nAChR. Sixteen highlighted residues on GluCl β were mutated to alanine. At Y182 and Y232 (yellow residues), tyrosine was also mutated to phenylalanine and tryptophan. Y182 aligns with W149 at nAChR, the site of a cation-π interaction with the ligand. T229 and Y232 (yellow residues) align with the crucial nAChR Y190 and Y198, respectively. I269 aligns with I244 in glycine receptor. Six additional mutations to alanine in Loop C were performed, where the residue is not glycine. The other 6 residues are basic in GluCl α and GluCl β but not in the other receptors, suggesting they may interact with the acidic group of glutamate. These residues were also mutated to alanine.

We also generated and analyzed 6 additional X→A mutations in Loop C (Vandenberg et al., 1993; Rajendra et al., 1995), where X is not glycine (highlighted in green, Figure legends, Figure 3-1). They are T224A, S225A, H226A, T227A, N228A and S231A. Red residues in Figure 3-1 (R66, K70, R131, K202, K236 and K242) are basic in GluCl  $\alpha$  and GluCl  $\beta$ , but not in the other receptors, suggesting that they may interact with the acidic group of glutamate; we mutated these residues to alanine as well.

### **Glutamate and IVM responses of WT GluCl receptors**

Heteromeric receptors expressed robustly after injections of 25 pg each of cRNA for the GluCl  $\alpha$  and  $\beta$  subunits (termed WT). Response amplitudes were  $304 \pm 18$  nA (n = 33) to 1 mM glutamate and  $675 \pm 26$  nA to 1  $\mu$ M IVM (n = 26). Figure 3-2 (top panel) presents an example of WT responses to the agonists. 1 mM glutamate induced a rapid and reversible current (348 nA) while 1  $\mu$ M IVM induced a slow and irreversible current (596 nA). The  $EC_{50}$  and the Hill coefficient for WT are  $0.48 \pm 0.08$   $\mu$ M and  $1.76 \pm 0.31$  for IVM and  $0.32 \pm 0.05$  mM and  $1.69 \pm 0.07$  (n = 6) for glutamate, respectively.

As expected from previous data (Cully et al., 1994), responses were much smaller for equivalent injections of individual cRNAs, which presumably encoded homomeric receptors. When 25 pg cRNA of GluCl  $\alpha$  or GluCl  $\beta$  was injected, the average responses to 1  $\mu$ M IVM or 1 mM glutamate were  $24 \pm 6$  nA (n = 6) or  $79 \pm 8$  nA (n=10), respectively, some tenfold smaller than the heteromeric responses. Responses were considerably larger with injection of 250 pg cRNA for the individual subunits. Oocytes injected with 250 pg GluCl  $\alpha$  cRNA displayed an IVM dose-response relation with an  $EC_{50}$  of  $0.52 \pm 0.06$   $\mu$ M, a Hill coefficient of  $2.24 \pm 0.35$ , and maximal responses of 1.68

FIGURE 3-2

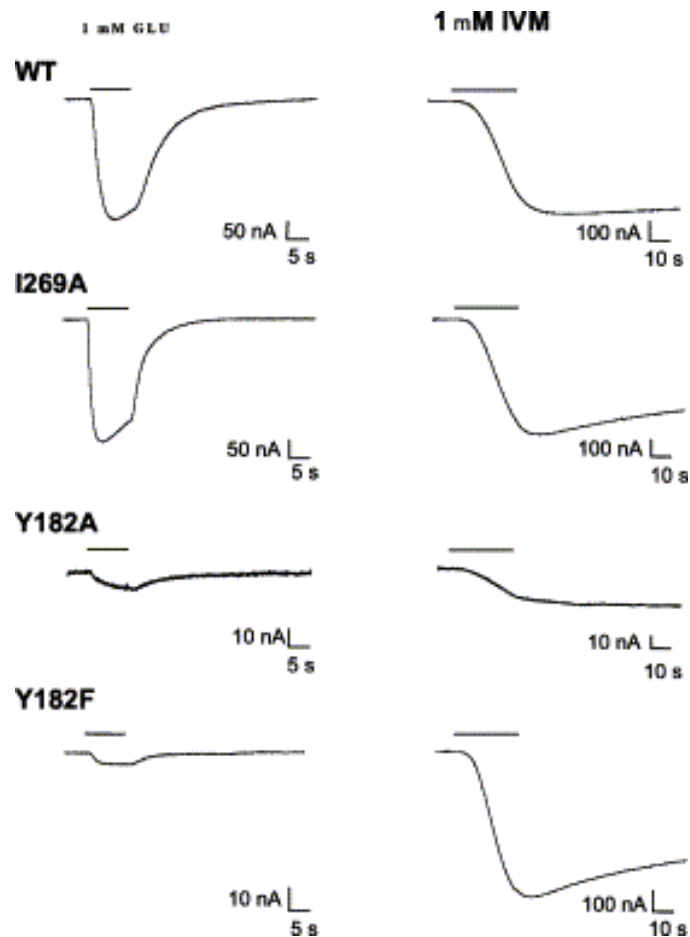


Figure 3-2: **Electrophysiological characterization of WT and three mutated GluCl constructs.** Left-hand column, responses to 1 mM glutamate (GLU); right-hand column, responses to 1  $\mu$ M ivermectin (IVM); the latter are slower than the glutamate responses and irreversible on the time scale of the experiments. The top row shows responses in an oocyte injected with GluCl  $\alpha\beta$ (WT) from *C. elegans*. Oocytes injected with GluCl  $\alpha\beta$ (I269A) responded well to both glutamate and IVM. The  $\alpha\beta$ (Y182A) mutant GluCl abolished both glutamate and IVM responses. The bottom row shows glutamate sensitivity was abolished but IVM sensitivity was retained in GluCl  $\alpha\beta$ (Y182F). For each mutant, the two traces shown were obtained from one oocyte. Horizontal line over the traces indicates the application time of agonists. *Xenopus* oocytes were injected with 25 pg of both WT  $\alpha$  RNA and WT (or mutated)  $\beta$  RNA.

$\pm 0.25 \mu\text{A}$  ( $n = 8$ ); there was little or no response to glutamate. For injections of 250 pg GluCl  $\beta$  cRNA, the responses to glutamate displayed an  $\text{EC}_{50}$  of  $0.24 \pm 0.01 \text{ mM}$ , a Hill coefficient of  $1.56 \pm 0.28$  ( $n=5$ ), and maximal response of  $0.90 \pm 0.13 \mu\text{A}$  ( $n = 15$ ); responses to IVM were small or absent. The homomeric receptors showed more rapid kinetics (activation, desensitization and deactivation) than the heteromeric responses; we did not study this phenomenon systematically.

### **Glutamate and IVM responses at mutant receptors**

In our first round of mutagenesis experiments, 4 constructs were tested in oocytes. GluCl  $\alpha\beta$ (T229A) and GluCl  $\alpha\beta$ (I269A) responded like WT: no significant difference was found ( $p > 0.05$ ,  $n = 20$ ). Figure 3-2 (second row) shows the currents induced from an oocyte injected with GluCl  $\alpha\beta$ (I269A), 360 nA and 710 nA for glutamate and IVM, respectively. On the other hand, GluCl  $\alpha\beta$ (Y182A) and GluCl  $\alpha\beta$ (Y232A) abolished both glutamate and IVM sensitivities (Figure 3-2, third row).

Fifteen additional mutants were examined in the second round (summarized in Table 1). Mutations to Ala (X $\rightarrow$ A) at H226, T227, N228, or S231 did not affect functional expression ( $p > 0.05$ ,  $n = 6$ ); mutations of T224, R131 or K202, did not affect glutamate response but modestly reduced (2-3 fold) the IVM response; and mutations at R66, K70, R236 and K242 decreased both glutamate and IVM responses. Mutations (Y $\rightarrow$ W) at Y182 and Y232 also destroyed both glutamate and IVM sensitivities. GluCl  $\alpha\beta$ (S225A) significantly increased the glutamate response to 223% of WT levels ( $p < 0.05$ ,  $n = 6$ ). Thus, none of these mutations achieved the desired results.

TABLE 3-1

GluCl	Glutamate $I/I_{\alpha\beta(WT)}$	IVM $I/I_{\alpha\beta(WT)}$
$\alpha(WT)$	0	$0.13 \pm 0.04$
$\beta(WT)$	$0.10 \pm 0.02$	0
$\alpha\beta(WT)$	1	1
$\alpha\beta(Y182A)$	$0.01 \pm 0.01$	$0.05 \pm 0.02$
$\alpha\beta(T229A)$	$0.98 \pm 0.17$	$0.85 \pm 0.29$
$\alpha\beta(Y232A)$	$0.02 \pm 0.01$	$0.12 \pm 0.05$
$\alpha\beta(I269A)$	$1.36 \pm 0.20$	$1.29 \pm 0.48$
$\alpha\beta(Y182F)$	$0.16 \pm 0.03$	$1.06 \pm 0.27$
$\alpha\beta(Y182W)$	$0.14 \pm 0.05$	$0.32 \pm 0.14$
$\alpha\beta(Y232F)$	N/A	N/A
$\alpha\beta(Y232W)$	$0.14 \pm 0.06$	$0.29 \pm 0.16$
$\alpha\beta(T224A)$	0.739	0.352
$\alpha\beta(S225A)$	2.23	0.87
$\alpha\beta(H226A)$	1.10	0.91
$\alpha\beta(T227A)$	0.85	0.73
$\alpha\beta(N228A)$	0.93	1.20
$\alpha\beta(S231A)$	0.76	1.40
$\alpha\beta(R66A)$	0.15	0.45
$\alpha\beta(K70A)$	0.48	0.58
$\alpha\beta(R131A)$	0.85	0.51
$\alpha\beta(K202A)$	1.17	0.55
$\alpha\beta(R236A)$	0.02	0.21
$\alpha\beta(K242A)$	$0.13 \pm 0.06$	$0.56 \pm 0.15$

Table 3-1: **Summary of glutamate and ivermectin effects on WT and mutant GluCls.** All mutants were in the  $\beta$  subunit. All values were averaged from at least 5 oocytes. For those mutants examined in more than 2 batches of oocytes, data are presented as mean  $\pm$  S.E.M.

### **GluCl $\alpha\beta$ (Y182F) eliminates glutamate responses while retaining IVM responses**

At position Y182 of the GluCl  $\beta$  subunit, 3 mutations were constructed (Y $\rightarrow$ A, W, F). The mutants GluCl  $\alpha\beta$ (Y182A) and GluCl  $\alpha\beta$ (Y182W) abolished the response of both glutamate and IVM. However, GluCl  $\alpha\beta$ (Y182F) meets our requirement. An example is shown in Figure 3-2 (bottom row). 1 mM glutamate induced a tiny current ( $\sim 5$  nA) in the oocyte that expressed GluCl  $\alpha\beta$ (Y182F), while 1  $\mu$ M IVM induced a current of 827 nA. On average, Y182F, when coexpressed with WT GluCl  $\alpha$ , reduced the glutamate response to  $15.8 \pm 3.4\%$  of WT levels but hardly changed IVM responses ( $106 \pm 27\%$ ) ( $n = 78$ ) (Figure 3-3A). For GluCl  $\alpha\beta$ (Y182F), the  $EC_{50}$  and Hill coefficient for glutamate is  $0.32 \pm 0.05$  mM and  $1.33 \pm 0.25$  ( $n = 5$ ), respectively, similar to those of WT ( $0.36 \pm 0.04$  mM;  $1.78 \pm 0.22$ ,  $n = 6$ ) (Figure 3-3B), indicating that the mutant decreases the efficacy of glutamate, but not the potency.

Tyr-182 aligns with nicotinic receptor residue Trp149, which plays an important role in a cation- $\pi$  interaction with the quaternary ammonium moiety of acetylcholine (Zhong et al., 1998; Brejc et al., 2001). We conclude that this residue also plays an important role in the binding or response to both glutamate and IVM in the GluCl  $\beta$  subunit. The interaction with both ligands is abolished by mutating the Tyr to Ala or to Trp, but only the interaction with glutamate is weakened by mutations to Phe. The available data did not allow a decision about the nature of the moiety that interacts with Tyr182, or the nature of the interaction.

### **Functional Expression of fluorescent protein-tagged constructs**

Three fluorescent proteins (EGFP, EYFP, ECFP; XFP) were separately inserted into

## FIGURE 3-3

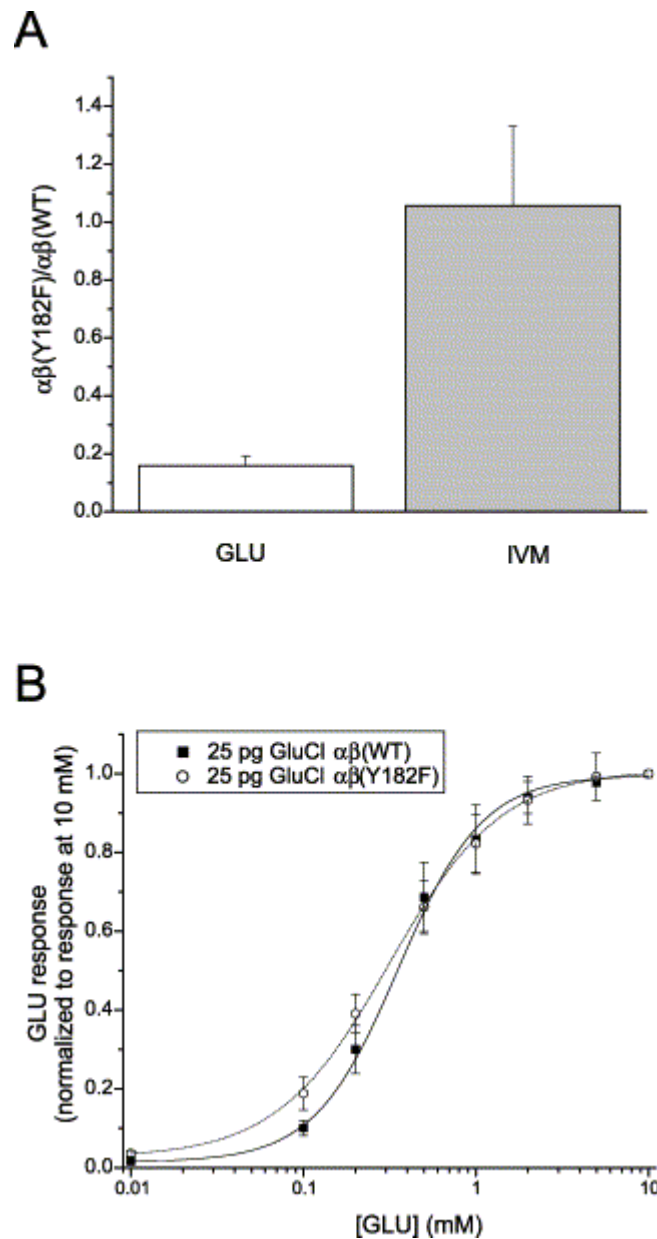


Figure 3-3: **GluCl  $\alpha\beta$ (Y182F) eliminates glutamate sensitivity and retains ivermectin sensitivity.** A, GluCl  $\alpha\beta$ (Y182F) reduces the glutamate response to 15.8 % of WT levels but hardly changes IVM responses (106% of WT values). The values were pooled from 78 oocytes of 6 batches, injected with 25 pg to 250 pg of cRNA for each subunit. Error bars are S.E.M. B, normalized glutamate dose-response relations for WT and GluCl  $\alpha\beta$  (Y182F). For GluCl  $\alpha\beta$  (Y182F) (open symbols, dashed line), the curve represents an EC<sub>50</sub> of 0.32 mM and an n<sub>H</sub> of 1.33 (n = 5), similar to those of the WT GluCl  $\alpha\beta$  (closed symbols, solid line) (0.36 mM; 1.78, n = 6).

the M3-M4 loop of the GluCl  $\alpha$ ,  $\beta$  and  $\beta$ (Y182F). Firstly, functional expression of GluCl  $\alpha$ (GFP), GluCl  $\alpha$ (YFP), GluCl  $\beta$ (CFP) and GluCl  $\beta$ (Y182F)(CFP) were expressed as homomers in oocytes and compared with GluCl  $\alpha$ ,  $\beta$  and  $\beta$ (Y182F), respectively. No significant difference was observed ( $p > 0.05$ ,  $n > 6$ , data not shown). Then heteromers with XFP tags in only the  $\alpha$  or  $\beta$  subunit constructs were examined. Data for one of these constructs are given in Figure 3-4A. No significant difference was found between GluCl  $\alpha\beta$ (Y182F) and GluCl  $\alpha\beta$ (Y182F)(CFP) ( $p > 0.05$ ,  $n = 9$ ). Like GluCl  $\alpha\beta$ (Y182F), GluCl  $\alpha\beta$ (Y182F)(CFP) abolished the glutamate response to 10.9% of the WT level and almost kept the IVM response (84.6% of the WT level) ( $n = 7$ ). Finally, doubly-XFP-tagged constructs were expressed to the oocytes. Three different molar concentrations of RNA were compared with WT and XFPs. There is no significant difference ( $p > 0.05$ ,  $n > 6$ ) between the responses in oocytes injected with equal molar concentration of WT and XFP RNA (Figure 3-4B). The grand averaged data from 30 oocytes showed that XFP hardly changed the response to both glutamate and IVM ( $90.8 \pm 14.2\%$  and  $92.0 \pm 7.1\%$  of WT level, respectively) (Figure 3-4C). The re-engineered GluCl channel, without glutamate sensitivity but with a fluorescent tag, may be more useful in GluCl silencing strategies.

### **Critique of the GluCl/IVM strategy**

Channel-based silencing strategies could mimic either the endogenous inhibition arising from activation of  $K^+$  channels (for instance,  $GABA_B$  receptors coupled to GIRK channels) or that arising from activation of  $Cl^-$  channels (for instance,  $GABA_A$  receptors). Most strategies employ  $K^+$  channels (Johns et al., 1999; Sutherland et al., 1999; Nadeau et al., 2000; Falk et al., 2001; Scarce-Levie et al., 2001; White et al.,

## FIGURE 3-4

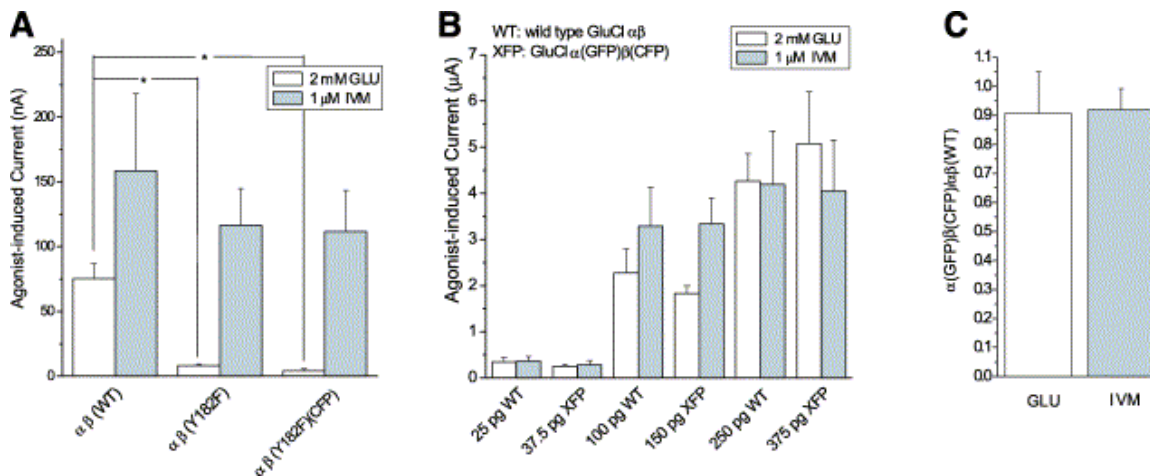


Figure 3-4. **Functional expression of fluorescent protein-tagged constructs.** *A*, comparison among GluCl  $\alpha\beta$ ,  $\alpha\beta$ (Y182F) and  $\alpha\beta$ (Y182F)(CFP). No significant difference is found between the functional expression of  $\beta$ (Y182F) and  $\beta$ (Y182F)(CFP). All values were averaged from 6 to 9 oocytes. Error bars are S.E.M and asterisks represent significant difference between 2 groups ( $P < 0.05$ ). Oocytes were coinjected with 25 pg WT  $\alpha$  RNA and 25 pg WT  $\beta$ ,  $\beta$ (Y182F) or 37.5 pg  $\beta$ (Y182F)(CFP) RNA, respectively. *B*, bar plots compare WT and GluCl  $\alpha(\text{GFP})\beta(\text{CFP})$  (termed XFP). There is no significant difference ( $P > 0.05$ ) between the responses in oocytes injected with equal molar concentration of WT and XFP RNA. *C*, grand average from 30 oocytes injected with 3 concentrations (25 pg, 100 pg and 250 pg for each subunit of WT; 37.5 pg, 150 pg and 375 pg for each subunit of XFP). The glutamate and IVM responses of XFP are 90.8% and 92.0% of WT levels, respectively.

2001a; White et al., 2001b; Lechner et al., 2002).  $K^+$  channels have the advantage that they can be chosen, or modified, to display various voltage-dependent and rectifying characteristics.  $K^+$  channels have the disadvantage that sustained  $K^+$  efflux (or  $Na^+$  entry) causes apoptosis under some circumstances (Nadeau et al., 2000).

The GluCl/IVM strategy (Slimko et al., 2002) is, to our knowledge, unique among artificial silencing strategies because it employs  $Cl^-$  channels. In most cells, intracellular  $[Cl^-]$  is on the order of a few mM; as a result, if  $G_{Cl}$  rises, intracellular  $Cl^-$  is expected to be driven by the  $K^+$  gradient. Therefore a high  $Cl^-$  conductance is expected to clamp the cell near  $E_K$ , or slightly hyperpolarized from the normal resting potential, and to cause only minor changes in intracellular  $Cl^-$ . One possible disadvantage to this strategy involves such neurons as dorsal root ganglia neurons and many immature central nervous system neurons, whose complement of transporters leads to a relatively high intracellular  $Cl^-$  and therefore a depolarized  $E_{Cl}$ . In such a cell, the GluCl/IVM strategy might cause  $E_{Cl}$  and  $E_K$  to approach each other, possibly leading to KCl loss and to cell shrinkage. It is encouraging that in previous experiments on dorsal root ganglion cells, a heterologously expressed, continuously active  $Cl^-$  conductance did cause a hyperpolarizing shift in  $E_{Cl}$ , but neither shrank nor killed the cells (Staley et al., 1996).

**Acknowledgments:** We thank Kira Kostenko and Carrie Shilyansky for help with the oocytes and members of our research group for helpful discussion. This research was supported by a grant from the National Institutes of Health (NS-11756) and by internal Caltech venture funds.

## References

- Brejč K, van Dijk WJ, Klaassen RV, Schuurmans M, van Der Oost J, Smit AB, Sixma TK (2001) Crystal structure of an ACh-binding protein reveals the ligand-binding domain of nicotinic receptors. *Nature* 411:269-276.
- Corringer PJ, Le Novère N, Changeux JP (2000) Nicotinic receptors at the amino acid level. *Annu Rev Pharmacol Toxicol* 40:431-458.
- Cully DF, Vassilatis DK, Liu KK, Paress PS, Van der Ploeg LH, Schaeffer JM, Arena JP (1994) Cloning of an avermectin-sensitive glutamate-gated chloride channel from *Caenorhabditis elegans*. *Nature* 371:707-711.
- Curtis L, Chiodini F, Spang JE, Bertrand S, Patt JT, Westera G, Bertrand D (2000) A new look at the neuronal nicotinic acetylcholine receptor pharmacophore. *Eur J Pharmacol* 393:155-163.
- Dougherty DA, Lester HA (2001) Neurobiology. Snails, synapses and smokers. *Nature* 411:252-253, 255.
- Etter A, Cully DF, Liu KK, Reiss B, Vassilatis DK, Schaeffer JM, Arena JP (1999) Picrotoxin blockade of invertebrate glutamate-gated chloride channels: subunit dependence and evidence for binding within the pore. *J Neurochem* 72:318-326.
- Falk T, Kilani RK, Yool AJ, Sherman SJ (2001) Viral vector-mediated expression of K<sup>+</sup> channels regulates electrical excitability in skeletal muscle. *Gene Ther* 8:1372-1379.
- Gensler S, Sander A, Korngreen A, Traina G, Giese G, Witzemann V (2001) Assembly and clustering of acetylcholine receptors containing GFP-tagged epsilon or gamma subunits: selective targeting to the neuromuscular junction in vivo. *Eur J Biochem* 268:2209-2217.
- Han NL, Haddrill JL, Lynch JW (2001) Characterization of a glycine receptor domain that controls the binding and gating mechanisms of the beta-amino acid agonist, taurine. *J Neurochem* 79:636-647.
- Johns DC, Marx R, Mains RE, O'Rourke B, Marban E (1999) Inducible genetic suppression of neuronal excitability. *J Neurosci* 19:1691-1697.
- Lechner HA, Lein ES, Callaway EM (2002) A genetic method for selective and quickly reversible silencing of Mammalian neurons. *J Neurosci* 22:5287-5290.
- Nadeau H, McKinney S, Anderson DJ, Lester HA (2000) ROMK1 (Kir1.1) causes apoptosis and chronic silencing of hippocampal neurons. *J Neurophysiol* 84:1062-1075.

- Okada T, Yamada N, Kakegawa W, Tsuzuki K, Kawamura M, Nawa H, Iino M, Ozawa S (2001) Sindbis viral-mediated expression of Ca<sup>2+</sup>-permeable AMPA receptors at hippocampal CA1 synapses and induction of NMDA receptor-independent long-term potentiation. *Eur J Neurosci* 13:1635-1643.
- Pedersen SE, Dreyer EB, Cohen JB (1986) Location of ligand-binding sites on the nicotinic acetylcholine receptor alpha-subunit. *J Biol Chem* 261:13735-13743.
- Rajendra S, Vandenberg RJ, Pierce KD, Cunningham AM, French PW, Barry PH, Schofield PR (1995) The unique extracellular disulfide loop of the glycine receptor is a principal ligand binding element. *Embo J* 14:2987-2998.
- Scearce-Levie K, Coward P, Redfern CH, Conklin BR (2001) Engineering receptors activated solely by synthetic ligands (RASSLs). *Trends Pharmacol Sci* 22:414-420.
- Shan Q, Haddrill JL, Lynch JW (2001) Ivermectin, an unconventional agonist of the glycine receptor chloride channel. *J Biol Chem* 276:12556-12564.
- Slimko E, McKinney S, Anderson D, Davidson N, Lester HA (2002) Selective electrical silencing of mammalian neurons in vitro using invertebrate ligand-gated chloride channels. *J Neurosci* (in press).
- Staley K, Smith R, Schaack J, Wilcox C, Jentsch TJ (1996) Alteration of GABA<sub>A</sub> receptor function following gene transfer of the CLC-2 chloride channel. *Neuron* 17:543-551.
- Sutherland ML, Williams SH, Abedi R, Overbeek PA, Pfaffinger PJ, Noebels JL (1999) Overexpression of a Shaker-type potassium channel in mammalian central nervous system dysregulates native potassium channel gene expression. *Proc Natl Acad Sci U S A* 96:2451-2455.
- Vandenberg RJ, Rajendra S, French CR, Barry PH, Schofield PR (1993) The extracellular disulfide loop motif of the inhibitory glycine receptor does not form the agonist binding site. *Mol Pharmacol* 44:198-203.
- White B, Osterwalder T, Keshishian H (2001a) Molecular genetic approaches to the targeted suppression of neuronal activity. *Curr Biol* 11:R1041-1053.
- White BH, Osterwalder TP, Yoon KS, Joiner WJ, Whim MD, Kaczmarek LK, Keshishian H (2001b) Targeted attenuation of electrical activity in *Drosophila* using a genetically modified K(+) channel. *Neuron* 31:699-711.
- Xue H (1998) Identification of major phylogenetic branches of inhibitory ligand-gated channel receptors. *J Mol Evol* 47:323-333.
- Zhong W, Gallivan JP, Zhang Y, Li L, Lester HA, Dougherty DA (1998) From ab initio quantum mechanics to molecular neurobiology: a cation-pi binding site in the

nicotinic receptor. Proc Natl Acad Sci U S A 95:12088-12093.

*Chapter 4***Codon optimization of *C. elegans* GluCl ion channel genes for mammalian cells dramatically improves expression levels**

Text of this chapter is reproduced, with minor editing, from:

Slimko EM, Lester HA (2003). Codon optimization of *C. elegans* GluCl ion channel genes for mammalian cells dramatically improves expression levels. *J Neurosci Methods* 14: 75-81

## Abstract

Organisms use synonymous codons in a highly non-random fashion. These codon usage biases sometimes frustrate attempts to express high levels of exogenous genes in hosts of widely divergent species. The *C. elegans* GluCl $\alpha$ 1 and GluCl $\beta$  genes form a functional glutamate and ivermectin-gated chloride channel when expressed in *Xenopus* oocytes, but expression is weak in mammalian cells. We have constructed synthetic genes that retain the amino acid sequence of the wild-type GluCl channel proteins, but use codons that are optimal for mammalian cell expression. We have tagged the native and codon-optimized GluCl cDNAs with enhanced yellow fluorescent protein (EYFP, GluCl $\alpha$ 1 subunit) and enhanced cyan fluorescent protein (EFCP, GluCl $\beta$  subunit), expressed the channels in E18 rat hippocampal neurons, and measured the relative expression levels of the two genes with fluorescence microscopy as well as with electrophysiology. Codon optimization provides a six- to nine-fold increase in expression, allowing the conclusions that the ivermectin-gated channel has an EC<sub>50</sub> of 1.2 nM and a Hill coefficient of 1.9. We also confirm that the Y182F mutation in the codon-optimized  $\beta$  subunit results in a heteromeric channel that retains the response to ivermectin while reducing the response to 100 $\mu$ M glutamate by seven-fold. The engineered GluCl channel is the first codon-optimized membrane protein expressed in mammalian cells and may be useful for selectively silencing specific neuronal populations *in vivo*.

## Introduction

Comparative genomic studies show that organisms use synonymous codons in a nonrandom, species-specific fashion (Bernardi, 1985; Nakamura et al., 1996; Kanaya et al., 2001). In *E. coli*, this non-random codon usage appears to parallel expression levels of the cognate tRNAs (Ikemura, 1981a, b). Several authors suggest that high-level expression of genes containing non-optimal codons may be limited by the availability of tRNA for rare codons (Kane, 1995). Codon optimization strategies enable the high-level expression of therapeutically relevant human proteins in *E. coli* (Hernan et al., 1992; Makrides, 1996), and in the yeasts *P. pastoris* and *S. cerevisiae* (Woo et al., 2002). There are fewer examples in which genes from evolutionarily old organisms have been optimized for expression in mammalian cells. Three successful examples include the optimization of green fluorescent protein from the jellyfish *A. porins* (Haas et al., 1996), the tetracycline transactivator from *E. coli* (Wells et al., 1999), and Cre recombinase (Shimshek et al., 2002). To date, there are no publications describing codon optimized membrane bound proteins.

We are developing a strategy that selectively and reversibly silences specific neuronal subpopulations in mammals via expression of the GluCl $\alpha$ 1 and GluCl $\beta$  genes from *C. elegans* (Li et al., 2002; Slimko et al., 2002); and we seek high-level expression of these two genes within mammalian neurons. Genes in the GluCl gene family are found in many invertebrates and are part of the nicotinic receptor superfamily, characterized by a large extracellular N-terminus, four transmembrane domains, and a

large loop between the third membrane spanning segment (M3) and the fourth segment (M4) (Cully et al., 1994). Many GluCl receptors are activated by the anthelmintic drug ivermectin (IVM), which is used both in humans and animals to treat a variety of parasitic diseases (del Giudice, 2002; Winnen et al., 2002). Our strategy is to express both GluCl $\alpha$ 1 and GluCl $\beta$  in specific neurons using tissue-specific promoters in transgenic animals or through local injection of viruses engineered to express these genes. Systematic administration of IVM will then reversibly activate a chloride conductance in the target neurons, reducing their excitability.

We are optimizing this GluCl / IVM strategy. First, the wild type GluCl channel genes seem to express poorly in mammalian neurons. While the weak expression appears partially due to the multi-subgenomic promoter Sindbis virus expression system (Slimko et al., 2002), we asked whether some of the problem arises from suboptimal codon usage. We have synthesized genes with codon usage similar to a compendium of highly expressed mammalian genes. Because previous work showed that tagging the channels with fluorescent proteins in the M3-M4 loops provides a convenient assay for membrane expression but does not alter function of the receptor (Gensler et al., 2001; Li et al., 2002), we also incorporated enhanced yellow and cyan fluorescent proteins (EYFP and ECFP) in the wild type and optimized genes. We find that codon optimization alone generates nearly a six- to nine-fold increase in the fluorescence, indicating a much higher expression level. We also present electrophysiological data that correlates with the fluorescence measurement.

A second GluCl optimization tactic requires minimizing the endogenous glutamate response of these channels with no decrease in the IVM response. We

previously showed that the Y182F mutation to the  $\beta$  subunit (Li et al., 2002) produces the desired abolition of glutamate but not IVM responses in an oocyte expression system. However, robust GluCl responses require IVM concentrations some 100-fold higher in oocyte systems than in mammalian cells. We therefore tested whether these desirable pharmacological characteristics also hold for the codon-optimized Y182F GluCl $\beta$  channel expressed in mammalian neurons. Indeed, this seems to be the case.

## Material and methods

*Molecular Biology.* The codon-optimized cDNAs (optGluCl $\alpha$ 1 and optGluCl $\beta$ ) were synthesized by Entelechon GmbH (Regensburg, Germany) and cloned into pcDNA3.1/TOPO-HIST from Invitrogen (Carlsbad, CA). EYFP was amplified by PCR from pEYFP-N1 from ClonTech (Palo Alto, CA) with the primers 5'-ACCGGTGAATTCCATGGTGAGCAAGGGCGAGGAG-3' and 5'-GCGGCCGGAATTCTTGTACAGCTCGTCCATGC-3' and cloned into the EcoRI site of optGluCl $\alpha$ 1. ECFP was amplified by PCR from pECFP-N1 from ClonTech with the primers 5'-GATGGTGAGCAAGGGCGAGGAG-3' and 5'-GTCTTGTACAGCTCGTCCATGCCG-3' and cloned into the PmlI site of optGluCl $\beta$ . The wild type fusion genes GluCl $\alpha$ 1-EYFP and GluCl $\beta$ -ECFP have previously been described (Li et al., 2002). The mutation Y182F of optGluCl $\beta$  was performed using Stratagene's QuikChange mutation kit with the following primers: 5'-TGCAACTTCGACCTGGTGTCTTCGCCCACACCATGAACGACATC-3' and 5'-GATGTCGTTTCATGGTGTGGGCGAAGGACACCAGGTTCGAAGTTGCA-3'. The

sequences for the optimized genes (described in Results) have been deposited in GenBank, accession number AY195802 for optGluCl $\alpha$ 1 and AY195803 for optGluCl $\beta$ .

*Neuronal culture and transfection.* One  $\mu$ g DNA of each tagged subunit was incubated with 20  $\mu$ g of Nupherin-neuron (BioMol Research Laboratories, Plymouth Meeting, PA) in 400  $\mu$ l of Neurobasal medium without phenol (Invitrogen, Carlsbad, CA), while 10  $\mu$ l of Lipofectamine 2000 (Invitrogen) was mixed in 400  $\mu$ l Neurobasal. After 15 min, the two solutions were combined and incubated 45 min. E18 rat hippocampal neuronal cultures in 35 mm culture dishes, at least 14 days in culture, were incubated in the resulting 800  $\mu$ l mixture for 2 - 4 h, and then the mixture was removed and replaced with the original 2 ml medium. Recordings were made 24-48 h later.

*Electrophysiology.* The bath solution was (in mM): 110 NaCl, 5.4 KCl, 1.8 CaCl $_2$ , 0.8 MgCl $_2$ , 10 HEPES, and 10 D-glucose, pH 7.4, osmolarity 230 mOsm. Patch pipettes were filled with a solution containing (in mM): 100 K gluconate, 0.1 CaCl $_2$ , 1.1 EGTA, 5 MgCl $_2$ , 10 HEPES, 3 ATP, 3 phosphocreatine, and 0.3 GTP, pH 7.2, 215 mOsm. For studying glutamate responses, 100 mM CsCl replaced the K gluconate in the pipette solution and 100  $\mu$ M CNQX was added to the bath and drug perfusion solution. Whole-cell voltage clamp was maintained using an Axopatch-1D amplifier controlled by a personal computer running pCLAMP 8 software via a Digidata 1200 interface (Axon Instruments, Union City, CA). Data were filtered at 2 kHz and digitized at 5 kHz. Holding potential was  $-60$  mV. Input conductance was measured by a 5 mV hyperpolarizing pulse. 100  $\mu$ M glutamate was applied focally to single voltage-clamped

neurons using a Picospritzer with a U-tube system providing the wash (Khakh et al., 1995). Under these conditions, the chloride current measured upon GluCl activation was inward.

*Imaging.* 24 h after transfection with the various combinations of constructs, cells were fixed by a 20-minute incubation in PBS with 4% paraformaldehyde and mounted in Vectashield H-1000 (Vector Laboratories, Burlingame, CA). Neurons were then imaged with a 100x objective using the EYFP filter set XF104-2 (Omega Optical, Brattleboro, VT) or the ECFP filter set XF114-2 and the pixel intensity was averaged over the soma for each neuron.

*Statistics.* Pooled data are shown as means  $\pm$  SEM.

## **Results**

### *Codon optimization*

We used a compendium of 52 highly expressed mouse genes (ribosomal proteins, polymerases, elongation factors, and heat-shock proteins) to create the mouse codon usage table shown in Figure 4-1 (Sakai et al., 2001). The codon adaptation index (CAI) quantifies the similarity between the codon usage of a specific gene and a species of interest (Sharp and Li, 1987). Table 4-1 presents the mouse CAI of wild type GluCl $\alpha$ 1, GluCl $\beta$ , and green fluorescent protein (GFP). A CAI value of unity would indicate that each codon of the gene under analysis is optimal. The wild type GluCl $\alpha$  and GluCl $\beta$ ,

FIGURE 4-1

	Mouse	Native	Optimized		Mouse	Native	Optimized		Mouse	Native	Optimized		Mouse	Native	Optimized				
Ala	GCU	32	<b>36</b>	12	Cys	UGU	47	47	0	Leu	CUU	13	21	0	Ser	UCU	22	13	0
	C	<b>40</b>	24	<b>84</b>		C	<b>53</b>	<b>53</b>	<b>100</b>		C	21	22	1		C	<b>26</b>	11	40
	A	19	28	0	Gln	CAA	19	<b>71</b>	5		A	6	13	0		A	12	<b>37</b>	0
	G	9	12	4		G	<b>42</b>	12	<b>99</b>		G	<b>42</b>	12	<b>99</b>		G	6	11	3
Arg	CGU	10	17	0	Glu	GAA	36	50	0	UUA	4	7	0	AGU		11	19	0	
	C	<b>23</b>	9	<b>85</b>		G	<b>64</b>	50	<b>100</b>	G	14	<b>25</b>	0	C	23	9	<b>57</b>		
	A	15	<b>25</b>	0	Gly	GGU	21	23	0	Lys	AAA	32	<b>63</b>	8	Thr	ACU	22	27	3
	G	21	15	2		C	<b>40</b>	17	<b>97</b>		G	<b>68</b>	37	<b>92</b>		C	<b>42</b>	11	<b>93</b>
	AGA	16	23	10		A	21	<b>60</b>	0	Pro	CCU	28	18	0		A	22	<b>49</b>	0
G	15	11	3	G	18	0	3	A	29		<b>49</b>	0	G	14	13	4			
Asn	AAU	41	<b>74</b>	5	His	CAU	40	<b>67</b>	0	Tyr	UAU	37	49	5	Val	GUU	18	<b>39</b>	3
	C	<b>59</b>	26	<b>95</b>		C	<b>60</b>	33	<b>100</b>		G	9	21	2		C	24	31	21
Asp	GAU	46	<b>79</b>	0	Ile	AUU	34	<b>63</b>	0		Phe	UUU	38	<b>50</b>	0	A	9	20	0
	C	<b>54</b>	21	<b>100</b>		C	<b>58</b>	21	<b>98</b>	C		<b>62</b>	50	<b>100</b>	G	<b>50</b>	10	<b>76</b>	
						A	8	16	2										

Figure 4-1. **Codon usage of native GluCl $\alpha$ 1 and  $\beta$  subunits compared with the optimized GluCl $\alpha$ 1 and  $\beta$  subunits synthesized in this study.** Percentage frequencies of the synonymous codons are shown for each corresponding amino acid. The most prevalent codon is shown in bold.

Gene	Native CAI	Optimized CAI
GFP	0.604	0.950
GluCl $\alpha$ 1	0.552	0.953
GluCl $\beta$	0.585	0.951

Table 4-1: **Codon Adaptation Index calculations**

with values of 0.55 and 0.58 respectively, score slightly poorer than the wild-type GFP value of 0.6. Because codon optimization has successfully increased the expression of GFP (Haas et al., 1996), we perform analogous modifications to the GluCl genes.

We chose the one or two most prevalent mouse codons for each amino acid (Figure 4-1) to generate a nucleotide sequence for both GluCl $\alpha$ 1 and GluCl $\beta$ . We analyzed the resulting nucleotide sequence with a splice site prediction tool from the Berkley Drosophila Genome Project (Reese et al., 1997), which revealed several potential donor or acceptor sites. We iteratively modified the nucleotide sequence to eliminate these sites. Additionally, we removed and added a number of restriction sites for convenience in cloning. The final optimized cDNAs for the GluCl $\alpha$ 1 and GluCl $\beta$  genes contain 399 and 352 silent mutations, respectively, leaving the amino-acid sequences identical to the wild type genes. The new sequences are provided in GenBank, accession number AY195802 for the optimized GluCl $\alpha$ 1 gene, which we call optGluCl $\alpha$ 1, and accession number AY195803 for the optimized GluCl $\beta$  gene, which we call optGluCl $\beta$ . Figure 4-1 presents the codon usage of the GluCl genes in their native form as well as after our optimization procedure. Codon optimization yielded a significant increase in the calculated CAI, as shown in Table 4-, which present comparative data for GFP/EGFP. All three genes have a CAI of roughly 0.6 with their native codon usage, and are nearly 1.0 after optimization.

These sequences were synthesized and tagged with fluorescent proteins in the M3-M4 loop. We found that codon optimization yielded a dramatic increase of the fluorescent signal of both GluCl $\alpha$ 1-EYFP and GluCl $\beta$ -ECFP. Figure 4-2 presents images of neurons transfected with the wild type and codon optimized versions of the

FIGURE 4-2

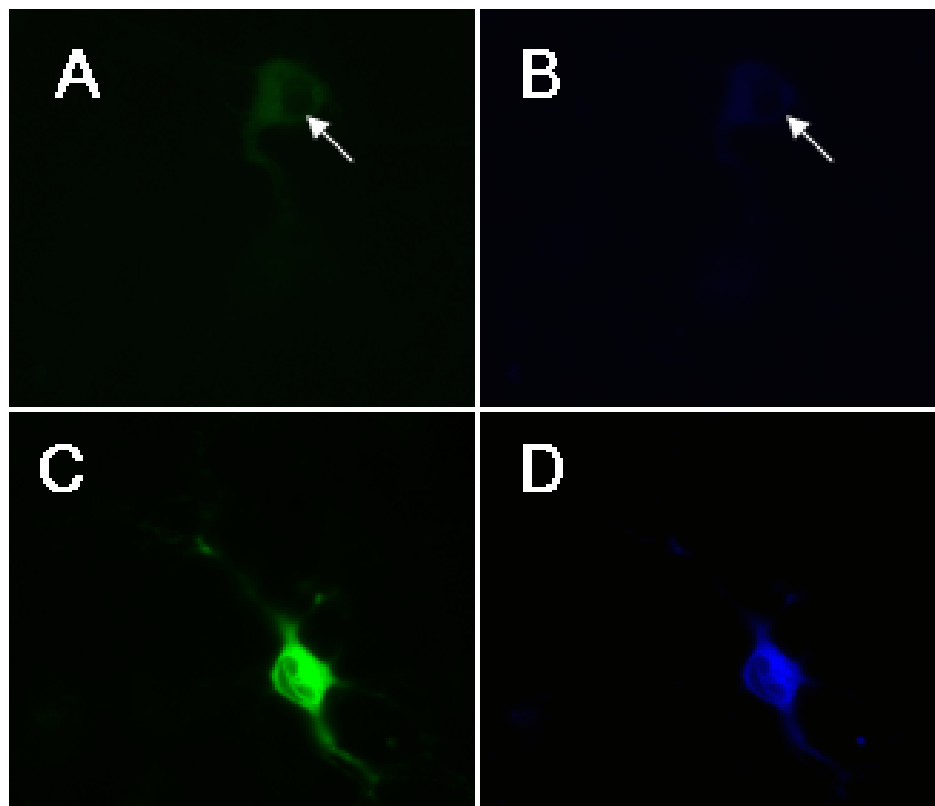


Figure 4-2. **Increase in channel expression as revealed by fluorescence microscopy.** (A,B) Native codon usage GluCl $\alpha$ 1-EYFP fusion and GluCl $\beta$ -ECFP fusion. The arrow indicates the position of the neuron in each panel. (C,D) Optimized codon usage optGluCl $\alpha$ 1-EYFP fusion and optGluCl $\beta$ -ECFP fusion. These are representative cells.

GluCl $\alpha$ 1 and GluCl $\beta$  genes. The increase in fluorescence is profoundly noticeable when the transfected cultures are viewed by eye: cells transfected with the wild type genes are barely visible, whereas those expressing the optimized genes are bright. The distribution of all four genes seems to be primarily somatic. There were no difference in localization between the wild type and optimized genes; this point has not been pursued systematically because a somatic localization is adequate for silencing. The average intensity of 10 cells transfected with each of the wild type and optimized GluCl $\alpha$ 1 and GluCl $\beta$  genes is shown in Figure 4-3A. Codon optimization alone has provided nearly a nine-fold increase in expression of the GluCl $\alpha$ 1 gene, and a six-fold increase in the expression of the GluCl $\beta$  gene. We attempted to achieve further increases in expression by replacing the signal peptide sequence and 5' untranslated region (UTR) of the optGluCl $\beta$  gene with that of a highly expressed mouse receptor, nAhCR  $\alpha$ 4. The result was no further increase in fluorescence intensity (data not shown).

Cotransfection of separate plasmids in this fashion yielded fluorescence signals that are highly correlated. Figure 4-4 shows the normalized ECFP fluorescence signal plotted against the normalized EYFP fluorescence signal for each of the 20 cells measured. In data not shown, we verified that there is no cross talk between the two channels. This satisfying result implies that there is roughly the same amount of each protein expressed in an individual cell, eliminating the potential complication that cell populations would contain GluCl channels of widely differing subunit compositions caused by variable expression of the two genes among cells.

We performed whole-cell patch clamping to measure the input conductance of neurons transfected with the heteromeric wild type GluCl and the heteromeric optimized

FIGURE 4-3

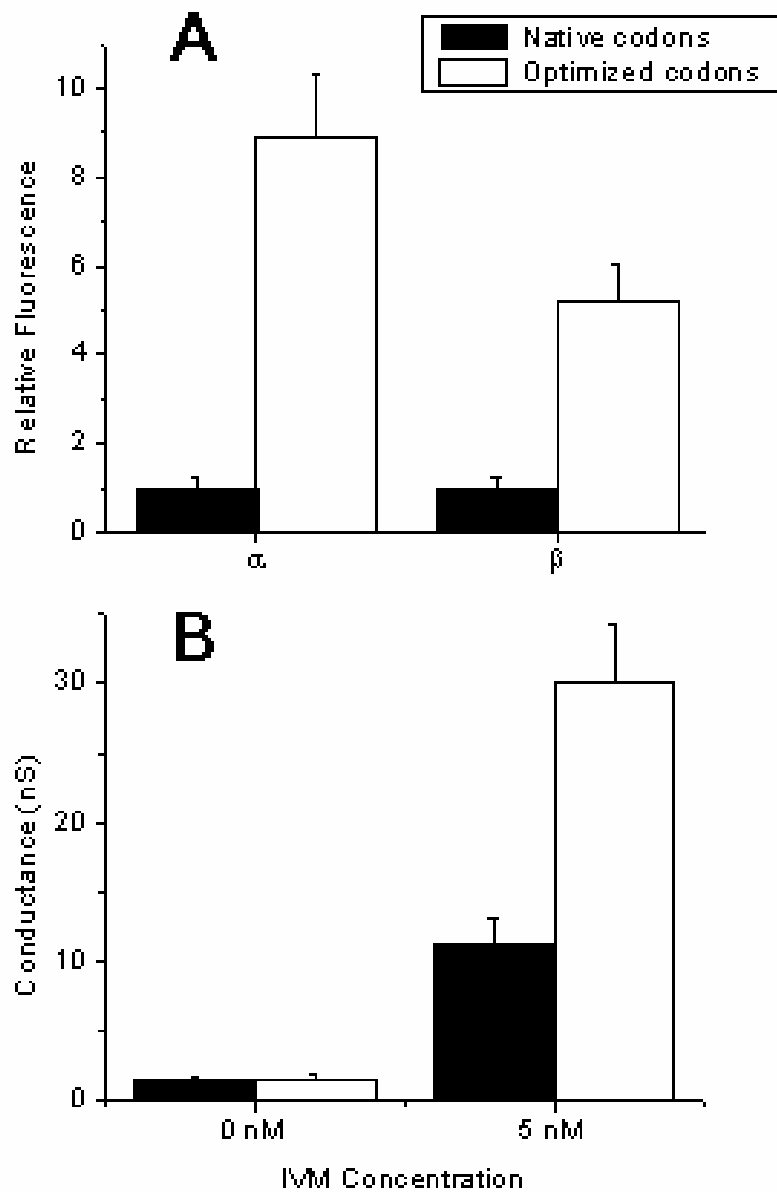


Figure 4-3. **Increase in expression measured by fluorescence microscopy and electrophysiology.**

(A) Increase in fluorescence measured by averaging 10 cells of both the native codon usage genes and optimized codon usage genes.

(B) Conductance of neurons in the absence and presence of 5 nM IVM. Each bar represents the average of 10 cells.

FIGURE 4-4

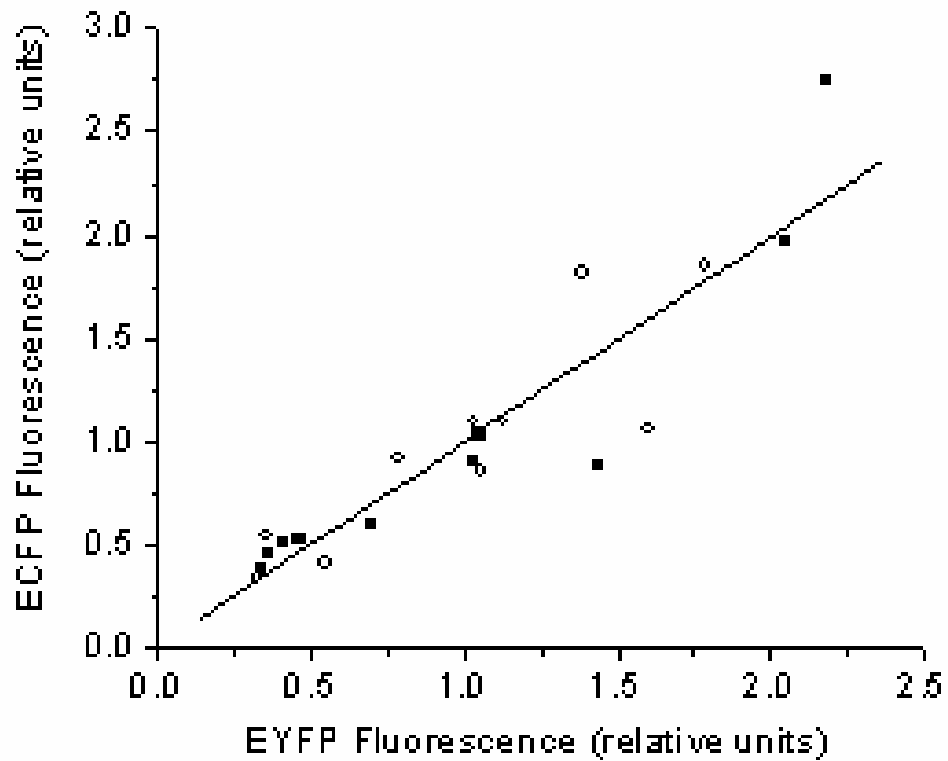


Figure 4-4: Correlation of signals in the two fluorescent channels, EYFP and ECFP, for neurons that have been cotransfected with both optGluCl $\alpha$ 1-EYFP and optGluCl $\beta$ -ECFP.

GluCl. Previous data show that an IVM concentration of approximately 5 nM applied to a GluCl-expressing neuron activates GluCl channel conductance sufficient to silence firing due either to glutamate activation or to current pulses (Slimko et al., 2002); but non-expressing neurons are unaffected by this concentration of IVM. The response of both the wild type and optimized constructs to this IVM concentration is presented in Figure 4-3B. The optimized GluCl genes lead to ~ three-fold greater IVM-induced conductance increase than in experiments with wild-type GluCl. This ratio is probably an underestimate, because only the most brightly fluorescent cells expressing nonoptimized subunits are chosen for patch-clamp study; and we believe that the results with fluorescence are closer to an unbiased average.

In a previous study, we were unable to measure accurate dose-response relations for IVM, due to variability in the expression levels of the genes. The higher expression level, combined with Nupherin-mediated transfection, enables more systematic study (Figure 4-5). The  $EC_{50}$  of the IVM-induced conductance is 1.3 nM, with a Hill coefficient of 1.9.

### ***Minimization of glutamate responses***

The native ligand for GluCl is glutamate, and we have been concerned that unintended GluCl activation by circulating or synaptically released glutamate may also inactivate neurons. Previously data showed that expression of GluCl $\alpha$ 1 and a mutated  $\beta$  subunit, GluCl $\beta$ Y182F, results in a heteromeric channel that retains its IVM response with an attenuated glutamate response (Li et al., 2002). We made the Y182F mutation in optGluCl $\beta$ -ECFP and co-expressed this gene with optGluCl $\alpha$ 1-EYFP in hippocampal cultures. The conductance increase caused by 5 nM IVM is statistically indistinguishable

FIGURE 4-5

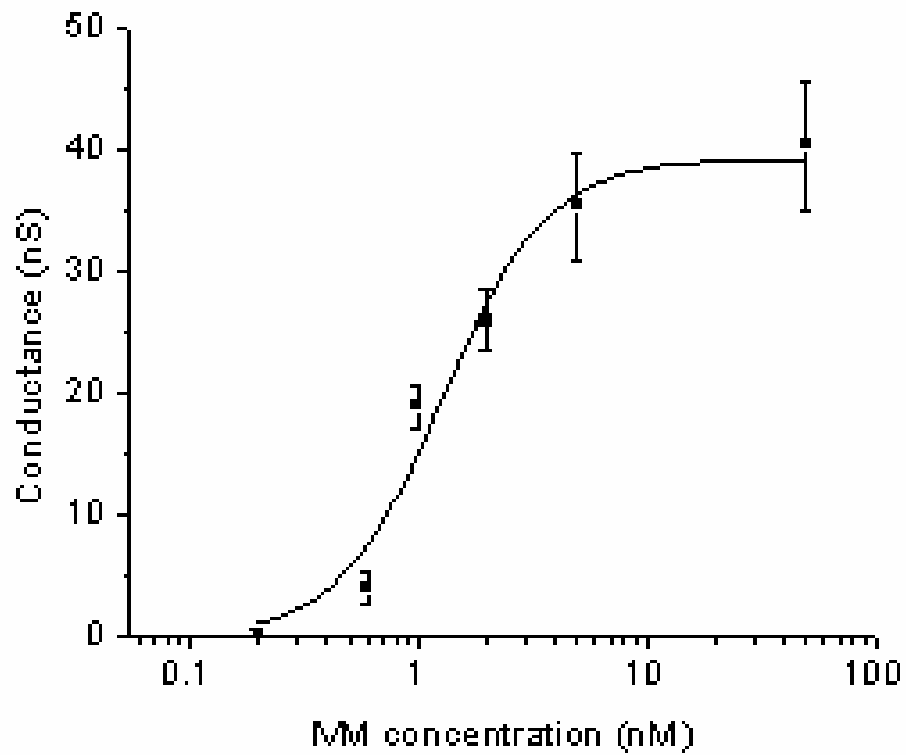


Figure 4-5: **Dose-response relation for activation of optGluCl channel by IVM.** EC50 is 1.2 nM and Hill coefficient is 1.9. Each point represents the average of the input conductance of 10 cells at the given concentration of IVM.

from the unmutated channel (Figure 4-6A). However, the maximal response to a 1 s application of 100  $\mu$ M glutamate is reduced seven-fold by this mutation, similar to previous *Xenopus* oocyte data (Figure 4-6B). In the glutamate response experiments, CsCl was used in the internal pipette solution and endogenous glutamate receptors were blocked with 100 $\mu$ M CNQX and untransfected control cells had no response to glutamate.

## Discussion

Researchers have used codon optimization to increase the expression of a variety of cytosolic proteins. The accompanying increase in expression ranges from modest, such as 1.6-fold for Cre (Shimshek et al., 2002) and 2-fold for rtTA (Wells et al., 1999), to dramatic, such as 40 to several hundred fold for both GFP and gp120 (Haas et al., 1996). This is the first published example of successful codon optimization to increase the expression of a membrane protein in mammalian cells. It is generally thought that membrane-bound proteins are limited in surface expression levels by trafficking, sorting, and exporting mechanisms, rather than by translation. However, we find that codon optimization provides a large (six- to nine-fold) enhancement of expression. There was little or no further enhancement when the signal peptide sequence of the optimized GluCl $\beta$  gene was replaced with the signal peptide of the mouse nicotinic  $\alpha$ 4 receptor. The codon optimization procedure may prove useful for other studies in which nonmammalian ion channels, transporters, and receptors are expressed in clonal mammalian cell cells, *e. g.*, for screening of antiparasitic drugs.

## FIGURE 4-6

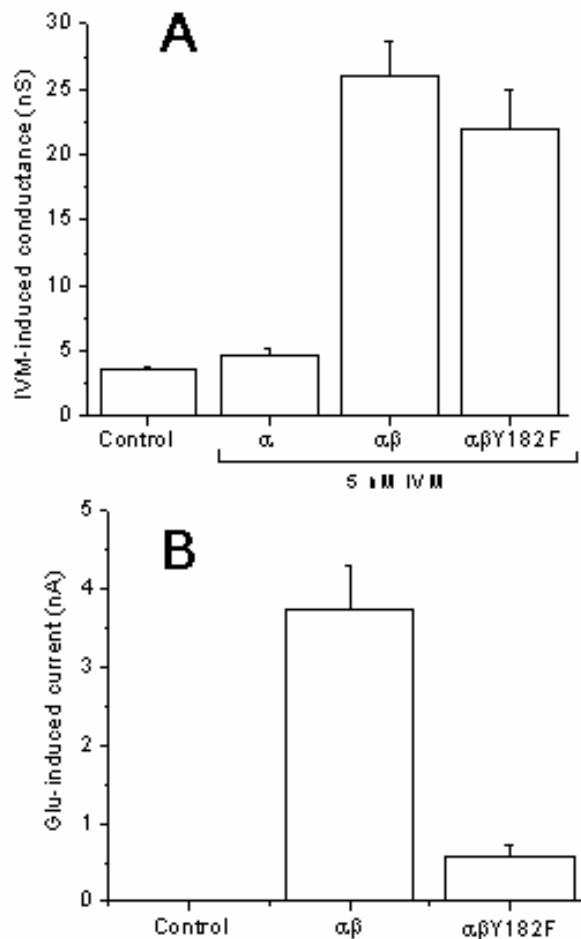


Figure 4-6. **Effects of optGluCl $\beta$  Y182F mutation.**

(A) Input conductance in the presence of 5 nM IVM. The control bar includes three groups of cells: cells that were not transfected and tested in the absence of IVM; cells that were not transfected and tested in the presence of 5 nM IVM; and cells transfected with optGlu $\alpha$ 1 and optGluCl $\beta$  or optGluCl  $\beta$ Y182F in the absence of IVM. There were no significant differences among these control groups. 5 nM IVM was applied to three groups of cells: cells transfected with optGluCl $\alpha$ 1 only ( $\alpha$ ); cells transfected with optGluCl $\alpha$ 1 and optGluCl $\beta$  ( $\alpha\beta$ ); and cells transfected with optGluCl $\alpha$ 1 and optGluCl $\beta$ Y182F ( $\alpha\beta$ Y182F). Note that the mutation has no effect on the IVM activation of the channel.

(B) The response to 100  $\mu$ M glutamate is severely attenuated with the  $\beta$ Y182F mutation. 100  $\mu$ M glutamate in the presence of 100  $\mu$ M CNQX was applied to three groups of cells: untransfected controls; cells expressing optGluCl  $\alpha$ 1 and optGluCl  $\beta$  ( $\alpha\beta$ ); and cells transfected with optGluCl  $\alpha$ 1 and optGluCl $\beta$ Y182F ( $\alpha\beta$ Y182F).

Several laboratories are developing genetic and pharmacological techniques for selectively silencing specific sets of neurons *in vivo* with mice or other animals (White et al., 2001; Lechner et al., 2002; Nitabach et al., 2002). Such techniques will presumably enable various experiments that may give us further insight into the system level functioning of the nervous system. The optimized, fluorescent GluCl constructs described here are activated by IVM concentrations of  $\sim 1$  nM, with little interference from endogenous glutamate responses, and with ready verification by fluorescence. This relatively low IVM concentration should help avoid known non-specific IVM effects (Krusek and Zemkova, 1994; Krause et al., 1998; Khakh et al., 1999; Shan et al., 2001). These GluCl subunits provide a robust system for high-efficiency silencing, and we consider that the channels are now appropriate for *in vivo* use. We are now turning our attention to efficient, specific *in vivo* expression. The two general strategies are (1) transgenic animals, and (2) local injection of viral vectors.

### **Acknowledgments**

This work was supported by National Institutes of Health (NS 11756 and MH 49176), by the Plum Foundation, and by the William T. Gimbel Discovery fund in Neuroscience. We thank David Anderson, Michael Fanselow, and Christof Koch for discussion and Sheri McKinney for help with cultures.

## References:

- Bernardi G. Codon usage and genome composition. *J Mol Evol*, 1985; 22: 363-5.
- Cully DF, Vassilatis DK, Liu KK, Paresse PS, Van der Ploeg LH, Schaeffer JM, Arena JP. Cloning of an avermectin-sensitive glutamate-gated chloride channel from *Caenorhabditis elegans*. *Nature*, 1994; 371: 707-11.
- del Giudice P. Ivermectin in scabies. *Curr Opin Infect Dis*, 2002; 15: 123-6.
- Gensler S, Sander A, Korngreen A, Traina G, Giese G, Witzemann V. Assembly and clustering of acetylcholine receptors containing GFP-tagged epsilon or gamma subunits: selective targeting to the neuromuscular junction in vivo. *Eur J Biochem*, 2001; 268: 2209-17.
- Haas J, Park EC, Seed B. Codon usage limitation in the expression of HIV-1 envelope glycoprotein. *Curr Biol*, 1996; 6: 315-24.
- Hernan RA, Hui HL, Andracki ME, Noble RW, Sligar SG, Walder JA, Walder RY. Human hemoglobin expression in *Escherichia coli*: importance of optimal codon usage. *Biochemistry*, 1992; 31: 8619-28.
- Ikemura T. Correlation between the abundance of *Escherichia coli* transfer RNAs and the occurrence of the respective codons in its protein genes: a proposal for a synonymous codon choice that is optimal for the *E. coli* translational system. *J Mol Biol*, 1981a; 151: 389-409.
- Ikemura T. Correlation between the abundance of *Escherichia coli* transfer RNAs and the occurrence of the respective codons in its protein genes. *J Mol Biol*, 1981b; 146: 1-21.
- Kanaya S, Yamada Y, Kinouchi M, Kudo Y, Ikemura T. Codon usage and tRNA genes in eukaryotes: correlation of codon usage diversity with translation efficiency and with CG-dinucleotide usage as assessed by multivariate analysis. *J Mol Evol*, 2001; 53: 290-8.
- Kane JF. Effects of rare codon clusters on high-level expression of heterologous proteins in *Escherichia coli*. *Curr Opin Biotechnol*, 1995; 6: 494-500.
- Khakh BS, Humphrey PP, Surprenant A. Electrophysiological properties of P2X-purinoreceptors in rat superior cervical, nodose and guinea-pig coeliac neurones. *J Physiol*, 1995; 484: 385-95.
- Khakh BS, Proctor WR, Dunwiddie TV, Labarca C, Lester HA. Allosteric control of gating and kinetics at P2X<sub>4</sub> receptor channels. *J Neurosci*, 1999; 19: 7289-99.

- Krause RM, Buisson B, Bertrand S, Corringer PJ, Galzi JL, Changeux JP, Bertrand D. Ivermectin: a positive allosteric effector of the alpha7 neuronal nicotinic acetylcholine receptor. *Mol Pharmacol*, 1998; 53: 283-94.
- Krusek J, Zemkova H. Effect of ivermectin on gamma-aminobutyric acid-induced chloride currents in mouse hippocampal embryonic neurones. *Eur J Pharmacol*, 1994; 259: 121-8.
- Lechner HA, Lein ES, Callaway EM. A genetic method for selective and quickly reversible silencing of Mammalian neurons. *J Neurosci*, 2002; 22: 5287-90.
- Li P, Slimko E, Lester H. Selective elimination of glutamate activation and introduction of fluorescent proteins into a *Caenorhabditis elegans* chloride channel. *FEBS Lett*, 2002; 528: 77.
- Makrides SC. Strategies for achieving high-level expression of genes in *Escherichia coli*. *Microbiol Rev*, 1996; 60: 512-38.
- Nakamura Y, Wada K, Wada Y, Doi H, Kanaya S, Gojobori T, Ikemura T. Codon usage tabulated from the international DNA sequence databases. *Nucleic Acids Res*, 1996; 24: 214-5.
- Nitabach MN, Blau J, Holmes TC. Electrical silencing of *Drosophila* pacemaker neurons stops the free-running circadian clock. *Cell*, 2002; 109: 485-95.
- Reese MG, Eeckman FH, Kulp D, Haussler D. Improved splice site detection in Genie. *J Comput Biol*, 1997; 4: 311-23.
- Sakai H, Washio T, Saito R, Shinagawa A, Itoh M, Shibata K, Carninci P, Konno H, Kawai J, Hayashizaki Y, Tomita M. Correlation between sequence conservation of the 5' untranslated region and codon usage bias in *Mus musculus* genes. *Gene*, 2001; 276: 101-5.
- Shan Q, Haddrill JL, Lynch JW. Ivermectin, an unconventional agonist of the glycine receptor chloride channel. *J Biol Chem*, 2001; 276: 12556-64.
- Sharp PM, Li WH. The codon Adaptation Index--a measure of directional synonymous codon usage bias, and its potential applications. *Nucleic Acids Res*, 1987; 15: 1281-95.
- Shimshek DR, Kim J, Hubner MR, Spengel DJ, Buchholz F, Casanova E, Stewart AF, Seeburg PH, Sprengel R. Codon-improved Cre recombinase (iCre) expression in the mouse. *Genesis*, 2002; 32: 19-26.
- Slimko EM, McKinney S, Anderson DJ, Davidson N, Lester HA. Selective electrical silencing of Mammalian neurons *in vitro* by the use of invertebrate ligand-gated chloride channels. *J Neurosci*, 2002; 22: 7373-9.

- Wells KD, Foster JA, Moore K, Pursel VG, Wall RJ. Codon optimization, genetic insulation, and an rtTA reporter improve performance of the tetracycline switch. *Transgenic Res*, 1999; 8: 371-81.
- White B, Osterwalder T, Keshishian H. Molecular genetic approaches to the targeted suppression of neuronal activity. *Curr Biol*, 2001; 11: R1041-53.
- Winnen M, Plaisier AP, Alley ES, Nagelkerke NJ, van Oortmarsen G, Boatin BA, Habbema JD. Can ivermectin mass treatments eliminate onchocerciasis in Africa? *Bull World Health Organ*, 2002; 80: 384-91.
- Woo JH, Liu YY, Mathias A, Stavrou S, Wang Z, Thompson J, Neville DM. Gene optimization is necessary to express a bivalent anti-human anti-T cell immunotoxin in *Pichia pastoris*. *Protein Expr Purif*, 2002; 25: 270-82.

*Chapter 5***Usage of the “GluCI/IVM” method in zebrafish to understand the role of retinal ganglion cells**

I thank Ethan Scott in Herwig Baier’s lab for performing the experiments reported here.

It has been a pleasure visiting Dr. Baier’s lab at UCSF to learn some of the visual behavior assays used in zebrafish. Text in this chapter is unpublished work.

## Abstract

We are developing a method for inducible and reversible cell-specific electrical silencing of vertebrate neurons *in vivo* called the “GluCl/IVM” method. The method employs a highly engineered chloride channel, optGluCl $\alpha$ -ECFP and optGluCl $\beta$ -Y182F-EYFP, from *C. elegans* that harbors three classes of modifications: 1) We identified a single mutagenesis site that ameliorates response to the native ligand glutamate while retaining response to the anthelmintic drug ivermectin, 2) we incorporated fluorophores into the two channel subunits to aid in visualization, and 3) we re-engineered the entire coding sequences to optimize expression levels in vertebrate systems. The *ath5* promoter drives expression in peripheral retinal ganglion cells (RGCs) in zebrafish. Using *ath5*, we generated transgenic zebrafish that express both optGluCl $\alpha$ -ECFP and optGluCl $\beta$ -Y182F-EYFP. Immunohistochemistry shows that the genes are expressed as expected in the retinal periphery at 5 days post fertilization. We performed three visual assays of these larvae, assessing behavioral changes of transgenic fish revealed by the presence of IVM: 1) visual background adaptation (VBA), 2) the optokinetic response (OKR), and 3) the optomotor response (OMR). Wild-type fish behavior is not modulated by IVM. While transgenic fish are normal in these assays when IVM is not present, they are completely deficient in VBA and significantly altered in OKR when IVM is present. OMR is normal in the presence of IVM. This finding allows us to conclude that the outer periphery of the retina is necessary for both normal VBA and normal OKR, while OMR does not require input from these cells. This is the second demonstration of a cell-specific selective silencing method driving a behavioral modulation in vertebrates.

## Introduction

Vertebrates exhibit numerous reflex behaviors that are driven by visual stimuli. In zebrafish and other teleosts, three prominent behaviors have been described, visual background adaptation (VBA), the optokinetic response (OKR), and the optomotor response (OMR) (Roeser and Baier, 2003). The VBA, used by the larvae to adapt its coloration to the local background, probably serves as a defensive reflex and the OKR and OMR probably serve to compensate for self-motion. The OKR (Figure 5-1A) encompasses smooth eye movements and rapid reset movements, or saccades. The OMR (Figure 5-1B) is a reflexive swimming in the direction of perceived motion. Fish use the OMR to maintain a stable position in a flowing river by responding to the apparent movement of visual cues present on the riverbed. VBA, OMR, and OKR can be reliably evoked in the laboratory at early larval stages. Numerous studies used these behaviors to identify mutations disrupting development and function of the visual system (Neuhauss et al., 1999; Kay et al., 2001).

It is not yet known where in the zebrafish brain, downstream of the retina, large – field motion is processed (Roeser and Baier, 2003). It is likely that dedicated circuits exist for these innate responses, but the neural substrates have not yet been identified. In zebrafish larvae, as early as 4 d post-fertilization (4 dpf), retinal ganglion cells (RGCs) project their axons to 10 different visual areas, referred to as “arborization fields” (Burrill and Easter, 1994). The proneural gene *atonal-homologue 5* (*ath5*) is closely associated with the activation of retinal neurogenesis in all vertebrates. The gene encodes a basic helix-loop-helix transcription factor expressed in a wave-like pattern that prefigures the wave of RGC genesis (Masai et al., 2000). *ath5* expression is first

## FIGURE 5-1

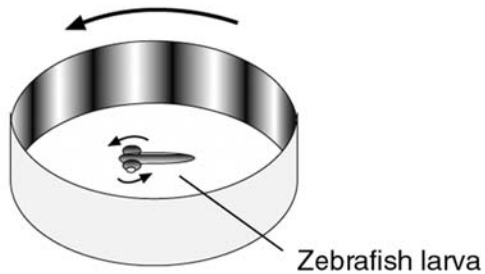
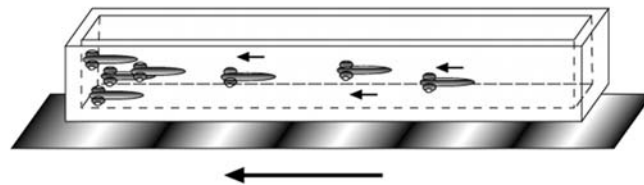
**A** The optokinetic response (OKR)**B** The optomotor response (OMR)

Figure 5-1. **Schematic of the two visuomotor behaviors investigated in this study.** A, During the OKR, immobilized fish respond with eye movements to a moving stimulus in their surroundings. B, During the OMR, fish swim to follow a moving stimulus displayed on the bottom of their tank. The direction of motion is indicated by the arrows. The figure is reproduced from Roeser and Baier, 2003 © (2003) The Society of Neuroscience

detected in the ventronasal retina at 25 hours post-fertilization (hpf), spreads from nasal to more dorsal and temporal retina over the next few hours, and is present throughout most of the neural retina at 36 hr. By 72 hr, when retinal ganglion cell, inner nuclear, and photoreceptor cell layers are distinct, *ath5* expression is downregulated in differentiated neurons but remains expressed in retinoblasts near the ciliary margin (ie, retina periphery). Retinoblasts that express *ath5* during this wave do so just after their final mitosis; immediately thereafter they begin to differentiate as RGCs (Yang et al., 2003). In the absence of functional *ath5*, these cells either ectopically re-enter the cell cycle or fail to exit the cell cycle (Kay et al., 2001)), causing both a failure of RGC genesis and an overall delay in the formation of the first retinal neurons.

We are developing a selective neuronal silencing strategy based upon glutamate-gated chloride channel subunits from *C. elegans* called the “GluCl/IVM” method (Li et al., 2002; Slimko et al., 2002; Slimko and Lester, 2003). In this strategy, this exogenous chloride channel is expressed in a tissue specific manner in a target organism. Upon systemic administration of the anthelmintic drug IVM, a potent agonist of GluCl, target neurons are electrically silenced due to the induction of a large standing chloride conductance, presumably leading to a change in organism behavior. Using enhancer elements from the *ath5* gene, which drives GFP expression in subsets of RGCs (Masai et al., 2003), in combination with the GluCl genes, we are able to modulate the excitability of these subsets of RGCs. These selective silencing experiments allow us to address the question of the involvement of specific RGCs in these three visual behaviors.

## **Materials and Methods**

*Zebrafish constructs and generation.* First the IRES segment from pIRES2-EGFP (Clontech) was cloned into poptGluCl $\beta$ -Y182F-EYFP (Slimko and Lester, 2003), such that the ATG start codon of the IRES and the ATG start codon of optGluCl $\beta$  were coincident. This resulting IRES-optGluCl $\beta$  cassette was then excised and cloned downstream of optGluCl $\alpha$  in poptGluCl $\alpha$ -ECFP (Slimko and Lester, 2003), resulting in poptGluCl $\alpha$ -ECFP-IRES-optGluCl $\beta$ -Y182F-EYFP. Approximately 7kb of 5'- and 3'-genomic fragments containing the untranslated regions of the *ath5* gene were inserted upstream and downstream of the expression cassette of poptGluCl $\alpha$ -ECFP-IRES-optGluCl $\beta$ -Y182F-EYFP. Linearization of the construct and microinjection of one-cell stage zebrafish embryos followed standard techniques (Xiao et al., 2005).

*Immunohistochemistry.* Transgenic larvae were fixed in 4% PBS-buffered paraformaldehyde (PFA), then cryoprotected in 30% sucrose/0.02% azide/PBS before sectioning at 12  $\mu$ m horizontally on a cryostat. Slides were incubated in blocking solution (PBS + 3% normal calf serum, 0.3% Triton X-100) for 30 min, then the GFP primary antibody (Molecular Probes) was applied (1:1000) overnight in blocking solution at 4 C. The immunohistochemical signal was detected with Alexa dye-conjugated secondary antibodies (Molecular Probes). Photographs were prepared with a cooled-CCD camera (SPOT-RT, Diagnostic Instruments).

*VBA Assay and analysis.* The VBA assay was performed as published previously (Neuhauss et al., 1999). 5 dpf clutches of mixed wild-type and transgenic animals were used for this experiment. One day before the experiment, 50 nM IVM was added to the tanks of half the clutches, the other half was left untouched. The larvae were taken from their tanks and put into a 25 cm Petri dish on a white background and given 15 min to

adapt their coloration. Afterwards, all dark fish were taken out of the dishes and genotyped, and a similar number of light fish were also removed and genotyped.

*OMR Assay and analysis.* The OMR assay was performed as published previously (Neuhauss et al., 1999). In short, transgenic fish and wild-type controls were individually transferred into 30-cm-long and 1-cm-wide Plexiglas tanks on an upward-facing computer monitor (Figure 5-1B). Fish were placed in the middle of the tank and a moving sine-wave grating (wavelength of  $200^\circ$ , temporal frequency of 10 Hz) was displayed for 30 sec. Ten fish of a given genotype were run simultaneously and scored as a group.

*OKR Assay and analysis.* The OKR assay (Figure 5-1A) was performed as published previously (Roeser and Baier, 2003). A liquid crystal display projector (In Focus LP 550) pointed upward into a white paper drum (50 mm height, 56 mm inner diameter) that rested on a transparent glass plate. A wide-angle conversion lens (Kenko VC-050Hi) and a close-up lens (King CU + 1) were inserted between the projector and the drum to focus the projector light into the drum. A neutral gray filter (Contax ND4) and an iris (12 mm diameter) were used to reduce the amount of light and to increase the depth of focus. Zebrafish larvae were placed in an inverted lid of a 40 mm Petri dish on top of the glass plate and immobilized in 2% methyl cellulose. The dish was shielded from the direct beam of the projector by a diffuser. Stimuli were generated on a laptop computer using plug-ins written for the public domain software NIH Image/J. The original image was a luminance-modulated spoked wheel, which was transformed into a set of vertical stripes by the projection process. Movement of the grating was generated by computer-animated rotation of the wheel. Stimulus velocity for the sine-wave gratings was  $20^\circ/\text{sec}$ .

## Results

### Codon usage for zebrafish closely matches the engineered optGluCl subunits

The original GluCl genes come from the invertebrate *C. elegans* (Cully et al., 1994). In previous work, we have found that the expression level of these genes can be increased significantly in mouse neurons by re-engineering the codon sequence to more closely match the codons preferred in highly-expressed mouse genes (Slimko and Lester, 2003). The codon adaptation index (CAI) quantifies the similarity between the codon usage of a specific gene and a species of interest. Before investing in the generation of transgenic zebrafish, we calculated the CAIs for both the native and mouse-codon-optimized GluCl genes (Table 5-1). With relatively high CAIs, the mouse-codon-optimized genes appear to have a good chance of expressing well in zebrafish.

Gene	Native CAI	Optimized CAI
GluCl $\alpha$	0.644	0.948
GluCl $\beta$	0.673	0.953

Table 5-1: **Codon Adaptation Index for GluCl and OptGluCl subunits relative to zebrafish highly expressed genes.**

### Ath5-driven GluCl expresses in a subset of Retinal Ganglion Cells (RGCs)

*Ath5*-optGluCl $\alpha$ -ECFP-IRES-optGluCl $\beta$ -Y182F-EYFP larvae 4 days post fertilization (dpf) express the optGluCl subunits in the retina periphery (Figure 5-2), similar to native *ath5* expression (Masai et al., 2000). As expected for an ion channel, the expression appears to be localized to the membrane of the cells. Unfortunately, our

## FIGURE 5-2

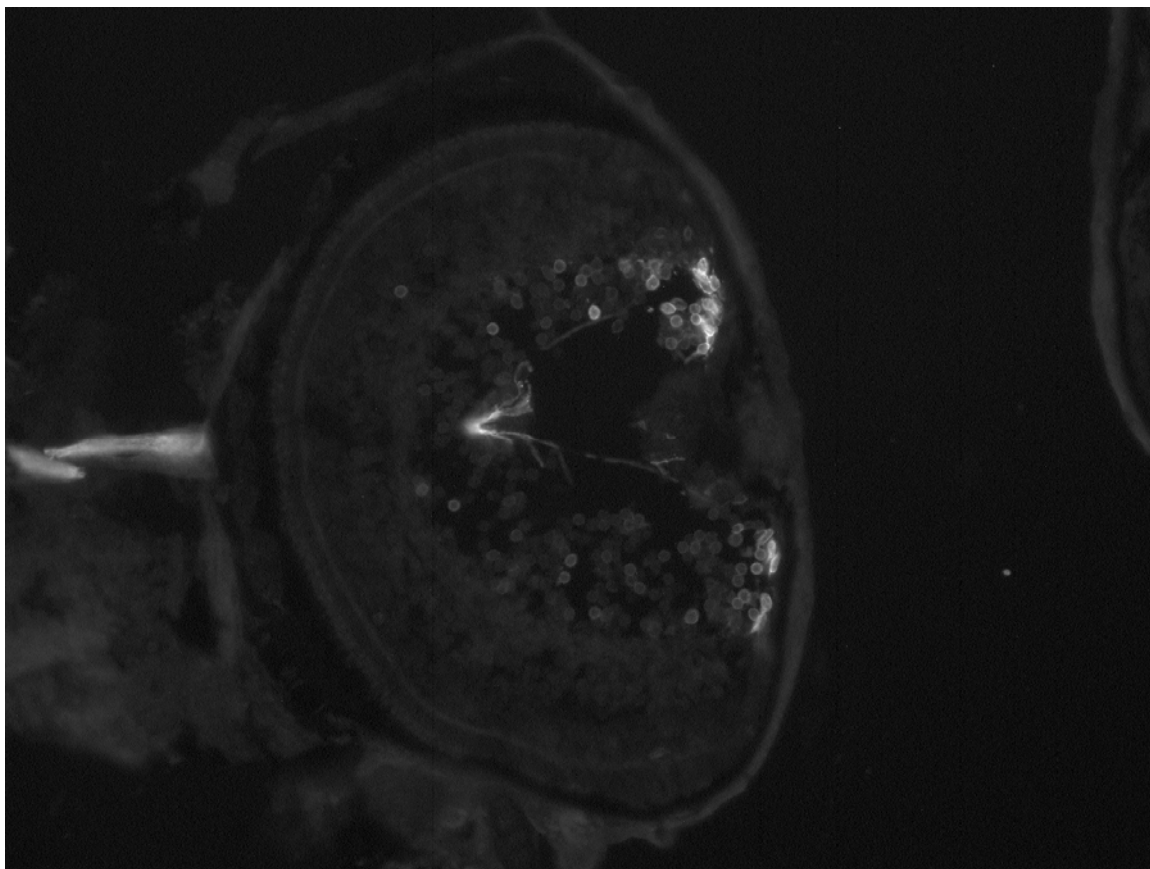


Figure 5-2: **Immunohistochemistry localization of GluCl.** Anti-GFP stain of a line 1 larvae 4 days post fertilization shows GluCl is strongly expressed in the periphery of the retina, near the ciliary margin, with decreasing expression toward the center. This is a 12 mm horizontal section, the top of the image is nasal and the bottom is temporal. Scale bar is 100  $\mu$ m.

attempts to directly visualize the ECFP and EYFP fluorophores failed, indicating that expression is not high.

### **The VBA in transgenic fish is eliminated in presence of IVM**

In clutches of 5-day-old zebrafish larvae from each of the founder lines (larvae will be mixed transgenic and wild-type), virtually all respond to a light background by adapting to a light coloration (Figure 5-3, row 1), exactly as wild-type larvae do. However, when clutches of larvae have been kept in tanks containing 50 nM IVM, in four of the five lines a substantial fraction stay darkly colored when put on the light background (Figure 5-3, row 2). Line 4 did not seem to respond in this fashion and must not express the optGluCl proteins. After this assay, the larvae were genotyped, and nearly all dark larvae were found to be transgenic (Figure 5-3, row 3), whereas the light larvae were found to be wild-type (Figure 5-3, row 4). This indicates that we have a specific behavioral deficit that requires both the larvae to be transgenic and the presence of IVM. Apparently, electrical activity in the periphery of the retina is essential for the VBA behavior.

Interestingly, the proportion of larvae that stayed dark in the +IVM experiment was not 50%, indicating that either some transgenic larvae were adapting properly or that the inheritance of the transgene was not the expected 50% in offspring of the founders. In data not shown, we used F2 larvae to show that 50% fail the VBA assay, indicating that the latter explanation is correct and most probably the germline of the founders is mosaic. Because we are able to induce the failure of the VBA task with IVM, we sought to assess the degree of their inducible visual impairment using additional behavioral assays.

### FIGURE 5-3

	Line #1	Line #2	Line #3	Line #4	Line #5
1. Darkness Rate (no IVM)	0/45	0/150	0/100	1/50	N/A
2. Darkness Rate (50 nM IVM)	8/34	23/200	26/200	1/150	19/150
3. Transgenesis Rate (Dark, 50 nM IVM)	7/8	18/23	27/27	0/1	18/19
4. Transgenesis Rate (Light, 50 nM IVM)	0/26	0/25	0/21	4/23	0/29

Figure 5-3: **Results of Visual Background Adaptation (VBA)**. For each line, clutches from the founder were moved from a dark background to a light background, both in the absence and presence of 50 nM IVM. After 15 min of exposure, light and dark larvae were counted. In the absence of IVM, all larvae behave normally and turn light (row 1). In the presence of 50 nM IVM, some larvae stay dark (row 2). Nearly all of these dark larvae are positive for GluCl (row 3), whereas all light larvae tested are wild-type (row 4).

### **The OMR in transgenic fish is unaltered in the presence of IVM**

For the OMR analysis, we restricted our experiments to using lines 1, 3 and 5. F2 clutches of 5 dpf larvae were first subject to VBA analysis to determine transgenesis. Approximately 50% of the larvae stayed dark on a light background when treated with 50 nM IVM, which we have shown in the previous section to be a reliable indicator of the presence of optGluCl. All of these larvae, including both transgenic and wild-type, were then put through the OMR analysis in groups of 10 (Figure 5-4). For each of the three lines, transgenic and wild-type performed similarly for both high-contrast and low-contrast stimuli. In data not shown, we verified that transgenic larvae without IVM also perform similarly to wild-type. Apparently, the periphery of the retina is not essential to maintain a robust OMR.

### **The OKR in transgenic fish is altered in the presence of IVM**

As a third visual behavior, we measured the OKR of wild-type and transgenic fish both with and without IVM (Figure 5-5). Although a number of parameters characterize saccades, including tracking rate, saccade frequency, and saccade amplitude, we chose to focus on saccade rate for these experiments. We investigated both a high-contrast and low-contrast stimulus. For two of the three lines, there is no difference in saccade rate between wild-type and transgenic larvae in the presence of IVM. In the third line, line 1, there is an approximately 60% deficit in transgenic fish exposed to IVM, compared to their wild-type counterparts. This reduction in performance occurs for both stimuli tested. While it is unclear why there is a difference between lines 1, 3, and 5, it is well-known that expression level can vary between transgenic lines and that this is a

Figure 5-4

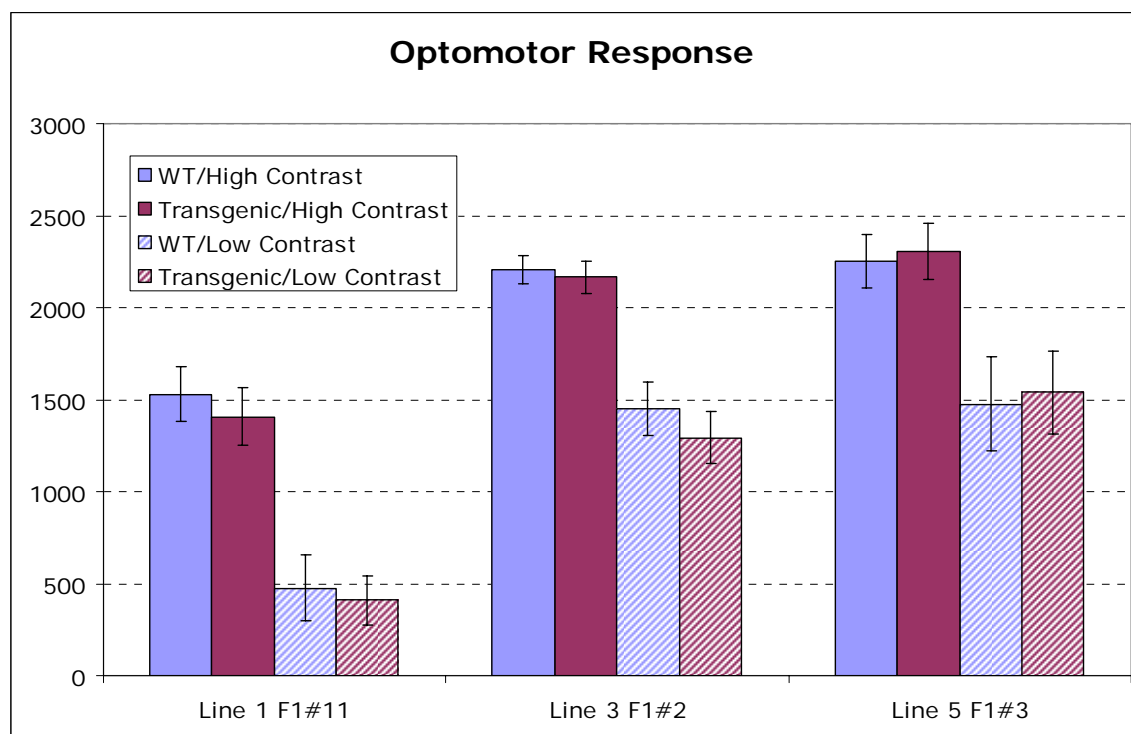


Figure 5-4: **Results from the optomotor response (OMR).** OMR scores for three of the transgenic lines show no difference between wild-type and transgenic animals. Both high contrast and low contrast stimuli were tried. For line 1, 3, and 5,  $n = 13, 13,$  and  $6,$  respectively, where one  $n$  represents a tank containing 10 larvae, scored as a group. Bars shown are standard error.

Figure 5-5

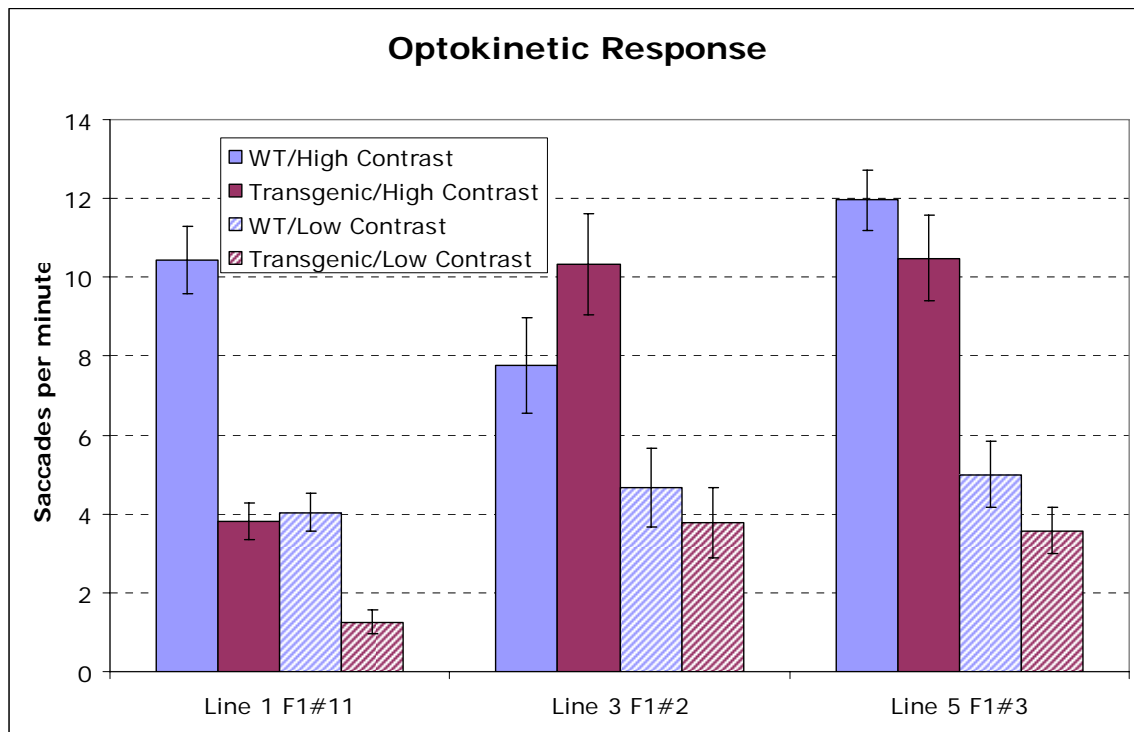


Figure 5-5: **Results for the optokinetic response (OKR).** Line 1 shows a clear deficit in measured saccades per minutes for transgenic larvae in the presence of 50 nM IVM, and no deficit for the other two lines. In the absence of IVM, all larvae behave normally (not shown). The deficit persists for both high contrast and low contrast stimuli. For lines 1, 3, and 5,  $n=29$ , 9, and 22, respectively, where each  $n$  represents a single larvae. Bars shown are standard error.

reasonable hypothesis for the cause. Future experiments are planned to understand this difference of behavior.

### **Spontaneous activity is identical between wild-type and transgenic**

We sought to verify that any deficit we observed was not merely the result of some generalized motor problem in the transgenic larvae. When in a Petri dish, larvae at this age generally show movement characterized by small bursts that appear uncorrelated to any external stimuli. Hence, we measured spontaneous movement of both wild-type and transgenic larvae in the presence of IVM (Figure 5-6). There is no difference between the two groups for each of the three lines tested.

## **Discussion**

In this study, we used the GluCl/IVM method to electrically silence the peripheral retinal ganglion cells of zebrafish and investigated the impact of this cell-specific silencing on three visually mediated behaviors. We discovered that the *ath5* promoter leads to expression of the optGluCl transgenes in the expected peripheral RGCs, although expression level was not so high as we would have liked. However, we found that IVM can modulate two important visual behaviors in these animals, the VBA task and the OKR, while leaving a third visual behavior, the OMR, unchanged. The VBA behavior is completely abolished in transgenics exposed to IVM, leading directly to the conclusion that electrical activity in peripheral RGCs is essential for VBA function. It remains an open question as to whether centrally located RGCs are also essential for VBA. In at least one line, saccade rates in the OKR are reduced by as much as 60% in IVM-treated transgenics compared to wild-type controls. This suggests an important role of peripheral RGCs in the pacing of the saccade-generating mechanism.

Figure 5-6

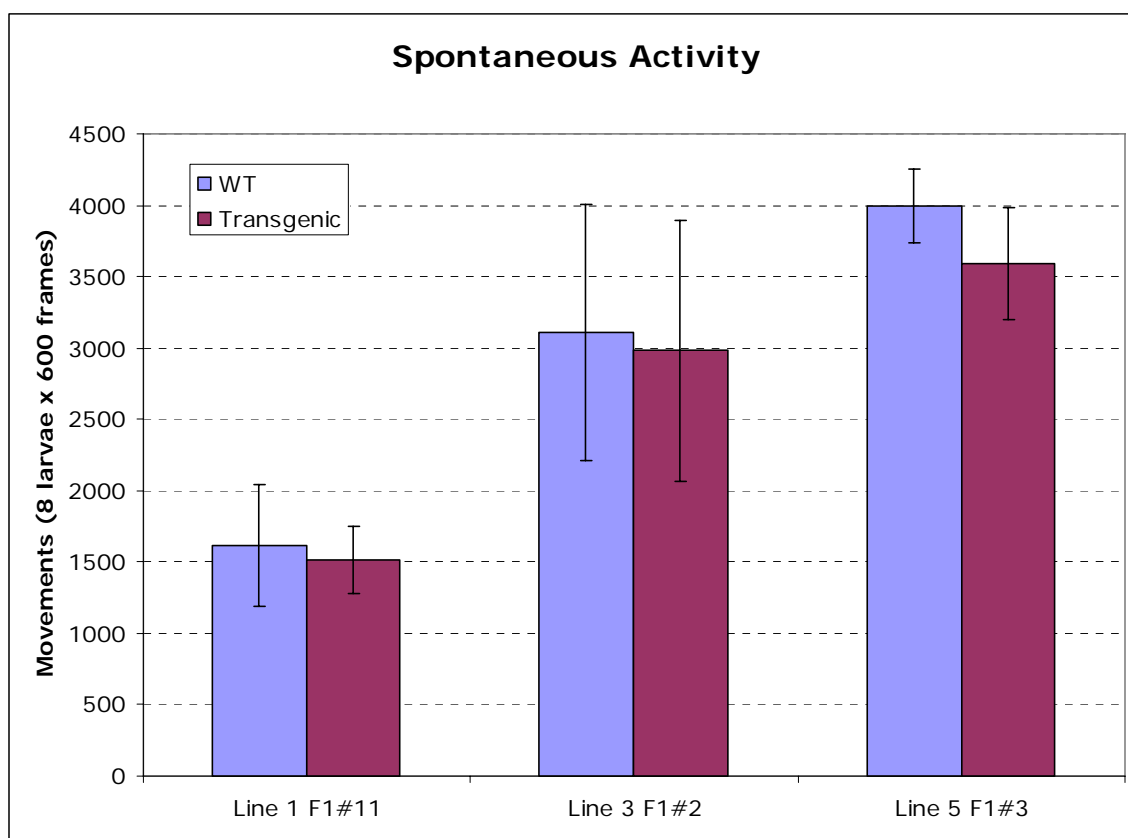


Figure 5-6: **Spontaneous swimming activity.** Wild-type and transgenic larvae from each of the three lines have equivalent spontaneous swimming activity, as measured by the number of movements per unit time. For lines 1, 3, and 5,  $n=9$ , 6, and 6 where each  $n$  represents 8 larvae scored as a group. Bars are standard error.

At this time, this is only the second publication to link an electrical silencing of cell-type specific neurons to a behavioral change in an intact vertebrate animal.

## References

- Burrill JD, Easter SS, Jr. (1994) Development of the retinofugal projections in the embryonic and larval zebrafish (*Brachydanio rerio*). *J Comp Neurol* 346:583-600.
- Cully DF, Vassilatis DK, Liu KK, Paress PS, Van der Ploeg LH, Schaeffer JM, Arena JP (1994) Cloning of an avermectin-sensitive glutamate-gated chloride channel from *Caenorhabditis elegans*. *Nature* 371:707-711.
- Kay JN, Finger-Baier KC, Roeser T, Staub W, Baier H (2001) Retinal ganglion cell genesis requires lakritz, a Zebrafish atonal Homolog. *Neuron* 30:725-736.
- Li P, Slimko EM, Lester HA (2002) Selective elimination of glutamate activation and introduction of fluorescent proteins into a *Caenorhabditis elegans* chloride channel. *FEBS Lett* 528:77-82.
- Masai I, Stemple DL, Okamoto H, Wilson SW (2000) Midline signals regulate retinal neurogenesis in zebrafish. *Neuron* 27:251-263.
- Masai I, Lele Z, Yamaguchi M, Komori A, Nakata A, Nishiwaki Y, Wada H, Tanaka H, Nojima Y, Hammerschmidt M, Wilson SW, Okamoto H (2003) N-cadherin mediates retinal lamination, maintenance of forebrain compartments and patterning of retinal neurites. *Development* 130:2479-2494.
- Neuhauss SC, Biehlmaier O, Seeliger MW, Das T, Kohler K, Harris WA, Baier H (1999) Genetic disorders of vision revealed by a behavioral screen of 400 essential loci in zebrafish. *J Neurosci* 19:8603-8615.
- Roeser T, Baier H (2003) Visuomotor behaviors in larval zebrafish after GFP-guided laser ablation of the optic tectum. *J Neurosci* 23:3726-3734.
- Slimko E, McKinney S, Anderson D, Davidson N, Lester HA (2002) Selective electrical silencing of mammalian neurons in vitro using invertebrate ligand-gated chloride channels. *J Neurosci* (in press).
- Slimko EM, Lester HA (2003) Codon optimization of *Caenorhabditis elegans* GluCl ion channel genes for mammalian cells dramatically improves expression levels. *J Neurosci Methods* 124:75-81.
- Xiao T, Roeser T, Staub W, Baier H (2005) A GFP-based genetic screen reveals mutations that disrupt the architecture of the zebrafish retinotectal projection. *Development* 132:2955-2967.

Yang Z, Ding K, Pan L, Deng M, Gan L (2003) Math5 determines the competence state of retinal ganglion cell progenitors. *Dev Biol* 264:240-254.

*Chapter 6***Attempts to use the “GluCl/IVM” method in mice**

Text of this chapter is unpublished work. I would like to thank Walter Lerchner in David Anderson's laboratory for support in doing the *in situ* hybridizations, immunohistochemistry, and *in vivo* AAV injections reported in this chapter.

## Abstract

We have been developing a technique for reversibly silencing specific neuronal populations in mouse brain, which we call the GluCl/IVM method. It relies on expression of a ligand-gated chloride channel from *C. elegans* engineered for optimal expression in mammalian neurons. In previous work we have demonstrated the applicability of the method in cultured hippocampal neurons. We have pursued four approaches to *in vivo* silencing of mouse brain using the GluCl/IVM method: 1) Sindbis virus injection into the brain, 2) adeno-associated virus (AAV) injection into the brain, 3) a *trkA* promoter-driven transgenic mouse, and 4) an *L7* promoter-driven transgenic mouse. Two of the methods, the Sindbis virus injection and the *trkA* mouse, were abandoned due to minimal expression levels. Our AAV experiments are incomplete, but appear to show a high level of expression, and behavioral experiments are forthcoming. With the *L7* promoter-driven transgenic, we have demonstrated expression of the GluCl channel through *in situ* hybridization, immunohistochemistry, direct fluorescent detection, and acute dissociated electrophysiology. Our behavioral assay, the rotarod, did not show a conclusive modulation in response to ip dosages of IVM, unfortunately. Low levels of expression of the transgenes probably account for this lack of effect.

## Introduction

A useful approach to understanding mechanisms underlying information processing and integration in neural circuits involves inactivating specific sets of neurons in the neural network. This approach has been used effectively in *Drosophila* and

*Caenorhabditis elegans* in some cases by reversibly inactivating a subset of neurons (Sweeney et al., 1995; Dubnau et al., 2001; McGuire et al., 2001; White et al., 2001; Nitabach et al., 2002). In mammals, selective ablation of particular cell types within the network has been achieved through a variety of genetic techniques (Nirenberg and Cepko, 1993; Kobayashi et al., 1995; Watanabe et al., 1998; Gogos et al., 2000). This technology has clarified mechanisms underlying development, information processing and integration, and behaviors, but also often has led to adaptive and compensatory changes in the neural function. The technology that allows reversible suppression of a specific neuronal activity in mammals is desired but still is limited (Callaway, 2005; Wulff and Wisden, 2005). In fact, at the time of this writing there has been only one publication of a successful application of reversible behavioral modulation due to selective silencing of a neuronal population in a mouse (Yamamoto et al., 2003). Additionally, there has been one report of *in vivo* circuit modulation due to selective silencing (Yu et al., 2004), although no behavior was reported.

Yamamoto and colleagues developed a “genetics-only” approach that relies on the tetracycline transactivator system to induce expression of the light chain of tetanus neurotoxin (TeNT) in cerebellar granule cells (Yamamoto et al., 2003). Because the tetracycline-controlled reverse activator (rtTA) requires doxycycline (DOX) to induce transcription, temporal control is achieved through addition of doxycycline in the animal’s diet. The light chain of tetanus toxin, once expressed in a neuron, proteolytically cleaves synaptobrevin (VAMP2), a protein which is required for synaptic vesicle exocytosis (Sudhof, 1995). The genetically manipulated expression of TeNT with the rtTA system thus confers inducible and reversible suppression of synaptic

transmission *in vivo* by DOX-dependent cleavage of VAMP2. The drawback of this approach is the time course. In Yamamoto's experiments, mice were treated with DOX for 13 days before the behavioral effect was seen, and required 21 days after DOX treatment to recover the original, untreated, behavior. There are three rate limiting steps in silencing a neuron with this technique: 1) the pharmacokinetics of doxycycline penetrating the target tissues, which are behind the blood-brain barrier, 2) the transcription and translation rate of TeNT once DOX is present, and 3) the rate at which TeNT cleaves VAMP2. Presumably, transcription and translation is the limiting step. There have been a number of other attempts to electrically silence neurons in mammals; these are summarized in Chapter 1.

Chloride current is a major mechanism of inhibition in the animal brain. We have been developing a technique that uses invertebrate ligand-gated chloride channels (Li et al., 2002; Slimko et al., 2002; Slimko and Lester, 2003). In these experiments, two subunits of a *C. elegans* glutamate-gated chloride channel (GluCl $\alpha$  and GluCl $\beta$ ) were expressed in mammalian neurons *in vitro* and, upon exposure to the anthelmintic drug ivermectin (IVM), neurons developed a large standing chloride conductance and were effectively silenced. To optimize these genes for *in vivo* silencing experiments, we have 1) ameliorated the activation by the endogenous ligand, glutamate (Li et al., 2002), by finding a site specific mutation, 2) incorporated fluorophore tags into each of the subunits (Slimko and Lester, 2003), and 3) re-engineered the coding sequences to reflect the mammalian preferred codons (Slimko and Lester, 2003). We call these derivatized genes optGluCl $\alpha$ -ECFP and optGluCl $\beta$ -Y182F-EFYP. In contrast to the TeNT technique, this approach does not require synthesis of new proteins to effect neuronal silencing. We

hope the pharmacological nature of this technique will result in a significantly faster time course of inactivation and activation.

We have used this engineered GluCl channel to make two different strains of transgenic mice. The first used a promoter for the neurons in the peripheral nervous system, *trkA*, shown to target DRG neurons (Ma et al., 2000). The second used a promoter for neurons in the central nervous system, L7 (sometimes called *Pcp2*), which targets Purkinje cells of the cerebellum (Oberdick et al., 1990). We have also used both Sindbis virus and adeno-associated virus (AAV) to express these genes in adult animals. Unfortunately, our results have not been conclusive. However, they are summarized in the remainder of this article, with advice given for future directions.

## **Materials and Methods**

*Mouse constructs and generation.* All procedures for animal treatments were performed according to the guidelines of the California Institute of Technology. The pL7-optGluCl expression plasmids (Figure 6-1B) coding for optGluCl $\alpha$ -ECFP and optGluCl $\beta$ -Y182F-EYFP under control of the L7 promoter were generated by inserting the two genes into the *Bam*HI site of the L7-pGEM3 plasmid (Oberdick et al., 1990). Note that there were two plasmids generated, one carrying optGluCl $\alpha$ -ECFP and the other carrying optGluCl $\beta$ -Y182F-EYFP. The plasmids were linearized with *Hind*III and *Eco*RI, purified, and co-injected into fertilized eggs from wild-type C57BL/6 mice. At four weeks of age, mice were tailed and founders were identified by PCR analysis. Two separate rounds of injection resulted in 72 lines, 5 of which were positive for both

Figure 6-1

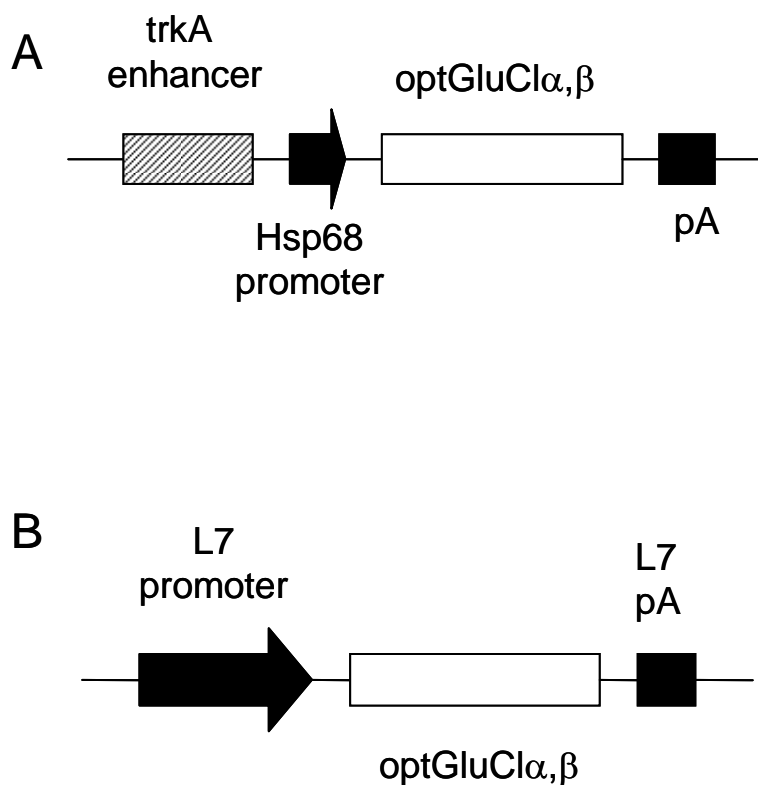


Figure 6-1. **Constructs used for transgenic mice generation.** A, the *trkA* promoter construct. B, the L7 promoter construct. Note that two different plasmids were generated for each mouse, an *optGluCl $\alpha$* -ECFP containing plasmid, and an *optGluCl $\beta$* -Y182F-EFYP containing plasmid. The constructs were co-injected to generate a mouse that would express both genes.

transgenes. All lines were back-crossed to C57BL/6 for one to three generations before physiological analysis.

Similarly, the *trkA*-optGluCl constructs (Figure 6-1A) were generated using the *trkA* promoter (Ma et al., 2000). Briefly, the two genes were cloned into the BamHI site of pJ21, the plasmids were linearized, purified, and co-injected into fertilized eggs from wild-type C57BL/6 mice. Five transgenic lines also resulted from these injections and were used for expression analysis.

*Sindbis vectors, preparation, and injection.* Sindbis vectors were prepared as described (Slimko et al., 2002). Virus was injected into the Rostral Ventral Lateral Medulla (RVLM) via a 30G stainless needle attached by polyethylene tubing to a 10- $\mu$ l Hamilton syringe. 0.5 – 1.0  $\mu$ l of the virus preparation was injected at a rate of  $\sim$ 0.2  $\mu$ l per minute. The needle remained in place for an additional 5 min to facilitate controlled delivery of the virus. 48 h post infection mice were culled for fluorescence and behavior analysis.

*AAV vectors, preparation, and injection.* pAAV-optGluCl $\alpha$  and pAAV-optGluCl $\beta$  were prepared by cloning optGluCl $\alpha$ -ECFP and optGluCl $\beta$ -Y182F-EYFP between the *KpnI* and *NotI* sites of pAAV-MCS (Stratagene, La Jolla, CA). Virus was prepared by ViraPur, LLC, San Diego, and supplied as two solutions tittered at  $10^{12}$ /ml. These solutions were mixed at a 1:1 ratio and 0.5  $\mu$ l was injected into either the amygdala or hippocampus, as described above. 48-96 h post infection, mice were culled for fluorescence analysis.

*Electrophysiology.* Acute dissociated Purkinje cell preparations were prepared as described previously (Raman and Bean, 1999). Transgenic and C57BL/6 mice (postnatal day 14-20) were anesthetized with methoxyflurane before decapitation, and the vermal

layer of the cerebellum was removed and minced in ice-cold, oxygenated dissociation solution containing (in mM): 82 Na<sub>2</sub>SO<sub>4</sub>, 30 K<sub>2</sub>SO<sub>4</sub>, 5 MgCl<sub>2</sub>, 10 HEPES, 10 glucose, and 0.001% phenol red (buffered to pH 7.4 with NaOH). The tissue was then incubated for 7 min in 10 ml of dissociation solution containing 3 mg/ml protease XXIII (Sigma, St. Louis, MO), pH 7.4 with NaOH, at 37°C, with oxygen blown over the surface of the fluid. The tissue was then washed in warmed, oxygenated dissociation solution containing 1 mg/ml bovine serum albumin and 1 mg/ml trypsin inhibitor, and then maintained in Tyrode's solution containing (in mM): 150 NaCl, 4 KCl, 2 CaCl<sub>2</sub>, 2 MgCl<sub>2</sub>, 10 HEPES, 10 glucose, pH 7.4 with NaOH, at room temperature, with O<sub>2</sub> blown over the surface of the fluid. Tissue was withdrawn as needed and triturated with a fire-polished Pasteur pipette to liberate individual neurons. Purkinje cells were identified by their large diameter and characteristic pear shape attributable to the stump of the apical dendrite. Cells were used between 30 min and 5 hr of trituration. For recording, the bath solution was (in mM): 110 NaCl, 5.4 KCl, 1.8 CaCl<sub>2</sub>, 0.8 MgCl<sub>2</sub>, 10 HEPES and 10 D-glucose, pH 7.4, osmolarity 230 mOsm. Patch pipettes were filled with a solution containing (in mM): 100 K gluconate, 0.1 CaCl<sub>2</sub>, 1.1 EGTA, 5 MgCl<sub>2</sub>, 10 HEPES, 3 ATP, 3 phosphocreatine and 0.3 GTP, pH 7.2, 215 mOsm. Holding potential was -60 mV. Input conductance was measured by a 5 mV hyperpolarizing pulse.

*In situ hybridization.* Nonradioactive *in situ* hybridization to frozen sections of mouse cerebellum was done as previously described (Ziringer et al., 2001). Templates for probes were synthesized by PCR using specific primers for optGluCl $\alpha$ -ECFP and optGluCl $\beta$ -Y182F-EYFP and their respective cDNA plasmids. Briefly, fresh frozen, 20  $\mu$ m thick coronal sections were cut with a cryostat. Sections were dried and fixed in 4%

paraformaldehyde, washed in PBS and subjected to acetylation using 0.25 % acetic anhydride in 1M triethanolamine-HCl pH 8.0. Slides were prehybridized for 1–3 hr, and hybridized overnight at 68°C, using a probe concentration of 0.5–1 µg/ml. Sections were washed twice in 0.2X SSC at 68°C for 30 min., incubated with anti-digoxigenin alkaline phosphatase-conjugated Fab fragments (Roche) at a 1: 2000 dilution in 0.1M maleic acid buffer, pH 7.5, with 0.2% Tween-20, 20% sheep serum and 2% blocking reagent (Roche). Staining was developed for 4–16 hours with NBT and BCIP (Roche) in alkaline phosphatase buffer to yield a purple product. Slides were fixed in 4% formaldehyde and mounted with glycerol.

*Immunohistochemistry.* The primary antibodies used were rabbit polyclonal anti-EGFP or anti-calbindin, from Molecular Probes (Eugene, OR). Briefly, fresh frozen, 20 µm thick coronal sections were cut with a cryostat. Sections were fixed in 4% PFA for 10 min, washed 4x in PBS with 0.1% Triton X100, and then blocked for 20 minutes in PBST supplemented with 10% goat serum. Sections were stained overnight at 4 C with a 1:1000 dilution of the primary antibody, then washed and blocked as above. The secondary antibody (either Alexa 488 or Alexa 568 from Molecular Probes) was then applied to the section as a 1:250 dilution for 2 h at room temperature. Finally, sections were washed 2x in PBS and mounted in 70% glycerol.

*Rotarod behavior tests.* The rotarod consisted of a grooved plastic roller (4 cm in diameter). A mouse was placed on the rotarod rotating at 30 rpm. For the static rotarod assay, mice (wild-type and transgenic) were subject to six sessions of three trials per session; two sessions were conducted per day. Each trial lasted until the mouse fell off or a maximum 180 seconds. At the end of six sessions, all mice could do the task without

failure. On the next day, mice were injected ip with varying dosages of IVM (5 – 20 mg/kg), and at various time points after, their performance on the rotarod was measured. For the learning rotarod assay, mice (wild-type and transgenic) were injected with 20 mg/kg IVM 24 hr before the training protocol, and their performance during the six training sessions was measured.

## Results

### Both Sindbis and AAV lead to *in vivo* neuronal expression

Initial viral injection experiments were performed using the Sindbis virus which has been described previously (Slimko et al., 2002). Our target area was the rostral ventral lateral medulla (RVLM). Unilateral inactivation of this region with muscimol leads to a profound apnea (Gatti et al., 1987), and we chose this as an appropriate simple behavioral assay. To verify the previous reports, we injected 0.5  $\mu$ l of 100  $\mu$ M muscimol into the left RVLM. Within 5 min, 3 of 3 mice completely stopped breathing. Buoyed by this result, we injected 3 mice with 1  $\mu$ l of the Sindbis virus solution that has been described (Slimko et al., 2002). This Sindbis virus has three cistrons to drive expression of GluCl $\alpha$ , GluCl $\beta$ , and green fluorescent protein (GFP). Forty-eight hours post injection animals were injected ip with 20 mg/kg of IVM. Animals were observed visually up to 3 h for signs of abnormal breathing; no lack or change in breathing was observed. 48 h after IVM administration, mice were culled; brains were removed, sectioned, and mounted so that we could attempt to estimate the expression level by searching for GFP fluorescence. We found that roughly 25% of neurons throughout the RVLM expressed GFP (Figure 6-2), which we felt was a reasonable level of infection. However,

Figure 6-2

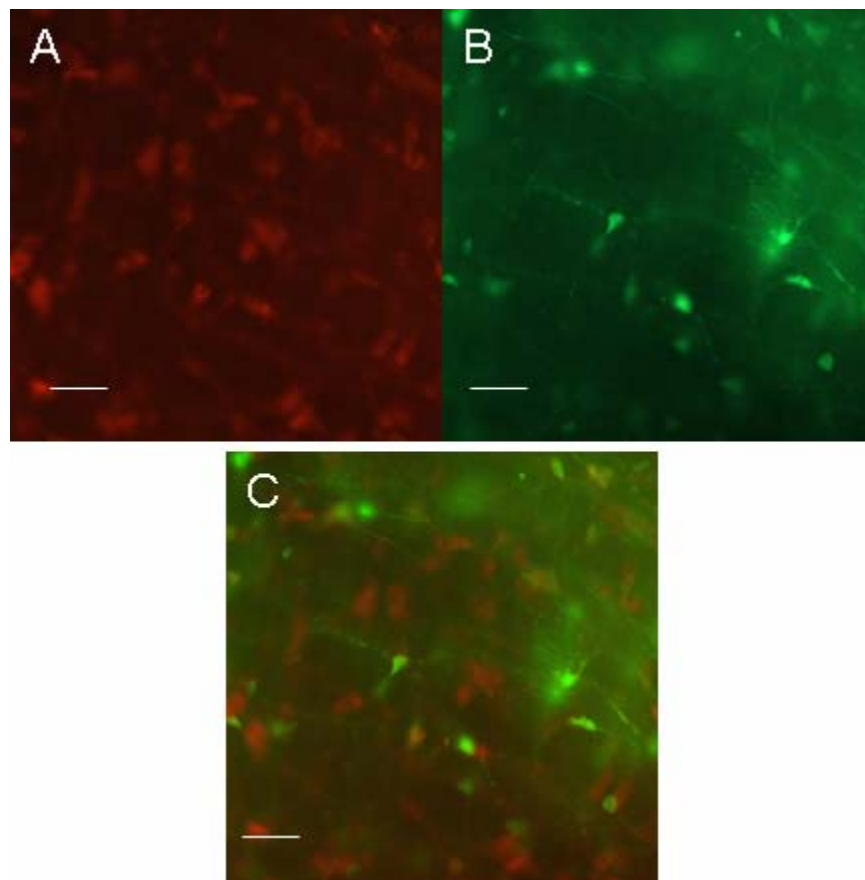


Figure 6-2: **RVLM sections**. A, Nissl staining. B, GFP fluorescence. C, Merged images. All scale bars shown are 50 mM. Note that the virus infects only ~25% of the neurons.

while doing these experiments, we learned that only a small percentage of cells expressing GFP express both subunits of GluCl (Slimko et al., 2002), which led us to believe that a very small number of neurons in the RVLM were actually being silenced. Hence, we were not surprised that we saw no behavioral phenotype. At this time, we abandoned these experiments.

We generated a recombinant adeno-associated virus type 2 (AAV2) as explained in Methods, using the engineered GluCl channel subunits, optGluCl $\alpha$ -ECFP and optGluCl $\beta$ -Y182F-EFYP. AAV has been used recently for gene expression experiments in the central nervous system (Davidson et al., 2000; Rabinowitz et al., 2002; Rabinowitz et al., 2004). Our target has been the hippocampus, where lesion studies produce decrements in contextual fear conditioning (Chen et al., 1996). We injected 1  $\mu$ l of a virus solution (tittered at  $10^{12}$ /ml) into the hippocampus. 48-96 h after infection, we sacrificed the animals and sectioned their brains to assay for expression level (Figure 6-3). We used a GFP antibody to enhance the signal from the optGluCl subunits and then counterstained with a Nissl antibody (Figure 6-3, A-D). Infectivity in the target region appears to be high, approaching 75%. Also, we are able to clearly resolve the native fluorescence of both subunits (Figure 6-3, E-H). The fluorescence does indicate, however, that there is substantial cell-to-cell variation of expression level. In experiments not shown, we have determined that the bleed-through from any of these three fluorophores into the other channels is minimal. These experiments are currently underway and, as of this writing, we have not yet attempted any behavioral experiments.

Figure 6-3(A-D)

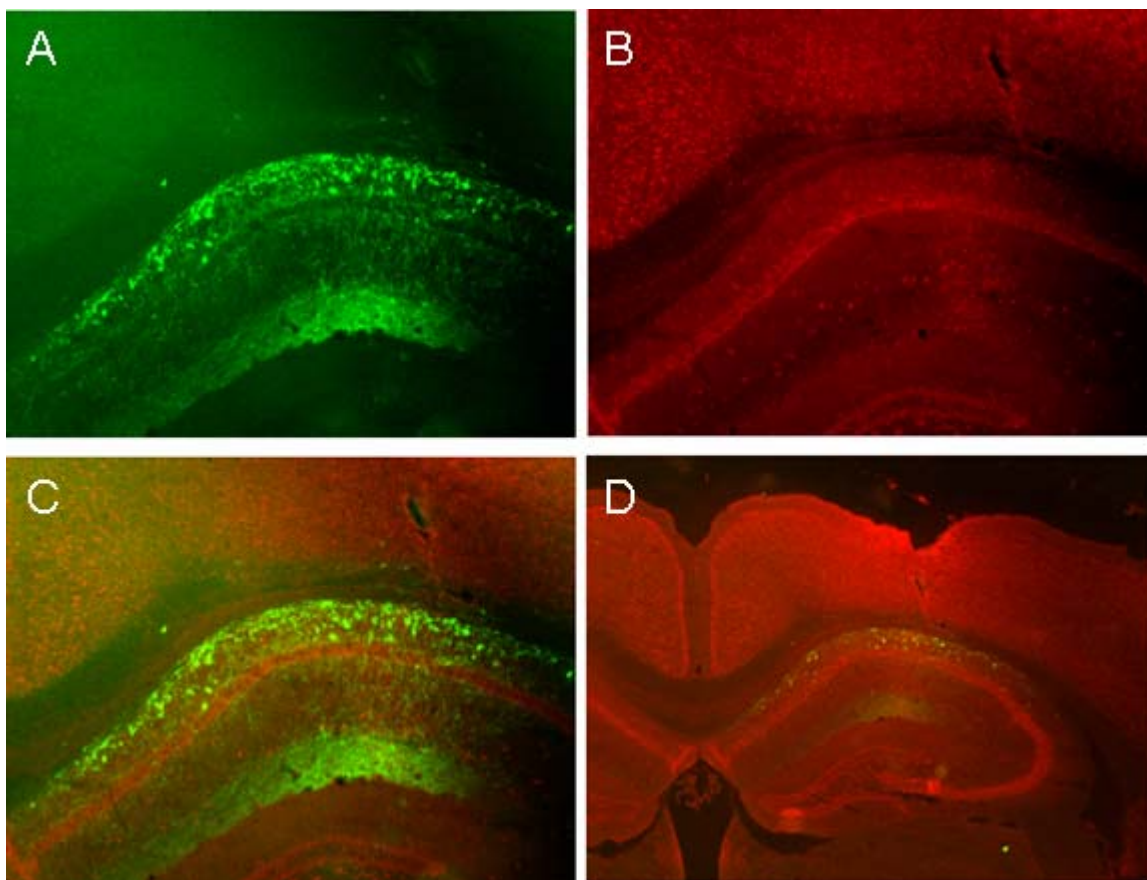


Figure 6-3(A-D): **Infection of the hippocampus with AAV.** A, anti-GFP staining showing successful infection of the target region, 20x. B, Nissl staining of the same region, 20x. C, overlay of A and B. D, 10x overlay view of hippocampus. Figure continued on next page.

Figure 6-3(E-H)

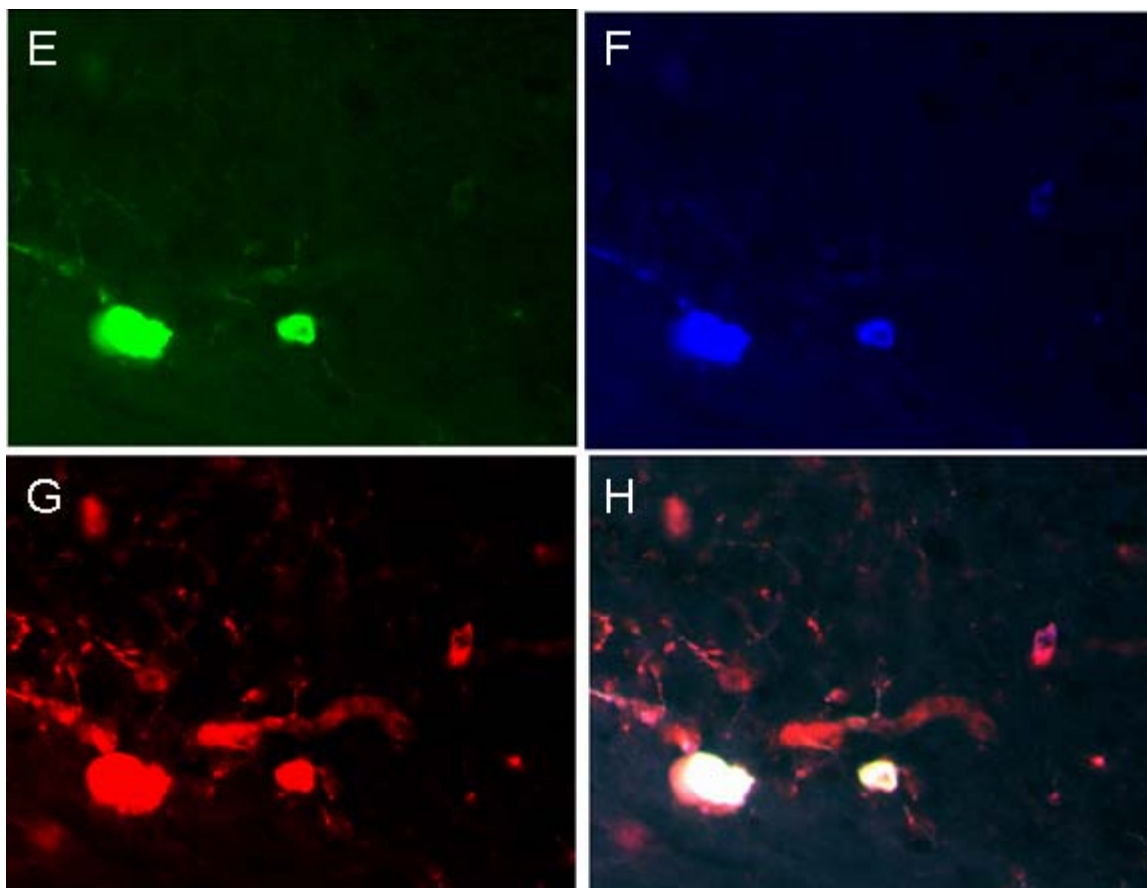


Figure 6-3(E-H). E, Native fluorescence of optGluClb-Y182F-EYFP, 60x. F, Native fluorescence of optGluCla-ECFP, 60x. G, Nissl staining of same view. H, Overlay of all three channels.

### **The *trkA* promoter does not lead to expression in adult DRGs.**

The *trkA* promoter drives expression of *lacZ* in embryonic dorsal root ganglion (DRG) neurons (Ma et al., 2000). The DRG is involved in the sensation of noxious stimuli (Scott, 1992). Unfortunately, there are no reports concerning the ability of the *trkA* promoter to drive gene expression in adult animals. However, we generated five lines containing the transgenes shown in Figure 6-1. Despite searching for expression with mRNA *in situ*, fluorescence microscopy, immunohistochemistry, and electrophysiology of DRG cultures, we found no evidence of expression in animals from P5 to P28. Because we were trying to develop a mouse with which we could do relevant behavioral characterization on adult animals, we decided to abandon this project.

### **Purkinje cell-specific mice show correct expression**

The L7, or *Pcp2*, promoter has been used to make several transgenic mouse lines with a variety of transgenes (see Table 6-1). All reports on the use of this promoter suggest that it is specific and works with high efficiency. However, the number of “highly-expressing” lines can be as low as 30% of the number of founder lines. Studies of mice with degenerative Purkinje cells (Hilber and Caston, 2001) indicate that mice lacking Purkinje cells typically have an ataxic phenotype. We felt that this type of phenotype would constitute a straightforward assay, and hence an L7-driven silencing mouse would be a good candidate for the first silencing mouse demonstration.

Five different lines of L7 mice were generated in two rounds of pronuclear injection using the construct described in Methods. Transgenesis was determined through PCR. The first round resulted in three lines and the second resulted in two. F2

Table 6-1

Reference	Gene	Founders	"High" Expressors
Oberdick et al (1990). Science 248:223-6	b-gal	3	3
Feddersen et al (1992). Neuron 9:955-66	*SV40 T Antigen	6	3
Smeyne et al (1995). MCN 6,230-51	Diphtheria toxin	5	3
Buffo et al (1997). J Neurosci 17:8778-8791	B-50/GAP-43	3	1
De Zeeuw et al (1998). Neuron 20:495-508	PKC Inhibitor	6	3
Baader et al (1998). J Neurosci 18:1763-73	Engrailed-2	6	4
Athanasiou et al (1998). MCN 12:16-28	*E2F-1	13	4
Yoshihara et al (1999). Neuron 22:33-41	WGA	4	3
Barski et al (2000). Genesis 28:93-98	Cre	3	3
Zhang et al (2001). Histo Cell Bio 115:455-464	EGFP & GFP	5	3
Tomomura et al (2001). Euro J Neurosci 14:57-63	EGFP	5	2
Carulli et al (2002). Euro J Neurosci 16:105-118	c-Jun	8	4
Flechsig et al (2003). EMBO J 22:3095-3013	PrP	3	3
Sekimjak et al (2003). J Neurosci 23:6392-6398	tau-EGFP	7	3
Brodie et al (2004). MCN 25: 602-11	*CREB	3	1
Anderson et al (2004). PNAS 101:3644-3649	Doppel	4	2

Table 6-1. **Mouse lines generated using L7 promoter**

mice were used for subsequent analysis. To determine the best expressing line with which to proceed with behavioral experiments, we performed both *in situ* mRNA hybridization and immunohistochemistry on cerebellar brain slices and looked for the lines with the strongest signal. Figure 6-4 shows the *in situ* results for two of the strongest expressing lines and a negative control. Both lines have signals for optGluCl $\alpha$ -ECFP and optGluCl $\beta$ -Y182F-EFYP mRNA above that of wild-type, and the signal is restricted to the Purkinje cell layer. Forebrain sections were also analyzed and found to have no signal. Line 70 has the stronger of the two signals. Two of the remaining three transgenic lines had signals that were barely detectable (data not shown), and the final line did not appear to have a positive signal.

The optGluCl $\alpha$ -ECFP and optGluCl $\beta$ -Y182F-EFYP genes used to generate these mice contain Enhanced Cyan Fluorescent Protein (ECFP) and Enhanced Yellow Fluorescent Protein (EYFP), respectively, as fusions (Chapter 3). This should allow for direct detection of the proteins with fluorescence microscopy. However, before proceeding to direct detection, we stained cerebellar sections of lines 70 and 43 with an EGFP antibody (Figure 6-5), which detects both EYFP and ECFP. Clearly, line 70 has stronger expression which correlates well with the previous *in situ* results. Again, the signal was restricted to the Purkinje cell layer and not found anywhere else in the brain.

Unfortunately, direct detection of the fluorophores was not straightforward. Previous *in vitro* results had suggested that the channel expressed quite well and was easy to detect (Slimko and Lester, 2003). Detecting the fluorescence in these mice was challenging and we spent a significant effort tuning the microscope to acquire a good image. Figure 6-6 presents one of the best high-magnification images that we were able

Figure 6-4(A-C)

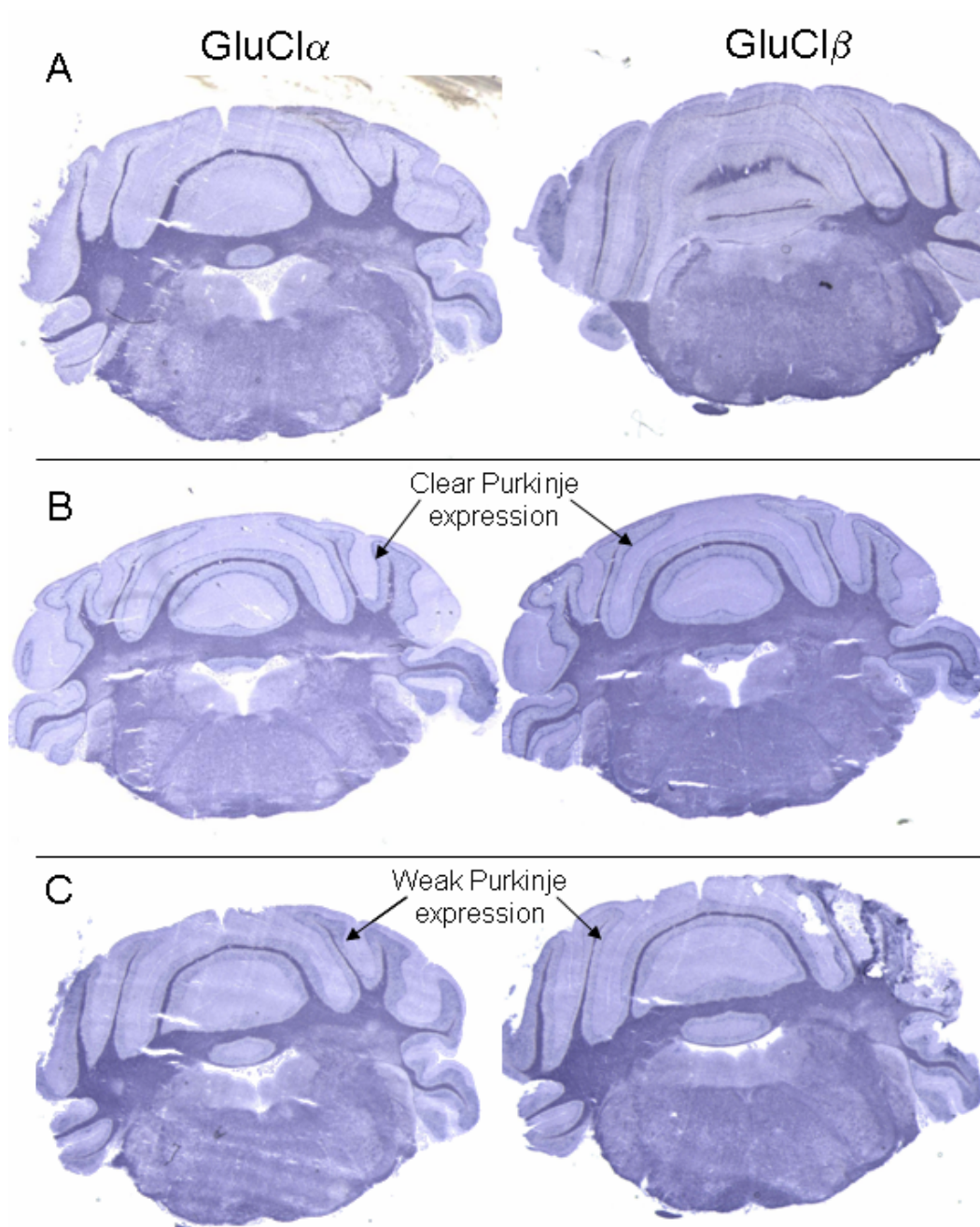


Figure 6-4(A-C): mRNA *in-situ* hybridizations for wild-type and two lines. A, wild-type, showing no existence of GluCl $\alpha$  or  $\beta$  mRNA. B, the strongest line, line 70, showing clear Purkinje expression of  $\alpha$  and  $\beta$  mRNAs. C, the next strongest, line 34, showing weaker Purkinje cell labeling.

Figure 6-4(D-E)

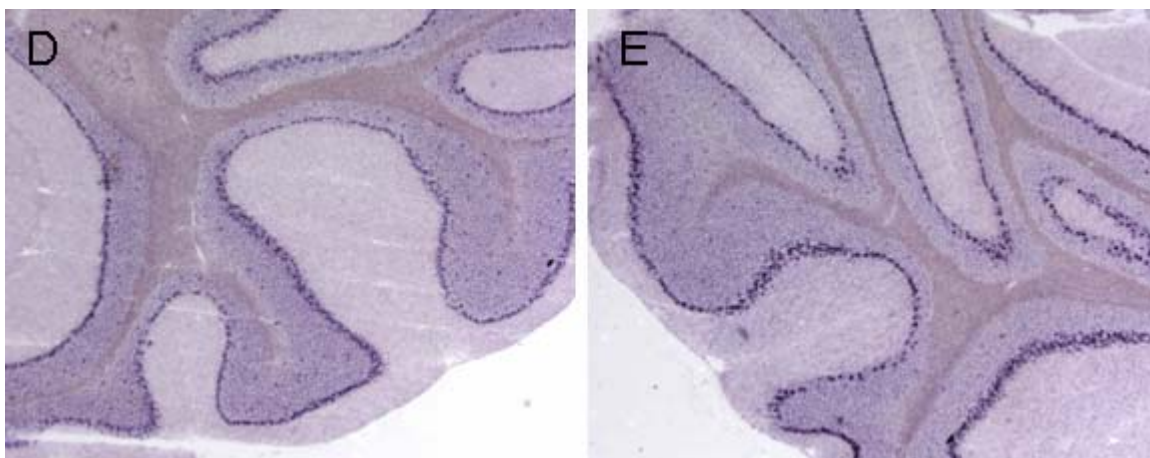


Figure 6-4(D-E): D and E, higher magnification images showing Purkinje cell staining of line 70. D is optGluCla-ECFP and E is optGluClb-Y182F-EYFP.

Figure 6-5

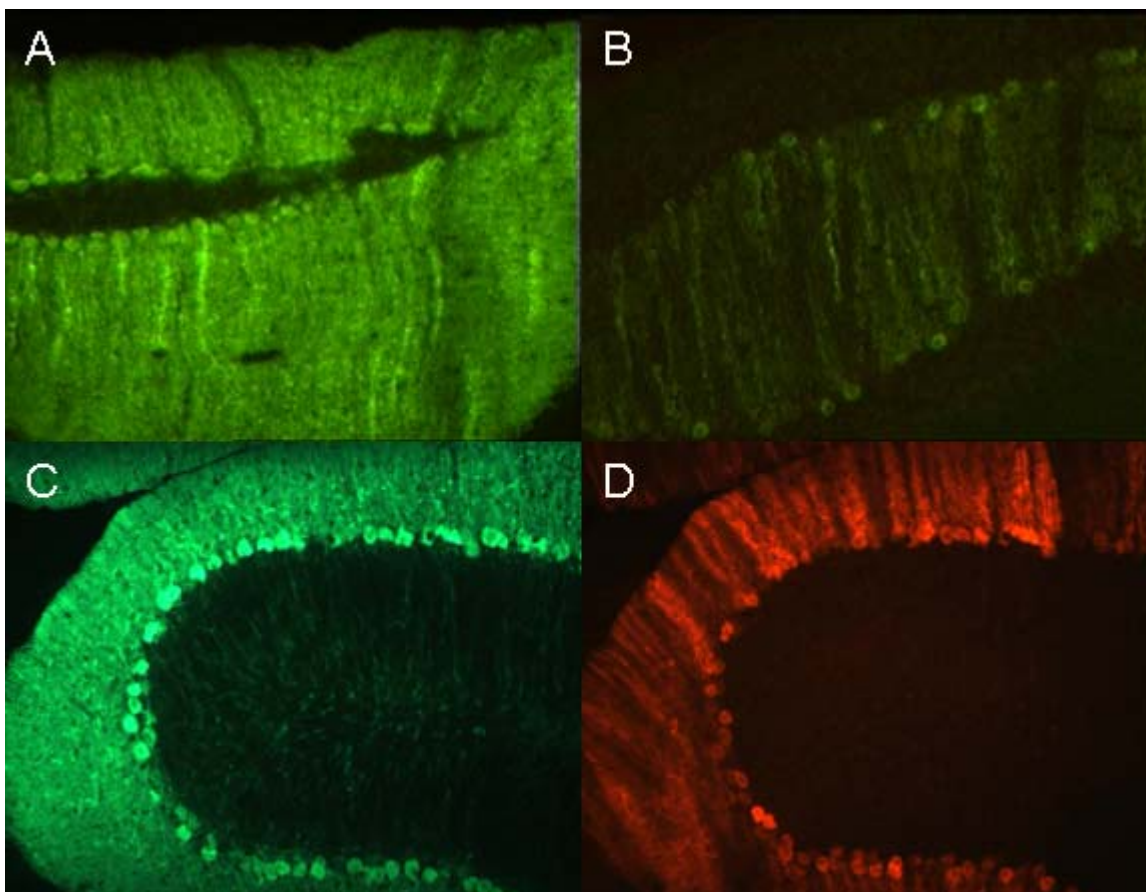


Figure 6-5: **Immunohistochemistry of cerebellar slices.** Slices were stained with an EGFP antibody, which recognizes both optGluCla-ECP and optGluClb-Y182F-EYFP. A, line 70, the strongest expressing line. B, line 43, a weaker line. Wild-type sections had no detectable fluorescence (not shown). C, staining of Purkinje neurons with calbindin. D, staining of the same section as B with an EGFP antibody. C and D done with line 70.

to achieve. In the ECFP channel, which corresponds to the optGluCl $\alpha$ -ECFP protein, we saw clear membrane-bound fluorescence in the Purkinje cell layer, although that fluorescence was dim. All slices exhibited significant background fluorescence in the EYFP channel, which made detection of the optGluCl $\beta$ -Y182F-EYFP protein even more difficult. However, as seen in Figure 6-6B, there is membrane labeling of Purkinje cells which is not seen in wild-type animals. This difficulty in detection could be the result of either low expression levels or the difficulty of detecting fluorescence in slices. There are a number of reports of detecting fluorescent molecules in cerebellar brain slices of transgenic mice (Zhang et al., 2001; Sekirnjak et al., 2003), which favors the former explanation.

### **Electrophysiology suggests expression is low**

We performed electrophysiological recordings on acute dissociated Purkinje neurons to estimate the expression level of optGluCl. These types of cultures have been shown to retain responses to ligand-gated ion channels such as GABA receptors, ameliorating the concern that the preparation technique somehow destroys membrane-bound proteins (Itier et al., 1996). The input conductance change in response to 10 nM IVM was small, approximately 40% (Figure 6-7). This is in stark contrast to our *in vitro* hippocampal culture results, where input conductance increased by 2000% to 3000% (Slimko et al., 2002; Slimko and Lester, 2003).

### **Rotarod behavior is inconclusive**

Despite the weak fluorescence signal and the rather small conductance change in the acute dissociated Purkinje cell experiments, we proceeded to assay the behavior of these animals. Our assay was the rotarod test, in which mice are placed on a rotating

Figure 6-6

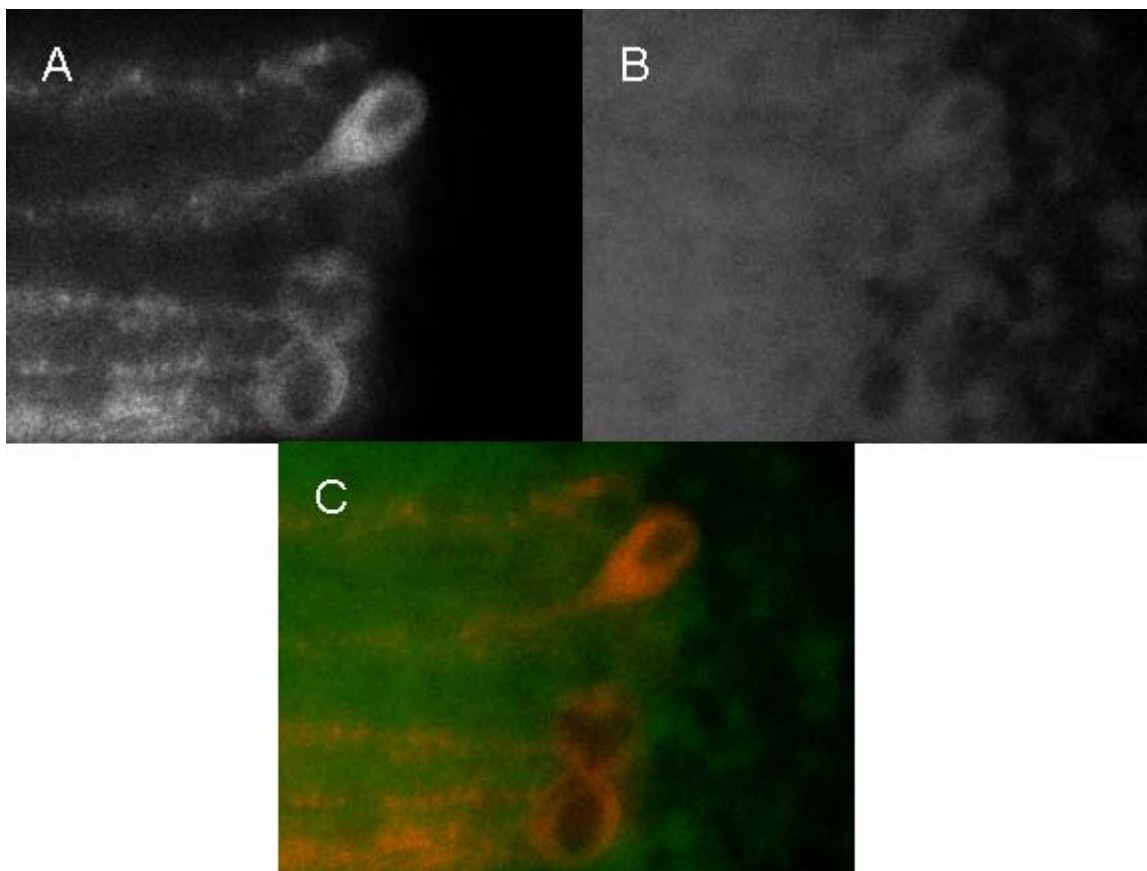


Figure 6-6: **Direct detection of ECFP and EYFP in L7 line 70.** A, image with ECFP filter set shows optGluCl $\alpha$ -ECFP localized to Purkinje cells. B, image with EYFP filter set shows optGluCl $\beta$ -Y182F-EYFP also localized to Purkinje cells, although background fluorescence was higher. Both images are grey-scale for clarity. C, A and B merges shows co-localization of the genes.

Figure 6-7

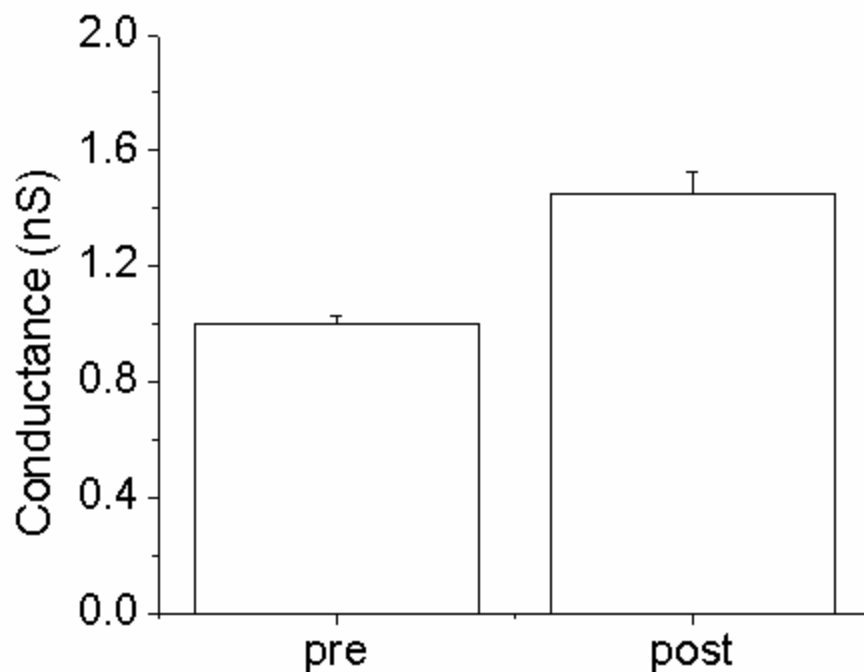


Figure 6-7: **Acutely dissociated Purkinje cell input conductance.** Cells were held at -60 mV and the input conductance was measured with 5 mV voltage steps. Data shown are for transgenic animals, 12 cells per group. Pre is prior to the addition of 10 nM IVM. Post is >20 minutes after addition of the drug. Wild-type animals were studied as well; pre and post IVM were statistically indistinguishable (not shown).

rod and the amount of time they are able to stay on this rod is measured. We performed two versions of this assay. The first is a static rotarod performance measurement. Over the course of 3 days we trained both wild-type and transgenic animals to run on a 30 rpm rotarod for at least 180 s. At the end of the three day training period, all wild-type and transgenic mice were able to perform the task without failure. At the beginning of testing on day 4, all mice were given an ip dosage of IVM, from 5 to 20 mg/kg. The rotarod performance of each mouse in the wild-type and transgenic groups was measured at 4 different time points post-injection (Figure 6-8). There was no significant difference between wild-type and transgenic groups for any of the time point/dosage combinations. Although the transgenics groups performed poorly at the 20 mg/kg dose and 30 min and 3 h time points, the wild-type mice performed poorly as well and there is no significant difference with the transgenic group. Very likely the performance decrement at these large dosages of 20 mg/kg caused non-specific effects in the animal (see Discussion). This was a disappointing result, but correlates with the weak fluorescence and the small conductance increase in the presence of IVM reported previously.

The second version of the assay was the rotarod learning measurement. In this assay, we administered a single 20 mg/kg of IVM 4 h prior to training the animals on the rotarod, and compared the rate at which the wild-type and transgenic animals were able to learn the task (Figure 6-9). There was no significant difference between the learning rates of the two groups.

Figure 6-8

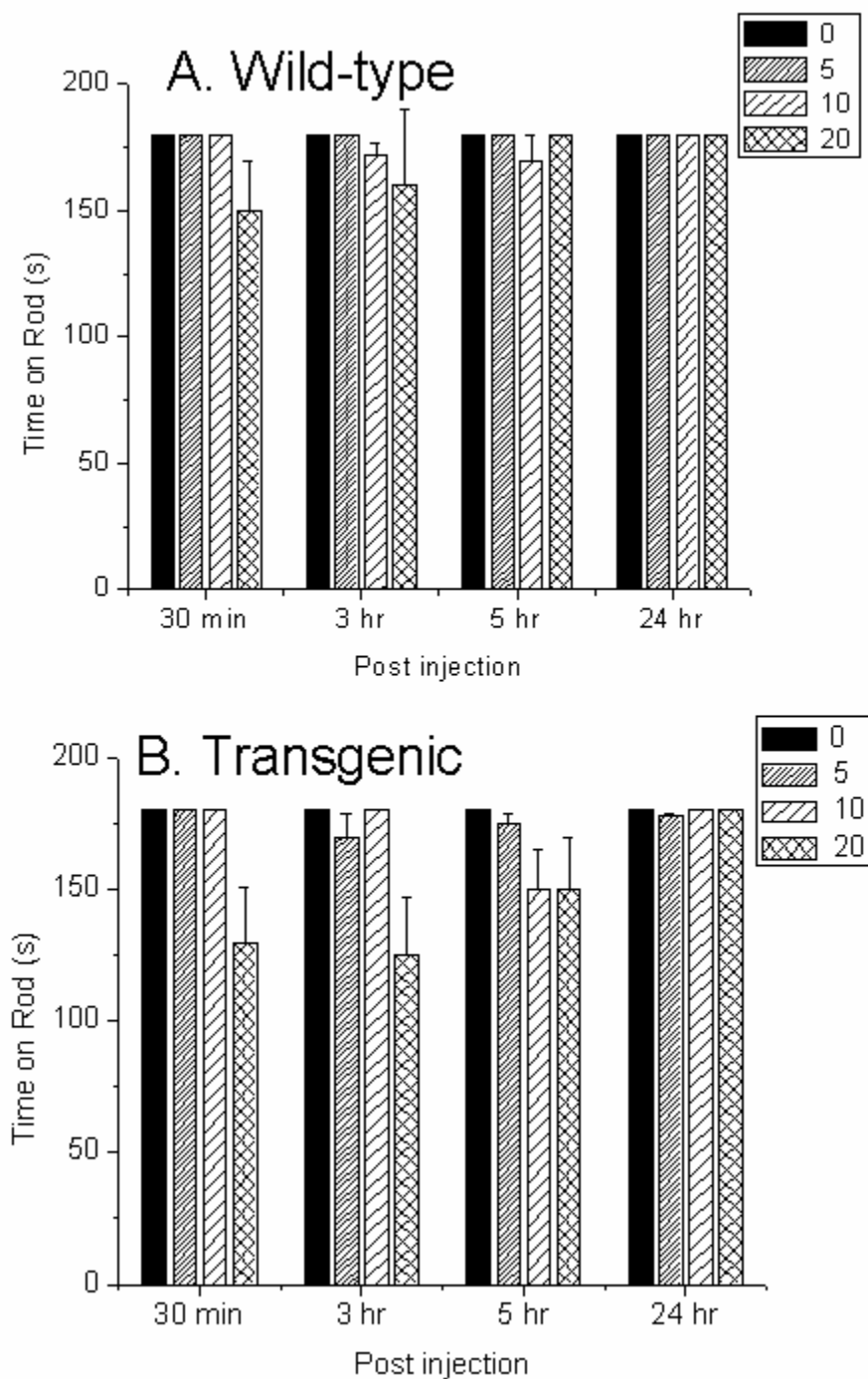


Figure 6-8. **Static rotarod performance.** A, wild-type mice performance on the rotarod at various time points after various dosages of IVM. B, transgenic performance on the rotarod under the same conditions. There is no significant difference between wild-type and transgenic.

Figure 6-9

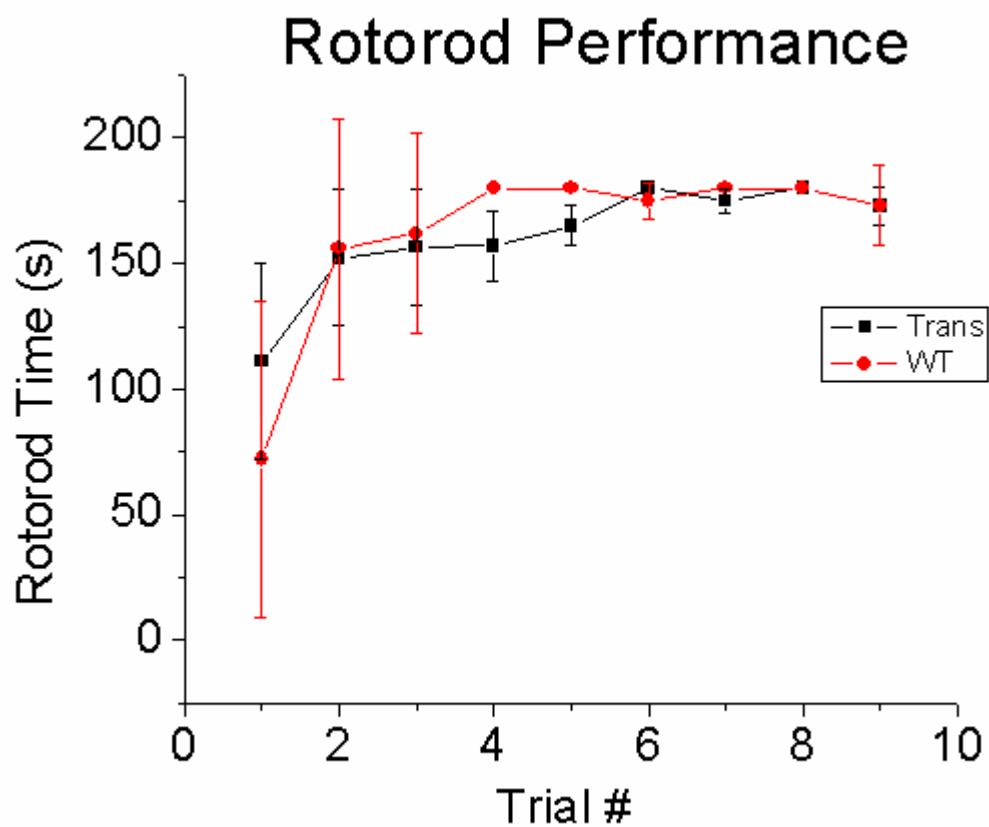


Figure 6-9: **Learning rotarod paradigm.** Wild-type and transgenic mice (5 each) were injected ip with 20 mg/kg of IVM. 4 hr later, they were trained on a 30 rpm for 10 trials, over the course of 3 days (during the final day the animal had 4 trials). There is no significant difference between wild-type and transgenic animals.

## Discussion

We have shown that transgenic mice made with the optGluCl genes under control of the L7 promoter express both mRNA and protein in the correct cell-types. The *in situ* experiments allowed us to detect mRNAs of both genes; however a limitation of using the EGFP antibody is that we cannot distinguish between the two proteins, optGluCl $\alpha$ -ECFP and optGluCl $\beta$ -Y182F-EYFP. Given that the fluorescence microscopy as well as mRNA *in situ*s indicated that both genes were present, we do not see this as a major limitation. A major concern, however, was that the observed fluorescence of these genes was low.

We expected to have a much larger electrophysiological signal in response to application of IVM. This technique relies upon activating enough chloride conductance to effectively clamp the neuron at or near resting potential, an effect we clearly saw in our earlier *in vivo* experiments. The change in conductance in the Purkinje neurons was  $\sim 0.4$  nS, compared to a  $\sim 20$  nS change in the previous hippocampal cultures. Assuming that the single-channel conductance and open probability of GluCl is the same when expressed in both Purkinje neurons and hippocampal neurons, this implies there is far less production of the GluCl proteins in the Purkinje neurons. This is problematic, for Purkinje neurons are typically larger than hippocampal neurons, and they would likely require more, not fewer, channels to effectively silence them.

Our behavioral experiments indicated no clear modulation in rotarod performance to IVM treatment. One criticism may be that we did not administer enough IVM. In previous experiments, we have determined the dosage of IVM that wild-type mice are able to handle without obvious toxic effects (Figure 6-10A). We found that

Figure 6-10

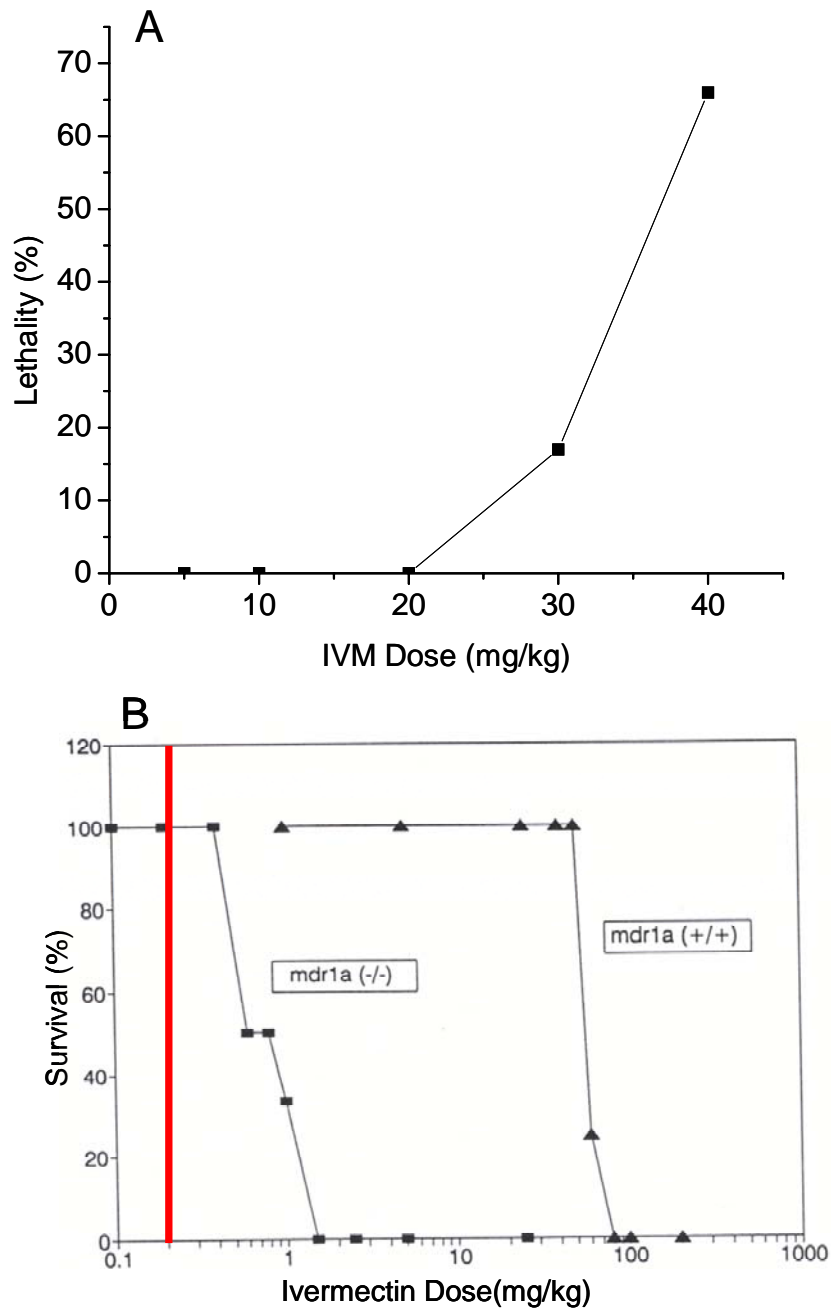


Figure 6-10: **Ivermectin can kill mice.** A, wild-type animals given various dosages of IVM. Above 20 mg/kg, IVM becomes lethal. B, Survival percentages for various dosages of IVM, comparing wild-type and *mdr1a* knockout mouse. The dose which we believe should be enough to activate GluCl in a wild-type mouse is shown with the red bar. Panel B adapted from Schinkel et al, 1994.

above 20 mg/kg, mice start to have severe ataxia and seizures, followed by death. Additionally, we were able to use reported pharmacokinetic data to estimate that an IVM dosage of 0.2 mg/kg results in approximately 5 nM IVM in the brain and thus should activate GluCl (Schinkel et al., 1994). This is nearly 100 times less than the dosage we used in our behavioral experiments. We believe we were using enough IVM to activate the channel; and any larger dosages of IVM would have severely interfered with behavioral tests (in fact, 20 mg/kg seemed to be the beginning of interference in rotarod behavior, see Figure 6-8). Hence, we used the highest possible dosage. Our most probable explanation for the lack of clear behavioral modulation, supported by the weak fluorescence signal and the small conductance change of acute dissociated Purkinje neurons, is that there simply is not enough GluCl protein to clamp the Purkinje neurons at resting membrane potential.

Our viral experiments are still under way. We are encouraged because the fluorescence observed after infection appears to be higher than that seen in our transgenic animals. Perhaps these experiments will lead to some behavioral data. Because of the significant behavioral modulation seen in zebrafish (Chapter 5) resulting from use of the GluCl/IVM method, we are still hopeful.

## References

- Callaway EM (2005) A molecular and genetic arsenal for systems neuroscience. *Trends Neurosci* 28:196-201.
- Chen C, Kim JJ, Thompson RF, Tonegawa S (1996) Hippocampal lesions impair contextual fear conditioning in two strains of mice. *Behav Neurosci* 110:1177-1180.

- Davidson BL, Stein CS, Heth JA, Martins I, Kotin RM, Derksen TA, Zabner J, Ghodsi A, Chiorini JA (2000) Recombinant adeno-associated virus type 2, 4, and 5 vectors: transduction of variant cell types and regions in the mammalian central nervous system. *Proc Natl Acad Sci U S A* 97:3428-3432.
- Dubnau J, Grady L, Kitamoto T, Tully T (2001) Disruption of neurotransmission in *Drosophila* mushroom body blocks retrieval but not acquisition of memory. *Nature* 411:476-480.
- Gatti PJ, DaSilva AM, Gillis RA (1987) Cardiorespiratory effects produced by injecting drugs that affect GABA receptors into nuclei associated with the ventral surface of the medulla. *Neuropharmacology* 26:423-431.
- Gogos JA, Osborne J, Nemes A, Mendelsohn M, Axel R (2000) Genetic ablation and restoration of the olfactory topographic map. *Cell* 103:609-620.
- Hilber P, Caston J (2001) Motor skills and motor learning in Lurcher mutant mice during aging. *Neuroscience* 102:615-623.
- Itier V, Depoortere H, Scatton B, Avenet P (1996) Zolpidem functionally discriminates subtypes of native GABAA receptors in acutely dissociated rat striatal and cerebellar neurons. *Neuropharmacology* 35:137-145.
- Kobayashi K, Morita S, Sawada H, Mizuguchi T, Yamada K, Nagatsu I, Fujita K, Kreitman RJ, Pastan I, Nagatsu T (1995) Immunotoxin-mediated conditional disruption of specific neurons in transgenic mice. *Proc Natl Acad Sci U S A* 92:1132-1136.
- Li P, Slimko EM, Lester HA (2002) Selective elimination of glutamate activation and introduction of fluorescent proteins into a *Caenorhabditis elegans* chloride channel. *FEBS Lett* 528:77-82.
- Ma L, Merenmies J, Parada LF (2000) Molecular characterization of the TrkA/NGF receptor minimal enhancer reveals regulation by multiple *cis* elements to drive embryonic neuron expression. *Development* 127:3777-3788.
- McGuire SE, Le PT, Davis RL (2001) The role of *Drosophila* mushroom body signaling in olfactory memory. *Science* 293:1330-1333.
- Nirenberg S, Cepko C (1993) Targeted ablation of diverse cell classes in the nervous system in vivo. *J Neurosci* 13:3238-3251.
- Nitabach MN, Blau J, Holmes TC (2002) Electrical silencing of *Drosophila* pacemaker neurons stops the free-running circadian clock. *Cell* 109:485-495.
- Oberdick J, Smeyne RJ, Mann JR, Zackson S, Morgan JI (1990) A promoter that drives transgene expression in cerebellar Purkinje and retinal bipolar neurons. *Science* 248:223-226.

- Rabinowitz JE, Bowles DE, Faust SM, Ledford JG, Cunningham SE, Samulski RJ (2004) Cross-dressing the virion: the transcapsidation of adeno-associated virus serotypes functionally defines subgroups. *J Virol* 78:4421-4432.
- Rabinowitz JE, Rolling F, Li C, Conrath H, Xiao W, Xiao X, Samulski RJ (2002) Cross-packaging of a single adeno-associated virus (AAV) type 2 vector genome into multiple AAV serotypes enables transduction with broad specificity. *J Virol* 76:791-801.
- Raman IM, Bean BP (1999) Ionic currents underlying spontaneous action potentials in isolated cerebellar Purkinje neurons. *J Neurosci* 19:1663-1674.
- Schinkel AH, Smit JJ, van Tellingen O, Beijnen JH, Wagenaar E, van Deemter L, Mol CA, van der Valk MA, Robanus-Maandag EC, te Riele HP, et al. (1994) Disruption of the mouse *mdr1a* P-glycoprotein gene leads to a deficiency in the blood-brain barrier and to increased sensitivity to drugs. *Cell* 77:491-502.
- Scott S (1992) *Sensory Neurons, Diversity, Development, and Plasticity*. Oxford: Oxford University Press.
- Sekirnjak C, Vissel B, Bollinger J, Faulstich M, du Lac S (2003) Purkinje cell synapses target physiologically unique brainstem neurons. *J Neurosci* 23:6392-6398.
- Slimko E, McKinney S, Anderson D, Davidson N, Lester HA (2002) Selective electrical silencing of mammalian neurons in vitro using invertebrate ligand-gated chloride channels. *J Neurosci* (in press).
- Slimko EM, Lester HA (2003) Codon optimization of *Caenorhabditis elegans* GluCl ion channel genes for mammalian cells dramatically improves expression levels. *J Neurosci Methods* 124:75-81.
- Sudhof TC (1995) The synaptic vesicle cycle: a cascade of protein-protein interactions. *Nature* 375:645-653.
- Sweeney ST, Broadie K, Keane J, Niemann H, O'Kane CJ (1995) Targeted expression of tetanus toxin light chain in *Drosophila* specifically eliminates synaptic transmission and causes behavioral defects. *Neuron* 14:341-351.
- Watanabe D, Inokawa H, Hashimoto K, Suzuki N, Kano M, Shigemoto R, Hirano T, Toyama K, Kaneko S, Yokoi M, Moriyoshi K, Suzuki M, Kobayashi K, Nagatsu T, Kreitman RJ, Pastan I, Nakanishi S (1998) Ablation of cerebellar Golgi cells disrupts synaptic integration involving GABA inhibition and NMDA receptor activation in motor coordination. *Cell* 95:17-27.
- White BH, Osterwalder TP, Yoon KS, Joiner WJ, Whim MD, Kaczmarek LK, Keshishian H (2001) Targeted attenuation of electrical activity in *Drosophila* using a genetically modified K(+) channel. *Neuron* 31:699-711.

- Wulff P, Wisden W (2005) Dissecting neural circuitry by combining genetics and pharmacology. *Trends Neurosci* 28:44-50.
- Yamamoto M, Wada N, Kitabatake Y, Watanabe D, Anzai M, Yokoyama M, Teranishi Y, Nakanishi S (2003) Reversible suppression of glutamatergic neurotransmission of cerebellar granule cells in vivo by genetically manipulated expression of tetanus neurotoxin light chain. *J Neurosci* 23:6759-6767.
- Yu CR, Power J, Barnea G, O'Donnell S, Brown HE, Osborne J, Axel R, Gogos JA (2004) Spontaneous neural activity is required for the establishment and maintenance of the olfactory sensory map. *Neuron* 42:553-566.
- Zhang X, Baader SL, Bian F, Muller W, Oberdick J (2001) High level Purkinje cell specific expression of green fluorescent protein in transgenic mice. *Histochem Cell Biol* 115:455-464.
- Zirlinger M, Kreiman G, Anderson DJ (2001) Amygdala-enriched genes identified by microarray technology are restricted to specific amygdaloid subnuclei. *Proc Natl Acad Sci U S A* 98:5270-5275.